AD-A136 473 STIMULATED CERENKOV-RAMAN SCATTERING(U) DARTMOUTH COLL HANOVER N H DEPT OF PHYSICS AND ASTRONOMY J E WALSH 14 DEC 83 N00014-79-C-0760 1/2

UNCLASSIFIED F/G 20/8 NL

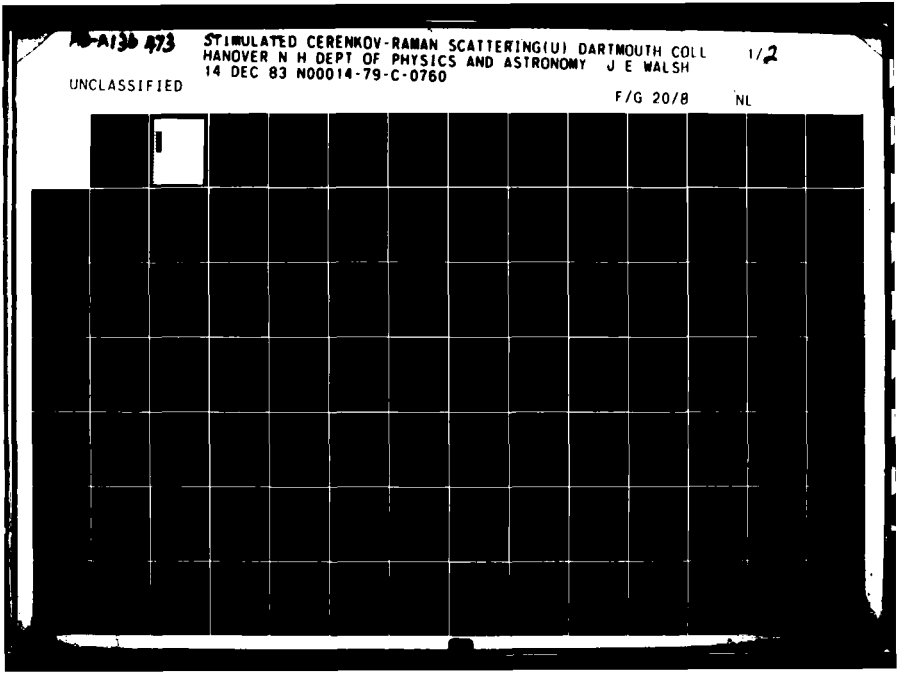

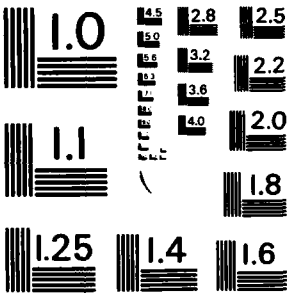

MICROCOPY RESOLUTION TEST CHART
NATIONAL BUREAU OF STANDARDS - 1963 - A

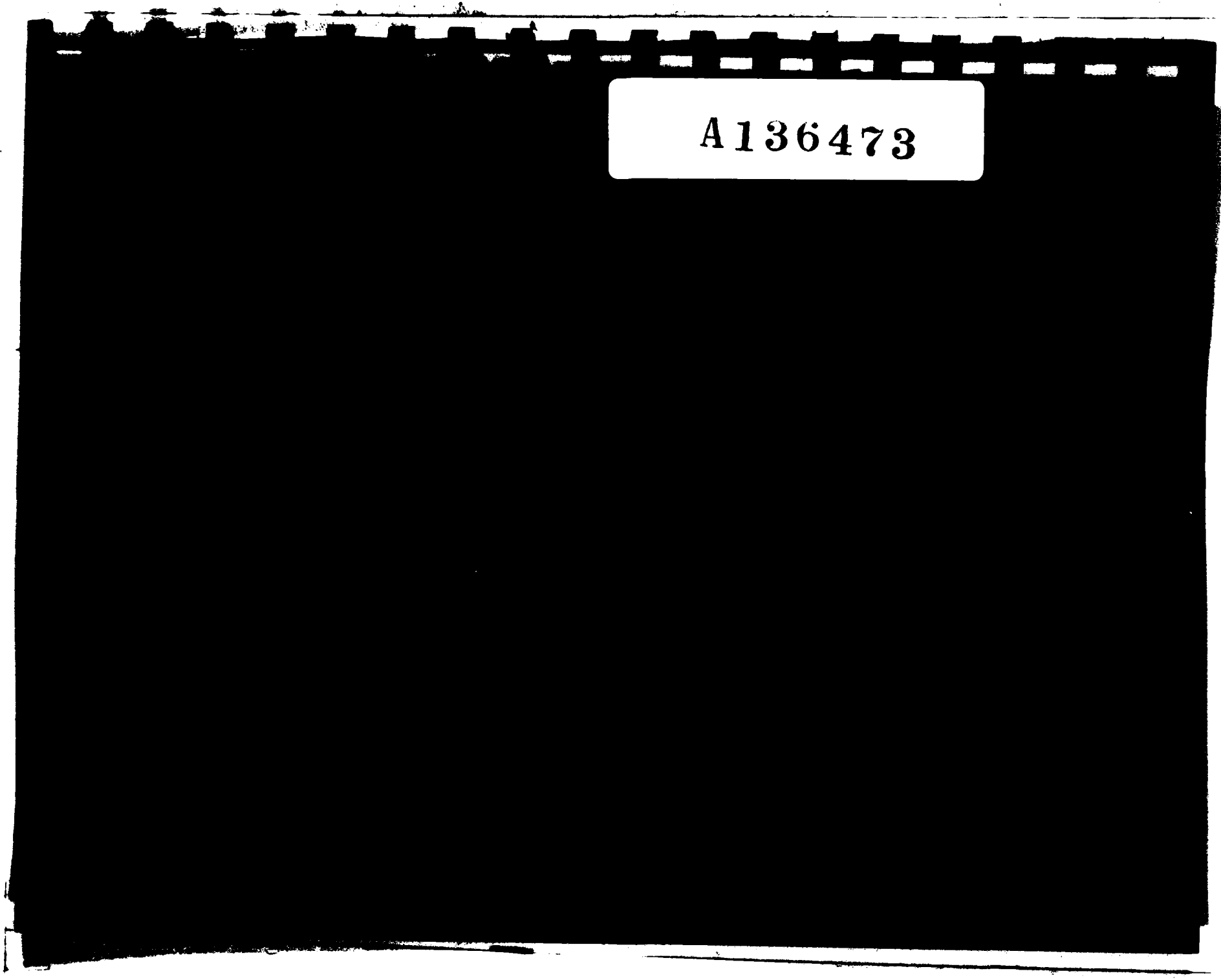

12

****

FINAL REPORT

OFFICE OF NAVAL RESEARCH CONTRACT NUMBER

N00014-79-C-0760

"Stimulated Cerenkov-Raman Scattering"

Prepared by

John E. Walsh
Department of Physics and Astronomy
Dartmouth College
Hanover, N.H. 03755

****

SECURITY CLASSIFICATION OF THIS PAGE (When Data Entered)

REPORT DOCUMENTATION PAGE		READ INSTRUCTIONS BEFORE COMPLETING FORM
1. REPORT NUMBER	2. GOVT ACCESSION NO. A136 473	3. RECIPIENT'S CATALOG NUMBER
4. TITLE (and Subtitle) Stimulated Cerenkov-Raman Scattering		5. TYPE OF REPORT & PERIOD COVERED Final: 8/1/79 - 7/31/83
		6. PERFORMING ORG. REPORT NUMBER
7. AUTHOR(s) John Walsh		8. CONTRACT OR GRANT NUMBER(s) N00014-79-C-0760
9. PERFORMING ORGANIZATION NAME AND ADDRESS Dartmouth College Hanover, New Hampshire 03755		10. PROGRAM ELEMENT, PROJECT, TASK AREA & WORK UNIT NUMBERS NR 395-058 (4330)
11. CONTROLLING OFFICE NAME AND ADDRESS Office of Naval Research 800 N. Quincy Street Arlington, VA 22217		12. REPORT DATE December 14 1983
		13. NUMBER OF PAGES 162
14. MONITORING AGENCY NAME & ADDRESS(if different from Controlling Office)		15. SECURITY CLASS. (of this report)
		15a. DECLASSIFICATION/DOWNGRADING SCHEDULE

16. DISTRIBUTION STATEMENT (of this Report)

Approved for public release; distribution unlimited

17. DISTRIBUTION STATEMENT (of the abstract entered in Block 20, if different from Report)

18. SUPPLEMENTARY NOTES

19. KEY WORDS (Continue on reverse side if necessary and identify by block number)

Millimeter-wavelength Cerenkov Sources; Cerenkov Raman Radiation

20. ABSTRACT (Continue on reverse side if necessary and identify by block number)

A Cerenkov-Raman Maser consists of an energetic electron beam, a dielectric resonator, and a static, rippled magnetic field pump. In the absence of the dielectric resonator, the device is, at longer wavelengths, identical to a stimulated Raman source and at shorter wavelengths, identical to the free electron laser. The addition of the dielectric resonator to the device gives a further degree of freedom to the doppler

DD FORM 1 JAN 73 1473 EDITION OF 1 NOV 65 IS OBSOLETE

SECURITY CLASSIFICATION OF THIS PAGE (When Data Entered)

shift relations. When the beam velocity is below the Cerenkov threshold energy of the dielectric resonator, the usual upshift factor, $\beta/(1-\beta)$ becomes $\beta/(1-\beta/\beta_\phi)$ where $\beta = v/c$ is the relative beam speed and β_ϕ is the relative phase velocity. If $\beta_\phi < 1$ then a given beam velocitywill have a higher frequency upshift. In addition, there is a further solution which is not allowed in the vacuum case. This has an upshift $\beta/(\beta)\beta_\phi-1)$ where $\beta/\beta_\phi > 1$. Both modes can be used to form a Cerenkov-Raman maser.

Contents

Introduction

This is the final report of research carried out under ONR Contract # N00014-79-C-0760 during the period August 1, 1979, through July 31, 1983. The work was primarily devoted to investigation of the Cerenkov-Raman Maser. This device consists of a relativistic electron beam, a rippled magnetic field pump, and a dielectric resonator. When the dielectric resonator is removed, the Cerenkov-Raman Maser becomes identical to the stimulated Raman maser, in the regime where the beam is to be regarded as a collective medium, or to the free electron laser in the single-particle regime.

In the latter devices, a transverse motion is imparted to the be by the rippled magnetic field. The beam electron in its rest frame "sees" the pump wavelength foreshortened by one doppler shift, and hence radiates at this upshifted frequency. Since this radiation is, in turn, viewed in the lab frame, a second doppler shift is introduced. In general the wavelength of the radiation, λ, and the pump wavelength, λ_p, are related by

$$\lambda = \lambda_p(1 - \beta)/\beta \qquad (1)$$

where $\beta = v/c$ is the relative (parallel) electron velocity. This radiation is enhanced the axial bunching which is, in turn, due to the axial component of the Lorentz force.

When the dielectric resonator is added to the system the doppler shift relations are modified in such a way that either

$$\lambda = \lambda_p(1 - \beta/\beta_p)/\beta \qquad (2a)$$

or when $\beta/\beta_\phi > 1$,

$$\lambda = \lambda_p(\beta/\beta_\phi - 1)/\beta \qquad (2b)$$

The symbol β_ϕ represents the relative phase velocity of the wave. Clearly, if $\beta_\phi < 1$ then the wavelength becomes shorter. Furthermore, the regime indicated by Eq. (2b) is not a possible vacuum mode.

The remainder of this report contains abstracts of papers presented at conferences and meetings, and reprints and preprints of published papers, including two papers, one of which appeared in Volume 7 of the series devoted to the Physics of Quantum Electronics, and the other from the series " Advances in Electronics and Electron Physics".

II. Personnel Supported in Part by ONR Contract:

Apart from the Principal Investigator, Robert Layman, a Senior Research Associate, and Richard Cook, a Junior R.A., have received some part of their support from the funding from this contract. Several undergraduate and graduate Research Assistants were also funded during the four years of the duration of this grant, and their names, present affiliations and the dates they received their degrees are listed below.

Kenneth Busby, Ph.D. 1980; Naval Research Lab.

Kevin Felch, Ph.D. 1980; Varian Associates.

Scott Von Laven, Ph.D. 1982; KMS Fusion.

Peter Heim, AB 1981; Dept. Physics, Dartmouth.

John Golub, AB 1981; Dept. Physics, Harvard.

James Murphy, Ph.D. 1982; Brookhaven National Lab.

Bernadette Johnson, Ph.D. 1984 (expected).

William Case, Visiting Faculty Fellow, Summers 1979-pres.
Dept. Physics, Grinnell College, Iowa.

Thomas Buller, Ph.D. 1984 (expected).

III. Abstracts

1. Excitation of the Slow Cyclotron Wave by a Superluminous Electron Beam, J.E. Walsh, W. Case and D. Kapilow, Bull. Am. Phys. Soc. 25, 949 (1980).

2. Cerenkov-Cyclotron Instability, J. Walsh and J. Golub, Bull. Am. Phys. Soc. 26, 798 (1981).

3. Cerenkov Radiation Sources in the Range 500μm-10μm, J.B. Murphy and J.E. Walsh, Bull. Am. Phys. Soc. 26, 935 (1981).

4. Excitation of the Slow Cyclotron Wave in a Dielectrically-Loaded Waveguide, W. Case, J. Golub and J. Walsh, Bull. Am. Phys. Soc. 26, 936 (1981).

5. Cerenkov Radiation as a Source of Millimeter Radiation, J. Branscum and J. Walsh, Bull. Am. Phys. Soc. 26, 93 (1981).

6. Cerenkov Masers: A Possible Plasma Heating Source, J. Walsh, J. Branscum, J. Golub, R. Layman, D. Speer and S. Von Laven, 11th Anomalous Absorption Conference, Montreal, Canada, June 1981.

7. Cerenkov-Raman Free Electron Lasers, J. Walsh, S. Von Laven, J. Branscum, R. Layman, I.E.E.E. International Conference on Infrared and Millimeter Waves, Miami Beach, Florida, December 1981.

8. Excitation of the Slow Cyclotron Wave Using an Axially-Propagating Superluminous Electron Beam, W. Case, R. Kaplan, J. Walsh and J. Golub, Bull. Am. Phys. Soc. 27, 1074 (1982).

Abstract Submitted
For the Twenty-second Annual Meeting
Division of Plasma Physics
November 10 to 14, 1980

Subject Category Number 4.8

Excitation of the Slow Cyclotron Wave by a Superluminous Electron Beam. W. CASE, Grinnell College and J. WALSH and D. KAPILOW, Dartmouth College--A monoenergetic electron beam passing through a dielectric is found to generate an exponentially growing, circularly polarized, electromagnetic wave when $v_o > c/\sqrt{\epsilon}$. The growth of the wave is due to the interaction of the wave with the cyclotron motion of the charges in the beam and is maximized when $\omega - k_z v_o = -\Omega/\gamma$, where $\Omega = eB_o/mc$, $\gamma = (1-\beta^2)^{-\frac{1}{2}}$ and $\beta = v_o^z/c$. The growth rate for wave propagating in the beam direction is $\omega_o [(\sqrt{\epsilon}\beta-1)/2\gamma\epsilon]^{\frac{1}{2}} \sec^{-1}$ where the frequency of the wave is $\omega = \Omega/[\gamma(\sqrt{\epsilon}\beta-1)] \sec^{-1}$. Growth rates for other propagation directions at syncronism have also been calculated. Saturation occurs when the beam is slowed down to a point where $\omega + \Omega/\gamma - k_z v_o$ is sufficiently large and the growth rate becomes zero. Wave energy at saturation is found for the special case of a wave propagating in the beam direction. A comparison is made between this instability and the usual Cerenkov instability.

Supported in part by the Office of Naval Research
Grant #N00014-79-C-0760

( ) Prefer Poster Session

(X) Prefer Oral Session

( ) No Preference

( ) Special Requests for placement of this abstract:

( ) Special Facilities Requested (e.g., movie projector)

Submitted by:

[signature]
(signature of APS member)

William Case
(same name typewritten)

Grinnell College
(address)

This form, or a reasonable facsimile, plus *Two Xerox Copies* must be received NOT LATER THAN WEDNESDAY, AUGUST 13, 1980 at the following address:

Division of Plasma Physics Annual Meeting
Ms. Diane Miller
Jaycor
P.O. Box 370
Del Mar, California 92014

relativistic electron beam accelerated along the axis of a dielectric lined waveguide has produced coherent Cerenkov radiation at kilowatt power levels in the millimeter region. Theory, a description of the experimental apparatus, and some experimental results will be presented.

Work supported in part by U.S. Army Grant No. DAAG 29-79-CO 2030.

F4 Relativistic Beam Propagation in a Dielectric Lined Waveguide. J. BRANSCUM, J.E. WALSH, R.W. LAYMAN, Dartmouth College, Hanover, N.H. 03755--Relativistic electron beams propagating along the axis of a dielectric lined cylindrical waveguide have been shown to produce coherent millimeter radiation.[1] Surface charge collecting on the dielectric liner causes problems of beam dynamics which could limit the practical uses of this process. Experiments demonstrating the effects of charge collection and some possible solutions will be described.

1. K. Felch, K. Busby, R. Layman, and J. Walsh, Bull. Am. Phys. Soc. 24, 1076 (1979).

Work Supported in part by U.S. Army Grant No. DAAG-29-79-CO 2030.

F5 Cerenkov-Cyclotron Instability. J. GOLUB and J.E. WALSH, Dartmouth College, Hanover, N.H. 03755--It has been shown that a slow cyclotron wave propagating along an electron beam, both in a dielectric medium, is unstable.[1] A slow space charge wave propagating at the Cerenkov angle in a similar system is also unstable. We have investigated the off-angle propagation of a slow cyclotron wave. The system is shown to be unstable at a wavelength given by

$$\lambda = (\beta n - 1)/(\Omega_c/2\pi c)$$

where $\beta = v/c$ is the relative beam velocity; n is the index of refraction of the dielectric; and Ω_c is the relativistic cyclotron frequency. A small signal temporal growth rate has been derived for propagation at a general angle. At the Cerenkov angle, using realistic experimental parameters and $\lambda = 500\mu m$, this growth rate is approximately one order of magnitude greater than that of the on-angle case. Potential application of this instability to some practical free electron laser systems will be discussed.

1. D. Kapilow and J.E. Walsh, Bull. Am. Phys. Soc., 25, 6 (1980).

Supported in part by The Office of Naval Research Grant #N00014-79-C-0760.

SESSION G: GRAVITATION/COSMOLOGY
Saturday morning, 18 April 1981
Olin Hall, Room 223 at 9:00 A.M.
H. W. Hilsinger, presiding

G1 Mechanism of Electromagnetic Radiation.* H. W. HILSINGER, Worcester Polytechnic Institute.—Mach's principle asserts that inertial effects are caused not by acceleration relative to some reference frame but by acceleration relative to the rest of the mass of the universe; however, experimental confirmation of this principle is precluded largely by the impossibility of removing that ambient mass or of shielding a system from its effect. The corresponding electromagnetic principle would attribute radiation by a charge to acceleration relative to the ambient charge. An experiment will be described that can, in principle, investigate the mechanism of electromagnetic radiation: does a charge radiate because it has absolute acceleration or because it has an acceleration relative to other charges? The possible results of such an experiment and their interpretation will also be discussed.

*Submitted by L. R. Ram-Mohan

G2 A Novel View of the Solar System - Part I. HAROLD F. SCHWEDE, Retired. The solar system has a new number 293.9823 with dimensions of kms/sec in the plane of the ecliptic. The Newtonian relation for orbital bodies is a limiting form of the expression derived. Jupiter has an influential role. A non-linear relation is quantized where $P^{2/3} \times (\eta + \frac{1}{2})^{1}$ is a constant. With κR_o as the constant, where κ has the value unity and takes care of the dimensions, R_o has the value of 0.010260 A. U. The number η takes integral values while P is the period in sidereal tropical years. The value of η for Venus and Earth are 70 and 97 respectfully. Values of η for such diverse bodies as "Object Kowal", Halley's comet and Ceres are 1867, 1749 and 269. The number $(\eta + \frac{1}{2}) \times R_o$ gives the average semi-major axes. The secular variations for the outer planets are discussed.

G3 Quarks and Particles. HAROLD F. SCHWEDE, Retired. Kinematic considerations of the masses of particles show intriguing results. Phase paths for Pions and Kaons are indicated. A derived number 0.511004091 is considered as the mass of the electron in Mev/c^2 and a number of about 100 ev/c^2 is obtained which is perhaps related to the electron neutrino. Relations are given for the proton and the neutron. The twin primes centered at 138 and 1020 play a role. Rational fractions same as the alleged fractionally charged quarks appear naturally. Elliptic functions, particularly the Weierstrass relations, are revealing. A fundamental relation is easily suitable to cover many types of forces.

SESSION H: GENERAL
Saturday morning, 18 April 1981
Olin Hall, Room 126 at 9:00 A.M.
P. Glanz, presiding

H1 Association of Hemoglobins as Studied by Intensity Fluctuation Spectroscopy. K. J. LaGATTUTA, Univ. of Connecticut — (1) Normal adult hemoglobin (HbA) exists in vivo as a tetramer, two chains of which are of the α form and two chains of which are β. The extent of the association of these four chains into tetramer, in vitro, was measured by intensity fluctuation spectroscopy (IFS) and a pH dependent reaction equilibrium constant deduced. Results are compared with values obtained by other methods. (2) Formation of multi-tetrameric aggregates of HbA is found to occur, in vitro, at low ionic strength. The average size of an aggregate and the dispersion in sizes was determined by IFS[1]. Indications of limited aggregation at very high ionic strength was also observed. (3) Application of IFS to studies of so-called sickling hemoglobins (HbS) will be discussed. The formation of the gel phase of deoxy-HbS may be preceded by states of limited aggregation. These states should be amenable to study by IFS.

[1]K. J. LaGattuta, etal., Biophys. J. 33, 63 (1981).

H2 Hand Held Calculators in Quantitative Analysis of Speckleograms. K. J. PRYFUTNIEWICZ, Worcester Polytechnic Inst.--Recent advances in speckle metrology based on the concept of projection matrices, lead to the development

Abstract Submitted
For the Twenty-third Annual Meeting
Division of Plasma Physics
October 12 to 16, 1981

Category Number and Subject Microwave Generation - 4.8

☒ Theory ☐ Experiment

Cerenkov Radiation Sources in the Range 500μm-10μm*. J.B. MURPHY and J.E. WALSH, Dartmouth College--A single slab dielectric waveguide is examined as a resonator for a Cerenkov free electron radiation source.[1] Properties of the resonator, such as transverse mode spacing, power distribution, scaling of resonator thickness with frequency, are examined. Starting currents are computed based on the linear theory of the single particle interaction mechanism for beams of experimental interest ($\Delta\gamma/\gamma \gtrsim 10^{-3}$). The linear gain of the device is compared to the undulator type device in the 500μm-10μm range. Nonlinear estimates of the saturated power are calculated based on a particle trapping model. We find that the small signal gain of this device compares favorably with undulator coupled devices and thus that operation in the infrared portion of the spectrum is a realistic possibility.

1. J.E. Walsh, in Phys. Quan. Elec. Vol. 7, 255. (Addison-Wesley, Reading, Mass. 1980).

*Work supported by ONR Contract # N00014-79-C-0760.

☒ Prefer Poster Session

☐ Prefer Oral Session

☐ No Preference

☐ Special Requests for placement of this abstract:

☐ Special Facilities Requested (e.g., movie projector)

Submitted by:

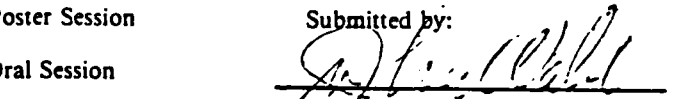

(signature of APS member)

John Walsh

(same name typewritten)

Dartmouth College, Hanover NH 03755

(address)

This form, or a reasonable facsimile, plus *Two Xerox Copies* must be received NO LATER THAN Thursday, July 9, 1981, at the following address:

Division of Plasma Physics Annual Meeting
c/o Ms. Joan M. Lavis
Grumman Aerospace Corporation
105 College Road East
Princeton, New Jersey 08540

Abstract Submitted
For the Twenty-third Annual Meeting
Division of Plasma Physics
October 12 to 16, 1981

Category Number and Subject Microwave Generation - 4.8

☒ Theory ☐ Experiment

Excitation of the Slow Cyclotron Wave in a Dielectrically Loaded Waveguide*. W. CASE, Grinnell College, J. GOLUB AND J. WALSH, Dartmouth College.--
We have continued our studies of the interaction of the modes of a dielectrically loaded waveguide and the slow cyclotron mode of a cold relativistic electron beam.[1] For the limit $\omega >> \Omega/\gamma >> \omega_p$ the growth rate is found to be:

$$\Delta = \left(\frac{\omega_p(\beta^2\varepsilon-1)}{2\beta\varepsilon}\right)\left(\frac{\omega}{\Omega}\right)^{\frac{1}{2}}$$

where: $\Omega \equiv eB_o/mc$, ω is the operating frequency, ω_p is the plasma frequency, and $\beta \equiv v_o/c$. The growth rates for the cylindrical guide are similar and will be presented. A comparison will be made between this instability and the slow space charge interaction (Cerenkov Instability). The physical mechanism which leads to the growth will also be discussed.

1. W. Case, J. Walsh, and D. Kapilow, 22nd. Annual Meeting of Division of Plasma Physics (1980).

*Work supported by ONR Contract # N00014-79-C-0760.

☒ Prefer Poster Session

☐ Prefer Oral Session

☐ No Preference

☐ Special Requests for placement of this abstract:

☐ Special Facilities Requested (e.g., movie projector)

Submitted by:

William Case
(signature of APS member)

William Case
(same name typewritten)

Grinnell College, Grinnell, Iowa (address)

This form, or a reasonable facsimile, plus *Two Xerox Copies* must be received NO LATER THAN Thursday, July 9, 1981, at the following address:

Division of Plasma Physics Annual Meeting
c/o Ms. Joan M. Lavis
Grumman Aerospace Corporation
105 College Road East
Princeton, New Jersey 08540

[3]J. C. Phillips, Covalent Bonding in Crystals, Molecules, and Polymers (U. of Chicago Press, 1969); H. Watanabe as cited in ref. 1.

D 3 Nonlinear screening of negative point charges in diamond, silicon, and germanium. P. CSAVINSZKY and K.R. BROWNSTEIN, Univ. of Maine.--Cornolti and Resta[1] (CR) have recently formulated a Thomas-Fermi (TF) theory of nonlinea impurity screening in semiconductors. CR have obtained th spatially-variable dielectric function for charges ± $1e_0$, ± $4e_0$ (e_0 is the proton charge) embedded in pure diamond, Si and Ge. The nonlinear results differ importantly from the results of the linearized TF theory[2]. We have previously solved the nonlinear TF equation of CR by an equiv alent variational principle[3]. We have used a two-parameter trial solution and considered the cases of $+1e_0$, $+2e_0$, $+3e$ and $+4e_0$ in pure diamond Si and Ge. We have now extended our variational approach to the negative charges $-1e_0$, $-2e$ $-3e_0$, and $-4e_0$ in the above semiconductors[4]. Our analytic results, using again a two-parameter trial solution, agree remarkably well with the numerical results of CR.

[1]F. Cornolti and R. Resta, Phys. Rev. B 17, 3239 (1978).

[2]R. Resta, Phys. Rev. B 16, 2717 (1977).

[3]P. Csavinszky and K.R. Brownstein, Phys. Rev. B (to be published).

[4]P. Csavinszky and K.R. Brownstein, Phys. Rev. B (to be published).

D 4 Phonon Conduction in Elastically Anisotropic Cubic Crystals. A.K. McCurdy, Worcester Polytechnic Institute.-- Striking differences in the boundary-scattered phonon conductivity are predicted along the principal axes of cubic crystals. The results are due to phonon focusing arising from elastic anisotropy. Normalized curves of phonon conductivity have been calculated for samples of square cross-section as a function of the elastic anisotropy $A = 2C_{44}/(C_{11}-C_{12})$ and the elastic ratio C_{12}/C_{11}. Anisotropies of more than 50% are possible for different rod axes. Silicon and calcium fluoride, materials in which this anisotropy was first reported, are shown to be very favorable materials to demonstrate this anisotropy. For silicon and calcium fluoride samples of rectangular cross-section the thermal conduction is shown to depend upon the crystallographic orientation and width ratio of the side faces for samples with the same <110> rod axis. Results are expressed in a convenient form for predicting the phonon conductivity of elastically anisotropic crystals given the linear dimensions, the density and the elastic constants.

D 5 Equilibrium Configuration of an Ethylene Monolayer Adsorbed on Graphite by Eric Ehrhardt, Larry Pratt, Howard Patterson[1] (University of Maine, Orono, Maine 04469) and Larry Passell (Brookhaven National Laboratory, Upton, N.Y. 11973).

In this talk we will describe computer calculations which have been carried out to determine the equilibrium configuration of an ethylene monlayer phys-adsorbed on graphite. A four sublattice structure was assumed from the results of elastic neutron scattering studies. In the calculation we have included ethylene-ethylene interaction as well as the ethylene-graphite substrate interactions. Our results for ethylene adsorbed on graphite are very similar to those of Fusilier, Gillis, and Raich[2] for nitrogen adsor on graphite. That is, the ethylene molecules show a herri bone pattern with the ethylene C=C axis almost perpendicul to the graphite basal plane.

1. Research partially supported by NSF, Department of Materials Research DMR 77-07140.

2. C. R. Fuselier, N.'S. Gillis and J. D. Raich, Solid State Communications 25, 747 (1978).

SESSION E: CONDENSED MATTER (EXPERIMENT)
Saturday morning, 3 October 1981
Room 141 Bennett at 8:45 A.M.
James Hutchison, presiding

E 2 Cerenkov Radiation as a Source of Millimeter Radiation. J. BRANSCUM, J. WALSH*.-- An electron moving with a velocity greator than the phase velocity of an electromagnetic wave produces radiation. This situation can be achieved physically in a number of ways, one of which is to have the electron move through (or near) a dielectric. The resultant radiation is known as Cerenkov radiation. This phenomenon may be used as the basis of a practical millimeter-infrared radiation source. Three problems must be considered: 1) method for making $\omega/ck < 1$. 2) dependence of beam-wave coupling on k, γ, and position. 3) method of insuring that energy moves into the wave from the beam. The first problem is solved by using a dielectric resonator with internal reflection types of modes. The second is approached by examining the phase-velocity dependence of the strength of the electric field which is undergoing total internal reflection. The third problem is approached by constructing a dielectric Fabry-Perot resonator. Each component will be discussed briefly.

*Supported in part by Office of Naval Research Grant # N000-16-79-C-0760.

E 3 Millimeter Wave Generation with a Relativistic Electron Beam. R.W. LAYMAN, J. BRANSCUM, and J. WALSH* --Production of electromagnetic radiation in the 35 to 150 GHz range by a mildly relativistic electron beam accelerated along the axis of a dielectrically lined cylindrical waveguide has been reported elsewhere[1]. This process shows potential as a tunable source of high power millimeter radiation. Results of experimental work to demonstrate this possibility will be described.

1. K. Felch, K. Busby, R. Layman, and J. Walsh, Bull. Am. Phys. Soc. 24, 1076 (1981).

*Work supported in part by U.S. Army Research Office Grant # DAAG-29-79-C-0203.

E 4 Evidence of Bifurcation Universality for First Sound Subharmonic Generation in Superfluid He^4.* C.W. SMITH, D.A. FARRIS, and M.J. TEJWANI, University of Maine, Orono.--Measurement of the subharmonic responses of superfluid helium-4 to ultrasound at 3 MHz is reported. A matched pair of PZT4 thickness mode transducers are positioned parallel on a common axis in an open geometry. One transducer is employed as a first sound source and the other as a receiver. The received signal is Fourier analyzed. Several subharmonic frequencies (f_0/n, where n = 2,3,4,..) of the applied frequency f_0 are observed above specific sound thresholds. Preliminary results for n = 2,4,8 have been analyzed in terms of the bifurcation theory for a nonlinear system in transition to chaos[1]. To within experimental error the thresholds for the onset of the subharmonics agree with the theoretically predicted value of the universal geometric convergence constant, 4.7. Comparison of the observed decrease in the amplitude of successive subharmonics with theoretical prediction, the sequence n = 3,6,12 and apparent phase-locking behavior are currently under investigation.

*Supported by NSF, DMR8005358 and AFOSR, NP 80-151.

[1]M.J. Fergenbaum, J. Stat. Phys. 19, 25 (1978).

E 5 Photoacoustic Studies of Iodine Vapor. A. BHAN, M. SAKLANGUE and B. DI BARTOLO, Boston College. We constructed a photoacoustic apparatus, using an acoustical cylindrical cavity operating in a longitudinal mode and used molecular iodine vapor as specimen and Argon as buffer gas to study the photoacoustic characteristics of the system. The iodine molecules, excited periodically

11th Anomalous Absorption Conference in Montreal, Canada

Cerenkov Masers: A Possible Plasma Heating Source

J. Walsh, J. Branscum, J. Golub, R.W. Layman,
D. Speer, S. Von Laven

Dartmouth College
Hanover, N.H.

June, 1981

A Čerenkov maser consists of an electron beam, a dielectric resonator and output coupling optics. The beam velocity can exceed the phase velocity of the wave in this system, and when it does, a coherent instability leads to beam bunching and a transfer of energy to the wave. The field in the beam channel is also evanescent. The decay rate, however, scales as k/γ where k is the axial wavenumber of the wave and γ is the ratio of the energy of the electron and its rest mass. Hence by using mildly relativistic electron beams (γ = 1.1-1.6) good beam-to-wave coupling can be obtained in the lower mm part of the spectrum. Depending upon their complexity and ultimate performance characteristics, devices of this kind may have a number of applications in plasma diagnostics and heating.

In order to test the basic ideas underlying such devices, a high-voltage (400 Kv max.) pulse transformer-based e-beam generator has been used to drive tubular quartz resonators. At the present time, coherent output has been obtained over the range 10mm-1.5mm. A summary of theoretical expectations and recent experimental results will be presented.

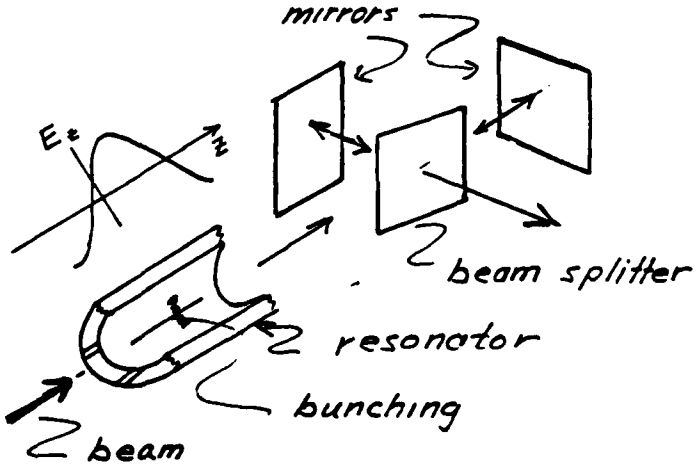

Čerenkov Maser

Work supported in part by: AFOSR Grant #77-3410B, ARO Grant #DAAG-29-79-C-0203 and ONR Grant #N00-14-79-C-0760.

IEEE Int. Conf. on Infrared and
Millimeter Waves, Miami Beach, Florida
Dec. 1981.

Cerenkov-Raman Free Electron Lasers

John E. Walsh, S. Von Laven,
J. Branscum, R.W. Layman

Dartmouth College, Hanover, N.H.

A Cerenkov-Raman Maser consists of a relativistic electron beam, a dielectric resonator, a magnetic wiggler and output coupling optics. The device differs from conventional free electron lasers in that the region of anomalous doppler shift ($\beta\sqrt{\epsilon} > 1$) is accessible. Theory and Experiment will be discussed.

Work supported by Office of Naval Research Grant N00014-79-C-0760.

Session: Free Electron Oscillator and Laser

Abstract Submitted
For the Twenty-fourth Annual Meeting
Division of Plasma Physics
November 1 to 5, 1982

Category Number and Subject 4.8 Microwave Generation

☒ Theory ☐ Experiment

Excitation of the Slow Cyclotron Wave Using an Axially Propagating Superluminous Electron Beam*, WILLIAM B. CASE and ROBERT D. KAPLAN, Grinnell College, JOHN E. GOLUB and JOHN E. WALSH, Dartmouth College.

We consider a relativistic electron beam propagating along a guide field in a dielectric. The calculation is carried out using the linearized fluid model and the resulting dispersion relation analyzed. When $\varepsilon^{-\frac{1}{2}} < \beta < c$ we find the usual instability involving the slow space charge wave (space charge Cerenkov). In addition we find that the slow cylcotron wave is unstable (cyclotron Cerenkov) with a cold beam growth rate:

$$\Delta = \frac{\omega_p [c^2 k_\perp^2 (\varepsilon\beta^2 - 1) + 2\varepsilon\Omega^2/\gamma^2]^{\frac{1}{2}}}{2\varepsilon (\omega\Omega)^{\frac{1}{2}}}$$

where the symbols have their usual meanings. Effects due to thermal width will be presented. A comparison of the two instabilities will also be given.

*Work supported in part by ONR Contract # N00014-79-C-0760-P2.

☒ Prefer Poster Session
☐ Prefer Oral Session
☐ No Preference
☐ Special Requests for placement of this abstract:
☐ Special Facilities Requested (e.g., movie projector)

Submitted by:

[signature] (signature of APS member)

William Case (same name typewritten)

Physics Dept., Grinnell College, Grinnell, Iowa (address)

This form. or a reasonable facsimile. plus *Two Xerox Copies* must be received NO LATER THAN NOON, July 30, 1982, at the following address:

Ms. Barbara Safarty
Princeton Plasma Physics Laboratory
P.O. Box 451
Princeton, New Jersey 08544

IV. Manuscripts and Publications

A Cerenkov-Raman Maser, Ph.D. Thesis, Kenneth Busby, Dartmouth College, Hanover, N.H., May, 1980. (This manuscript is not included with this final report, but has been issued as a separate document. Further copies can be obtained from the Dartmouth College Plasma Laboratory.

1. Stimulated Cerenkov Radiation, John Walsh, in Advances in Electronics and Electron Physics; Vol. 58, edited by C. Marton (Academic Press), 1982.

2. Cerenkov and Cerenkov-Raman Radiation Sources, John Walsh, in Physics of Quantum Electronics, Vol. 7 (Addison-Wesley, MA), 1980.

3. Cerenkov Lasers, J. Walsh, B. Johnson, E. Garate, R. Cook, J. Murphy and P. Heim, Proc. of the Free Electron Laser Conference, Bendor Island, France, September 1982.

4. A Cerenkov Gas Laser, John Walsh and Bernadette Johnson, SPIE-Los Alamos Conference on Optics, Los Alamos, N.M., April 1983, paper 380-158.

*To appear in book of Proceedings Dec. '83 or Jan. '84.

STIMULATED ČERENKOV RADIATION

JOHN E. WALSH

Department of Physics and Astronomy,
Dartmouth College

* * *

* * *

INTRODUCTION

I A. ČERENKOV RADIATION

The electromagnetic wave produced by a charged particle moving with greater than light velocity in a dielectric medium is known universally as Čerenkov[1] radiation. Čerenkov's experiments, which were performed independently during the 1930's, and the subsequent analysis of the phenomena by Frank and Tamm[2] did, however, have some precursors.

Heaviside,[3] in 1889, analysed the problem of the radiation produced by a charged particle when it moved with uniform velocity. This work was done prior to the development of the special theory of relativity, and Heaviside assumed that it was possible for a particle to move with a velocity greater than that of light in a vacuum. When it was so assumed, radiation was produced. In a formal sense, his results were similar to those of Frank and Tamm. Sommerfeld,[4] in 1904, without apparent knowledge of Heaviside's results, performed a similar analysis. There were also some experimental precursors to Čerenkov's work. M. Curie,[5] in 1911, observed that radiation produced in the walls of glass containers holding radioactive material was probably due in part to the penetration of the glass by fast-charged particles. Some experiments performed by Mallet[6] in

in 1926 were, in part, observations of Čerenkov radiation. None of this early work, however, lessens the importance of pioneering experiments of P.A. Čerenkov.

Following the initial experiments of Čerenkov and theory of Frank and Tamm, an extremely large number of both theoretical and experimental contributions have appeared. General discussions, with hundreds of additional references, may be found in Jelley,[7] in Zrelov[8] and in the review article by Bolotovski.[9] The interest of many contributors has been the potential use of the Čerenkov process as a practical radiation source. Notable among these contributions were the papers of Ginzburg,[10] in which he considered a number of ways in which electrons could be coupled to dielectrics and be made to produce radiation in the millimeter and submillimeter regions of the electromagnetic spectrum.

Much of the early work dealt with the radiation produced by single electrons. As we shall see, however, this spontaneous radiation is a relatively weak process for all wavelengths longer than that of the blue ultra-violet regions of the spectrum. Hence, in order to produce useful amounts of radiation, it was natural to consider the radiation produced by a bunched electron beam. At wavelengths long compared to the length of the bunch, the radiated power is proportional to the square of the number of electrons involved, and hence the power emitted rises dramatically. A number of experiments were designed to explore the properties of the

Čerenkov radiation produced by prebunched electron beams moving in close proximity to a dielectric surface. Important contributions were made by Coleman,[11] by Danos,[12] by Lashinsky,[13] and by Ulrich.[14] In these experiments, no provision was made for feeding back the emitted radiation on subsequent bunches and hence they could be categorized as observation of enhanced spontaneous emission.

Suggestions have also been made that Čerenkov radiation could be used as the basis of a microwave tube.[15,16,17] In these, a dielectric tube was used as a slow wave structure. The general configuration suggested was similar to that used in traveling wave tubes. When electron beams in the energy and current range found in conventional microwave tubes are used, however, the resulting devices are unsatisfactory for several reaons. We will develop this line of argument carefully in subsequent sections, since these difficulties must be surmounted in constructing a useful Čerenkov source.

A major difficulty in constructing a Čerenkov source that is capable of producing useful amounts of radiated power is the coupling of the electron beam to the dielectric. In elementary discussions, it is usually assumed that the electron is passing right through the dielectric. This can actually be done for the limiting case of very high energy particles and gaseous or liquid dielectrics. In this regime, Čerenkov radiation actually finds wide practical

application as a diagnostic tool.[7] There have also been serious attempts[18,19,20] to observe stimulated Čerenkov radiation in the visible and ultra-violet region from a high-energy beam/gaseous dielectric combination. In these latter experiments, momentum modulation[18,19] by an applied electromagnetic has been observed, but as yet there is no clear-cut evidence of true stimulated emission. An alternative to passing an electron beam directly through a dielectric is to let a beam propagate along a channel. Recent experiments[21,22,23] in which millimeter-wavelength stimulated Čerenkov radiation has been observed have been of this type.

A primary purpose of the present paper is to explore the potential of the latter option. We will establish criteria necessary for producing usable levels of stimulated Čerenkov radiation at wavelengths which are short compared to the characteristic scale length of both the transverse and longitudinal dimensions of a dielectric resonator.

I B. ČERENKOV MASERS

The goal of the general area of research pertaining to devices now often called free-electron lasers is to produce coherent, tunable, moderate, and high-power radiation in parts of the electromagnetic spectrum where such a source is not now available. All of the devices suggested to date have much in common with microwave tubes, and hence the designation "maser" or "laser" could be the subject of debate. It is possible, but not necessary, to formulate the equations of motion quantum-mechanically. The electron transitions are between continuum states. The recoil due to single-photon emission is negligible, and thus Planck's constant does not appear in any final working formula. A classical analysis based on either fluid or kinetic equations will lead to the same expressions. Therefore, much of what is know about microwave tubes will apply also to free-electron lasers. Microwave tubes, however, operate at wavelengths comparable to or greater than the device, while the opposite will be the case for any free-electron laser or maser. This difference, although minor from some viewpoints, accounts for many of the difficulties encountered in attempting to build short wavelength, beam-driven radiation sources.

A Čerenkov maser, Fig. 1, is a device consisting of a dielectric resonator, an electron beam, and an output coupling structure*. The device is, in essence, a traveling-wave tube with the dielectric resonator serving as the slow wave structure. When low relative dielectric constant materials are used for the resonator and, at least, mildly relativistic electron beams are used for the drive, gain can be obtained at wavelengths comparable to and less than the transverse dimension of the resonator. We will see from the subsequent analysis that a device such as the one shown in Fig. 1 could be expected to work in the lower millimeter, submillimeter and far-infrared portions of the spectrum.

In the device shown in the sketch, the resonator supports a wave going slower than the speed of light in vacuum. The electron beam propagates slightly faster than the wave, and hence it will bunch in the region of retarding field. Work is done and the wave grows. This process will be analyzed in detail in Section II.

Shown in Fig. 2 are two other possible configurations for a Čerenkov source. In the first, the beam runs over the top of a slab of dielectric, and in the second, it is assumed to pass through the dielectric. The first form may be used

*The name Čerenkov, in the designation, follows from the fact that it is the Čerenkov criterion that the beam velocity must satisfy if gain is to be obtained.

as it is shown, or it may be the limiting form of a thin, cylindrical resonator, hollow beam configuration. The second form is convenient for analysis since the boundary value problem implied in the first version is much simplified. We will use it for this latter purpose. When extremely relativistic electron beams and gaseous dielectrics are used, the second sketch might also serve as the basis of practical device. The fundamental problems of practical implementation of the direct device, which are the production of and the propagation of a sufficiently monoenergetic electron beam, are beyond the scope of the present analysis. Hence, we will not speculate seriously about experimentally realistic devices where the beam propagates through the dielectric.

Emphasis throughout the analysis and discussion will be on resonators which are separate from the beam. Furthermore, we will always assume that the devices operating at lower-millimeter wavelengths or less are the ones of interest. In Section II, we will establish conditions which must be obtained in this wavelength region. Discussion in Section III will be devoted to experimental matters. Then, some general conclusions will be given in Section IV.

II. THEORY

A series of calculations aimed at establishing the beam energy, current, and velocity spread, which are required in order to obtain growth of stimlated Čerenkov radiation, will be presented in this section. The analysis will proceed along classical lines similar to those used in traveling wave tube and beam plasma theory. In Sections II A and B we will examine the exponential gain of stimulated Čerenkov radiation obtained when it is assumed that either a strongly magnetized or a completely unmagnetized monoenergetic electron beam passes directly through a dielectric medium. The limit implied by the assumption that the beam is monoenergetic will be examined in Section II C, and modified gain formulas will be derived. Section II D will then be devoted to some resonator configurations which are more practical for the present application. Emphasis will be on the slab geometry, since in this case it is possible to present a reasonably compact analytic result. The results obtained from other geometries will be similar. A few brief comments and calculations related to nonlinear effects will be outlined in Section II E.

II A. ČERENKOV GAIN ON A STRONGLY MAGNETIZED BEAM

We consider first the case of a plane wave propagating at an angle to strongly magnetized electron beam. The geometry is shown in Fig. 3.

II A. 1. Current Modulation

When the beam is strongly magnetized, the beam density and modulation are one-dimensional and lie along the beam and magnetic axis. In this limit, the linearized equation for the velocity modulation has only one component, v_z, where:

$$\frac{dv_z}{dt} = -\frac{e}{m\gamma^3} E_z \qquad (1)$$

The solution of this equation for the assumed E_z is readily found:

$$v_z = -\frac{ie}{m\gamma^3} \frac{1}{\omega - k v_o} E_z \qquad (2)$$

This result together with a linearized equation of continuity gives for the density modulation n ,

$$n = \frac{n_o k_o v}{(\omega - kv)}$$

$$= - \frac{(in_o e)}{m\gamma^3} \frac{kE_z}{(\omega - k_1 v_o)^2} \tag{3a}$$

$$= - [in_o e/(m\gamma^3)] \; kE_z/(\omega - kv_o)^2 \tag{3b}$$

Thus the current produced by the wave is given by:

$$J_z = - n_o ev - nev_o \tag{4a}$$

$$= + \frac{i\omega_p^2}{4\pi\gamma^3} \frac{\omega E_z}{(\omega - k\, v_o)^2} \tag{4b}$$

where $\omega_p^2 = 4\pi n_o e^2/m$ is the beam plasma frequency.

II A. 2. The Wave Equation

The current given by eq. (4b) appears in Maxwell's equations as a source term. These are:

$$\nabla \times \underline{E} = - \frac{1}{c} \frac{\partial \underline{B}}{\partial t} \tag{5a}$$

and

$$\nabla \times \underline{B} = + \frac{4\pi}{c} \underline{J} + \frac{1}{c} \frac{\partial \underline{D}}{\partial t} \tag{5b}$$

In writing the second of these, we assume that the wave and the beam are in a dielectric medium where:

$$\underline{D} = \epsilon \underline{E} \tag{6}$$

Taking the time derivative of the second of Maxwell's equations and substituting the first gives a single-wave equation:

$$\nabla \times \nabla \times \underline{E} + \frac{\epsilon}{c^2} \frac{\partial^2 \underline{E}}{\partial t^2} = - \frac{4}{c^2} \frac{\partial \underline{J}}{\partial t} \tag{7}$$

There is no current component in the direction perpendicular to the beam and, hence, the perpendicular component of eq. (7) may be used to express E_x in the terms of E_z. Doing this and substituting into the longitudinal component of eq. (7), and making use of the assumed time and z-dependence, we obtain a single wave equation for E_z:

$$\frac{\partial^2 E_z}{\partial x} + \frac{\frac{\omega^2 \epsilon}{c^2} - k^2}{c^2} E_z = \frac{4\pi i}{\omega \epsilon} \left(\frac{\frac{\omega^2 \epsilon}{c^2} - k^2}{c^2} \right) J \tag{8}$$

Since we have also assumed a plane wave dependence in the perpendicular as well as longitudinal direction, we also obtain immediately:

$$\left[\frac{\omega^2 \epsilon}{c^2} - k^2 - p^2 - \frac{\omega_p^2}{\epsilon \gamma^3} \frac{\left(\frac{\omega^2 \epsilon}{c^2} - k^2 \right)}{(\omega - k v_o)^2} \right] E_z = 0 \tag{9}$$

where p is the perpendicular component of the wave number.

II A. 3. The Dispersion Relation

We are obviously interested in the case $E_z \neq 0$ and, hence, the coefficient of eq. (9) is the dispersion relation:

$$\frac{\omega^2\varepsilon}{c^2} - k^2 - p^2 - \frac{\omega_p^2}{\varepsilon\gamma^3} \frac{\left(\frac{\omega^2\varepsilon}{c^2} - k^2\right)}{(\omega - kv_o)^2} = 0 \qquad (10)$$

for a plane wave propagating through a dielectric medium at an angle to a strongly magnetized electron beam.

Equation (10) is a quartic in both ω and k and hence it has four roots. When $v_o < c/\sqrt{\varepsilon}$, all four roots are real, while if $v_o > c/\sqrt{\varepsilon}$ it has two real roots and a complex conjugate pair. One of the real roots is related to a wave propagating in the direction opposite to that of the beam (in the negative, z-direction). The other three result from the coupling of an electromagnetic wave propagating in the positive z-direction and two beam space charge waves. The latter two, fast and slow space charge waves, would be normal modes of the free beam. In the presence of the dielectric, however, they become coupled to the electromagnetic wave. When the velocity threshold $v_o/c = 1/\sqrt{\varepsilon}$ is exceeded, the beam-wave dielectric system becomes unstable.

II A. 4. Čerenkov Gain

The presence of the beam is obviously felt most strongly for waves near "synchronism", i.e. when

$$\omega \simeq kv_o \qquad (11a)$$

and

$$kv_o \lesssim \omega_{ok} \qquad (11b)$$

where we define ω_{ok}^2 as

$$\omega_k^2 = c^2(k^2+p^2)/\varepsilon \quad , \qquad (11c)$$

the dispersion relation of the electromagnetic waves in the absence of the electron beam.

In the region where eqs. (11a) and (11b) are valid, the dispersion relation, eq. (10), becomes an approximate cubic:

$$(\omega-kv_o)^3 - \frac{\omega_p^2}{2\gamma^3\varepsilon}\omega(1-1/\beta^2\varepsilon) = 0 \qquad (12)$$

Equation (12) follows from (10) when kv_o is set equal to ω in those terms where the substitution does not give zero. This is a valid assumption provided ω_p^2 is small in a sense which we will define shortly.

When $\beta^2\varepsilon < 1$ eq. (12) has three real roots while in the reverse case, the roots are:

$$(\omega - kv_o) = \left[\frac{\omega_p^2 \omega}{2\varepsilon\gamma^3}\left(1 - 1/\beta^2\varepsilon\right)\right]^{1/3} \qquad (13a)$$

and

$$(\omega - kv_o) = \left(\frac{\omega_p^2 \omega}{2\gamma^3 \varepsilon}\right)^{1/3} \left(1 - 1/\beta^2\varepsilon\right)^{1/3} \frac{(1 \pm i\sqrt{3})}{2} \qquad (13b,c)$$

The root corresponding to eq. (13b) is an exponentially growing wave in either time, $\mathrm{Im}\omega \neq 0$, or space, $\mathrm{Im}k \neq 0$. The choice between these will be determined by initial and boundary conditions.

We will, for the moment, assume that the spatial growth is of interest and we will let $\mathrm{Im}k = \alpha$, then:

$$\alpha = \frac{\sqrt{3}}{2}\left(\frac{\omega_p^2 \omega}{2\varepsilon\gamma^3}\right)^{1/3} \frac{\left(1 - 1/\beta^2\varepsilon\right)^{1/3}}{c\beta} \qquad (14)$$

Examination of eq. (14) shows that the spatial gain increases with the two-thirds power of the beam density and the one-third power of the frequency. It vanishes as the beam energy approaches the Čerenkov threshold and decreases as ε and γ become large.

Shown in Fig. 4 are sketches of free wave dispersion curves for two different perpendicular wave numbers, p_1 and p_2 . The curves leave the $k = 0$ axis at the point

$\omega/c = p/\sqrt{\varepsilon}$, cross the speed of light at $\omega/c = p/\sqrt{\varepsilon-1}$ and then asymptotically approach a wave prpagating in the z-direction. Along this curve, the angle of propagation is varying from $\theta = \pi/2$ to $\theta = 0$. Also shown in Fig. 4 is a beam "velocity" line, $\omega = ck\beta$. The points at which this line intercepts the dispersion curves are points at which the beam velocity and the phase velocity of the free waves are the same; they are in "synchronism".

Consideration of eqs. (11a) and (11b) shows that, at this point, the angle of propagation is the same as the Čerenkov angle, $\theta_c = \cos^{-1}(1/\beta\sqrt{\varepsilon})$. At this point, the dispersion is modified by the beam and the wave will grow at a rate given by eq. (14). If γ, ε, and the beam density are left unchanged, the rate of growth at the synchronous point on the p_1 curve will be greater than that on the p_2 curve by an amount equal to the frequency ratio to the one-third power. Thus the stimulated Čerenkov process is a potential short wavelength radiation source.

Growth will also occur at angles other than the Čerenkov angle. Shown in Fig. 5 is a numerical solution of the complete dispersion relation (eq. (10)). We see that there are three solutions in the positive , positive k quadrant of the ω - k plane. One is purely real, while the other two are a complex conjugate pair in the region below and near synchronism and real above this point. The gain peaks just below synchronism (the shift is equal to

the $Re(\omega-kv_o)$ given in eq. (13)) and goes identically to zero at the point $\omega = kv_o$. On the small k side the $Im(\omega/c)$ goes to zero more slowly. The exact shape of this curve will depend upon γ, ε and the beam density.

We have now established that by controlling the angle of propagation, ε, and the beam energy, the frequency at this maximum growth occurs increases as $\omega^{1/3}$. It will be instructive to consider the magnitude of the gain as these parameters are manipulated. In order to do this, we rewrite again eq. (14), now in this form:

$$\alpha = \left(\frac{\beta\omega_p^2\omega}{2c^3}\right)^{1/3} G(\gamma_T)\ F(\gamma,\gamma_T)\ \frac{\gamma_T}{\gamma} \qquad (15)$$

where

$$\gamma_T^2 = \frac{\varepsilon}{\varepsilon-1} \qquad (16a)$$

is the threshold energy ($\beta_T^2 = 1/\varepsilon$),

$$G(\gamma_T) = \frac{(1-1/\gamma_T^2)^{1/3}}{\gamma_T^{5/3}} \qquad (16b)$$

and

$$F(\gamma,\gamma_T) = \frac{(1-\gamma_T^2)^{1/3}}{(1-1/\gamma^2)} \qquad (16c)$$

One power of β has been inserted in front of ω_p^2 so that we may subsequently express it in terms of the beam current, a form which we will find convenient in our numerical evaluation of the gain. Before we do this evaluation, we will examine the functions G, F, and γ_T/γ.

The function G depends only upon the dielectric constant of the material. A sketch is shown in Fig. 6a. It shows a vertical rise at $\gamma_T = 1$, the point where the dielectric constant of the material approaches infinity, reaches a maximum at $\gamma_T^2 = 7/5$ ($\varepsilon = 7/2$), and finally decreases as $\gamma_T^{-5/3}$ as γ_T becomes large ($\varepsilon \to 1$). Thus, in considering a practical Čerenkov source, one cannot move profitably in the direction of low beam energy, optically-dense materials ($\gamma \to 1$, $\gamma_T \to 1$, $\varepsilon \to \infty$) since the gain vanishes rapidly in this limit. As a practical matter, one could not propagate a beam in this type of material in any event. In the opposite limit, we would have gasses ($\varepsilon \to 1$). In this region, the gain will also decrease, but conclusions as to the usefulness of this limit must also include consideration of the $\omega^{1/3}$ term. It is interesting, and perhaps important, for practical mm-submm wavelength devices that G peaks in the region of the dielectric constant of quartz.

The function F depends both upon the threshold energy, γ_T, and the beam energy of γ. It rises vertically from $\gamma = \gamma_T$ and asymptotically approaches unity from below.

Sketches of F, γ_T/γ and their product are shown in Fig. 6b. There is obviously a local maximum in the growth rate. The value of the product at this maximum is about .5 .

Before we consider some actual numerical values for the growth rate, it will be useful to consider one further scaling, which will be that of the beam density. We assume for the present that the beam is now a rectangular slab of thickness and that the variation of $\underline{E}$ in the x-direction is still given by exp (ipx). The term

$$\frac{\beta\omega_p^2}{2c^3} = \frac{4\pi\beta ne^2}{2mc^2}\ \frac{\omega}{c} \qquad (17a)$$

can be re-expressed as

$$\frac{\beta\omega_p^2}{2c^3} = \frac{2\pi I}{I} \cdot \frac{\omega a}{c} \cdot \frac{1}{a^3} \qquad (17b)$$

where

$$r_o = e^2/mc^2 \qquad (18a)$$

$$I_o = ec/r_o \qquad (18b)$$

and I is the electron beam current. When I is measured in amperes, I_o has the value 17 kA. Hence, the factors preceding the energy and material form factors in the expression for gain, eq. (15), are given by:

$$\left(\frac{\beta\omega_p^2\omega}{2c^3}\right)^{1/3} = \left(\frac{2\pi I}{I_o}\right)^{1/3} \left(\frac{\omega a}{c}\right)^{1/3} \frac{1}{a} \qquad (19)$$

When I is approximately 3A, the first of the three factors is approximately equal to 0.1, while if it 3ma it becomes 0.01. The second factor may, in principle, vary from zero to a moderately large number, and the characteristic scale length a may be anything from .01 to 1 centimeter. Hence, substantial gain is possible in principle. A discussion of ways in which this may be achieved in practical cases will be deferred until after we have made some mention of wave-guiding structures.

II B. GAIN FROM AN UNMAGNETIZED BEAM

The preceding analysis presumes that the current density modulation occurs only in the z-direction. As we will see in later discussion, one class of Čerenkov device will make use of mildly relativistic electron beams and will somewhat resemble microwave tubes. The beams in these devices will almost certainly propagate along a strong axial guide field, and, in this limit, the assumptions made in the last section be at least approximately valid.

Another class of device, however, might make use of a more relativistic beam such as that used in the injector of a linear accelerator, a linear accelerator itself, or perhaps some other type of accelerator. The beam in this case may very well not be magnetized. It will then have rapidly varying components in the transverse as well as the longitudinal direction, and the gain formulas will be modified.

When the beam is unmagnetized, the linearized equation for the perpendicular motion is:

$$\frac{d\underline{v}_\perp}{dt} = \frac{e}{m\gamma}\left(\underline{E}_\perp + \frac{\underline{v}_o}{c} \times \underline{B}\right) \qquad (20)$$

while the longitudinal motion is still governed by eq. (1). Assuming the same geometry given in Fig. 1, the one non-vanishing component of this equation will lie in the x-direction.

$$\frac{dv_x}{dt} = -\frac{e}{m\gamma}\left(E_x - \frac{v_o B_y}{c}\right) \tag{21}$$

Equation (21), with the aid of Faraday's law, may be restated in the form:

$$\frac{dv_x}{dt} = -\frac{e}{m\gamma}\left[\left(\frac{\omega - kv_o}{\omega}\right)E_x + \frac{pv_o}{\omega}E_z\right] \tag{22}$$

The $\underline{v} \times \underline{B}$ term gives rise to an E_z as well as E_x dependence for v_z.

The solution to eq. (21), together with the linearized equation of continuity, may be used to construct expressions for the current density. These are:

$$J_x = \frac{i p^2}{4\pi\gamma}\frac{1}{\omega}\left(E_x + \frac{pv_o}{\omega - kv_o}E_z\right) \tag{23a}$$

and

$$J_z = \frac{i\omega p^2}{4\pi\gamma}\frac{1}{\omega}\left[\frac{pv_o}{\omega - kv_o}E_x + \left(\frac{\omega^2}{\gamma(\omega - kv_o)^2} + \frac{p^2 v_o^2}{(\omega - kv_o)^2}\right)E_z\right] \tag{23b}$$

The current terms can now be substituted in eq. (7). When this is done, we have as our new wave equation:

$$\begin{pmatrix} k^2 + \frac{\omega_p^2}{c^2} - \frac{\omega^2\varepsilon}{c^2} & pk + \frac{pv_o}{\omega - kv_o}\frac{\omega_p^2}{c^2} \\ pk + \frac{pv_o}{\omega - kv_o}\frac{\omega_p^2}{\gamma c^2} & p^2 + \left(\frac{\omega_p^2}{\gamma c^2}\frac{\omega^2\gamma^2 + p^2 v_o^2}{\gamma^2(\omega - kv_o)^2}\right) - \frac{\omega^2\varepsilon}{c^2} \end{pmatrix}\begin{pmatrix} E_x \\ E_z \end{pmatrix} = 0 \tag{24}$$

The determinational equation for eq. (24) is now the dispersion relation for the unmagnetized beam-dielectric combination. It is:

$$\left(k^2 + \frac{\omega_p^2}{\gamma c^2} - \frac{\omega^2\varepsilon}{c^2}\right)\left(p^2 + \frac{\omega_p^2}{\gamma^3 c^2} \cdot \frac{\omega^2\gamma^2 p^2 v_o^2}{(\omega - kv_o)^2} - \frac{\omega^2\varepsilon}{c^2}\right) - \left(pk + \frac{pv_o}{\omega - kv_o}\frac{\omega_p^2}{\gamma c^2}\right)^2 = 0 \tag{25}$$

Equation (25), which appears quite cumbersome in comparison with eq. (9), is still a quartic in either ω, k or both. All qualitative comments made about the strongly magnetized case apply here as well. However, the results are quantitatively somewhat different. Again, the strongest coupling region of the beam to the wave is in the velocity synchronism ($\omega/ck = \beta$).

If terms proportional to $1/(\omega - kv_o)^2$ are collected separately, we obtain for the dispersion relation:

$$\frac{\omega^2\varepsilon}{c^2}\left(\frac{\omega^2\varepsilon}{c^2} - k^2 - p^2 - \frac{\omega_p^2}{c^2}\right) - \frac{\omega_p^2}{\gamma c^2}\frac{1}{(\omega - kv_0)^2}\left[\left(\frac{\omega^2\varepsilon}{c^2} - k^2 - p^2\frac{\omega_p^2}{c^2}\right)p^2 v_o^2 + \frac{\omega^2}{\gamma^2}\left(\frac{\omega^2\varepsilon}{c^2} - k^2\right) - p^2(\omega^2 - v_o^2 p^2 - v_o^2 k^2)\right] = 0 \tag{26}$$

Near synchronism, this reduces to:

$$\left(\frac{\omega^2\varepsilon}{c^2} - k^2 - p^2 - \frac{\omega_p^2}{\gamma c^2}\right) - \frac{\omega_p^2}{\gamma c^2}\frac{\omega^2(\varepsilon - 1)(\beta^2\varepsilon - 1)}{(\omega - kv_o)^2} \tag{27a}$$

or

$$\left(\frac{\omega-kv_o}{v_o^3}\right)^3 = \frac{\omega_p^2\omega}{2\gamma c^3}\ \frac{(1-1/\beta^2\varepsilon)}{\beta^3\gamma_T^2} \qquad (27b)$$

Once again, the dispersion relation is cubic and the frequency and the dependence upon the size of the Čerenkov angle ($\theta = \sin^{-1}(1-1/\beta^2\varepsilon)$) are the same. However, the beam energy and ε dependence are different. If we use the functions defined earlier, we have for the spatial growth rate:

$$\alpha = \left(\frac{\beta\omega_p^2\omega}{c^3}\right)^{1/3} G(\gamma)\ F(\gamma,\gamma_T)\left(\frac{\gamma_T}{\gamma}\right)^{1/3} \qquad (28)$$

The energy dependence is now $\gamma^{-1/3}$ in the high energy limit, as opposed to the more constrictive γ^{-1} dependence in the strongly magnetized limit. If all other factors are the same, the gain in the unmagnetized limit will be greater than that for the strongly magnetized beam. This is because the electrons in the beam can now do work on the wave in both the transverse and longitudinal direction.

II C. BOUNDED STRUCTURES

Excepting the possibly interesting limit of extremely relativistic beams and gaseous dielectrics, it is not practical to have the beam penetrating the dielectric. Hence, in assessing the practicality of Čerenkov sources, it is important to consider dielectric wave guides and resonators which have channels for the beam propagation. This complicates the analysis. Thus, before we take up the cases quantitatively, it will be useful to consider, at this point, the regime where the results of the preceding section are qualitatively useful.

First, we note that with minor changes, the results of the last section will apply exactly to a metal-bounded, cylindrical, dielectric waveguide through which an electron beam propagates. The perpendicular wave number, p, is now a root of zero order Bessel function and is no longer completely free. The only other change is that the factor π in the current term no longer appears, because the beam is now also cylindrical. The field symmetry is now transversely magnetic.

II C. 1. Cylindrical Guide with a Beam Channel

When the beam propagates in a hole in the dielectric, we have a situation such as that sketched in Fig. 7. If the diameter of the hold is sufficiently small, a concept which, shortly, will be quantitatively specified, the results of the preceding section might be expected to apply more or less exactly.

It is obviously the relative size of the hole which is the fundamental difference. Fortunately, it is possible to attain considerable insight into its effect with little analysis. We consider, for the moment, a metal-lined guide partially filled with dielectric. The dispersion curves sketched in Fig. 7 are similar to those shown in Fig. 4. The main difference is the shape near the light line, $\omega = ck$. The point where the curve crosses this line is now controlled by the relative filling factor, d/b, as well as the dielectric constant of the material. As d/b and ε become small, the point where the partially-filled guide becomes a slow wave structure, $\omega/ck \ll 1$, can thus still be made to occur at an arbitrarily high frequency.

When $\omega/ck > 1$, outside the light line, the field in the hole is proportional to $J_o(pr)$, an ordinary Bessel function. In this regime it peaks in the center of the hole. However, we must operate in the regime $\omega/ck < 1$, and in this case, the radial dependence is proportional to a modified Bessel function, $I_o(qr)$. The field is now

a minimum at r = 0, and the beam wave coupling is obviously decreased.

A sketch of the field dependence in the two regimes is shown in Fig. 8. The wave number in the dielectric, p, is still given by:

$$p^2 = \frac{\omega^2}{c^2} - k^2 \tag{29}$$

while the wave number in the hole, when $\omega/ck < 1$, is now given by

$$q^2 = k^2 - \frac{\omega^2}{c^2} \tag{30}$$

The latter is obviously one measure of the field depression in the hole. Since we operate near synchronism, $\omega = ck\beta$, we have for q:

$$q = k/\gamma \tag{31a}$$

$$q = \omega/c\beta\gamma \tag{31b}$$

or

$$q = 2\pi/\lambda\beta\gamma \tag{31c}$$

Hence, when non-relativistic beams are used $\beta\gamma \approx v/c$, the field drops off away from the dielectric in a distance small compared to a wavelength. If, however, the beam is at least mildly relativistic, $\beta\gamma \gtrsim 1$, the opposite limit

applies and we can operate with wavelengths that are small compared to the hole.

The latter considerations actually apply to any structure supporting a wave for which $\omega/ck < 1$. One might then ask about the relative advantages of a dielectric tube since, if $\beta\gamma \gg 1$, then coupling would be improved at short wavelengths for only slow wave structure.

The advantages of the dielectric tube also lie in the short wavelength range. In a conventional slow wave structure, the periodicity must also be comparable to the wavelength. Structures of reasonable length are, therefore, a great many wavelengths long and they become very difficult to fabricate at relatively long wavelengths (a few millimeters). It is possible, but not easy, to build conventional structures with a fundamental period smaller than a few millimeters. The dielectric is, however, a smooth structure and easy to fabricate. When the beam is relativistic, the coupling impedance becomes comparable to that of other structures. Modifications of this basic structure, such as a dielectric tube with no metal boundary and multiple coupled tubes, may also be of practical use. Another basic structure, a dielectric slab bounded on one side by a conductor, also shows promise for application in the shorter wavelength region. This follows from the fact that a greater mode separation at small wavelengths can be obtained from this more open structure. Hence, it may well

be easier to make single-mode devices with this type of structure, and for this reason we will analyze it in some detail.

The basic geometry is shown in Fig. 9. Assuming, for the moment, that no beam is present, we have for the TM modes of the guide:

$$\underline{E} = (0, E_y, E_z) \tag{32a}$$

where

$$\left[\frac{d^2}{dy^2} + \left(\frac{\omega^2\varepsilon}{c^2} - k^2\right)\right] E_z = 0 \tag{32b}$$

and

$$E_y = \frac{ik}{\frac{\omega^2\varepsilon - k^2}{c^2}} \frac{\partial E_z}{\partial x} \tag{32c}$$

In the region $0 \leq y \leq d$, the dielectric constant ε appears while in the region $y \geq d, \leq \infty$ is set equal to unity.

Anticipating the fact that we are concerned only with slow waves bound to the surface guide, we have for the electric fields:

$$E_z = A \sin py \tag{33a}$$

where

$$p^2 = \frac{\omega^2 \varepsilon}{c^2} - k^2 \qquad (33b)$$

in the region $0 \leq y \leq d$. Outside the dielectric, the field is:

$$E_z = Be^{-qy} \qquad (34a)$$

$$q^2 = k^2 \omega^2 / c^2 \qquad (34b)$$

Matching the tangential electric and magnetic fields can be used to eliminate the constants A and B. Thus we have for the dispersion relation of the dielectric slab wave guide:

$$\varepsilon q \cot pd = p \qquad (35)$$

A plot of the roots of this function is given in Fig. 10. The lowest order mode has no cutoff. It comes up along the light line, $\omega = ck$, until pd gets somewhat closer to the neighborhood of $\pi/2$. Thereafter, as ω becomes larger, it asymptotically approaches the speed of light in the dielectric. In the region $\pi/2 \leq pd \leq \pi$ there are no solutions to q. (45), while, when $\pi \leq pd < 3\pi/2$, a second mode which has a finite ω cutoff frequency can also propagate. At successively higher frequencies, more of these modes appear. Several are shown in Fig. 10.

II C. 2. Coupling of Beam to Bounded Resonator

Also shown in Fig. 10 is a beam speed line, $\omega = ck\beta$. It is obvious that if the beam velocity satisfies the Čerenkov conditions, $\beta > 1/\sqrt{\varepsilon}$, phase synchronization between an electron beam and a wave can be maintained. When the beam is added, the wave equation in the vacuum region becomes:

$$\left[\frac{d^2}{dy^2} + \left(\frac{\omega^2}{c^2} - k^2\right) \varepsilon_{\parallel}\right] E_z = 0 \qquad (36a)$$

where

$$\varepsilon_{\parallel} = 1 - \frac{\omega_p^2/\gamma^3}{(\omega - kv_o)^2} \qquad (36b)$$

In arriving at eqs. (36a) and (36b), it has been presumed that beam density modulation occurs only in the z-direction, that the left edge of the beam is close to the dielectric, and that the beam extends indefinitely in the region $y > d$. The size of the actual gap between the beam and the dielectric will be an important parameter in a short wavelength device and its role will be discussed separately.

II C. 3. The Beam-Guide Dispersion for a Bounded Structure

When a bounded structure is used to support the wave, as it must in almost any practical source, the dispersion relation becomes a transcendental as opposed to an algebraic

function. It will be more or less straightforward to obtain values for the roots by numerical means, but it is not immediately obvious how to obtain a good qualitative understanding of the roots.

One method which is appropriate for relatively weak beams is the following. Assume a relation of the form:

$$D(\omega, k, \omega_p^2) = 0 \qquad (37)$$

where the presence of ω_p^2 in eq. (37) indicates the presence of the beam. If the beam is weak, we can write:

$$D(\omega, k, \omega_p^2) = D^{(0)}(\omega, k) + \omega_p^2 \frac{\partial D}{\partial \omega_p^2} \qquad (38a)$$

where

$$D^{(0)}(\omega, k) = D(k, \omega, 0) \qquad (38b)$$

is the dispersion relation for the waves supported by the structure when no beam is present. This function can, in a region near to the solution $D^{(0)}(\omega, k) = 0$ be written as

$$D^{(0)}(\omega, k) = (\omega - \omega_k)\, \partial D^0/\partial\omega \qquad (39)$$

where ω_k are the roots of eq. (35).

The second term in eq. (38a) can also be further reduced. The dependence of the dipsersion relation upon ω_p^2 always enters through ϵ and hence the second term of

Equation (38a) will also have the form:

$$\omega_p^2 \frac{\partial D}{\partial \omega_p^2} = \frac{\omega_p^2 C(\omega,k)}{\gamma^3(\omega-kv_o)^3} \tag{40}$$

where $C(\omega, k)$ is a function which will depend upon the details of the structure. It may, for example, have zeros, but it will not have any poles near either $\omega = ky$, or $\omega = \omega_k$.

Thus, near synchronism, $\omega_k = kv_o$, and for beams which are not too strong, $I/I_o << 1$, we again have a cubic dispersion relation:

$$0 = (\omega-\omega_k)\frac{\partial D^0}{\partial \omega} + \frac{\omega_p^2}{\gamma^3(\omega-kv_o)^2} C(\omega_k,k) \tag{41a}$$

or

$$(\omega-kv_o)^3 = \frac{\omega_p^2}{\gamma^3} \frac{C(\omega_k,k)}{\partial D^0(\omega_k,k)/\partial\omega} \tag{41b}$$

Thus, the qualitative nature of the roots is rather independent of the exact geometry of the wave-supporting structure.

When the wave-supporting structure is a dielectric slab and the assumptions made earlier apply, the dispersion relation becomes:

$$q \cot pd = \frac{p}{\varepsilon}\sqrt{\varepsilon_{\parallel}} \tag{42}$$

The expansion procedure outlined in the preceding subsection then gives for eq. (41b):

$$\left(\frac{\omega-kv_o}{v_o}\right)^3 = \left(\frac{\beta\omega_p^2}{c^3}\right)\frac{(1-1/\beta^2\varepsilon)}{\varepsilon\beta^4\gamma^3}\cdot\frac{\sin^2 pd}{\frac{kd}{\gamma}+\frac{\gamma^2}{\varepsilon\gamma_T^2}\sin^2 pd} \qquad (43)$$

The first two groups of factors on the right-hand side of eq. (43) are identical to the results obtained when it was assumed that the beam propagated in the dielectric, and much of the discussion presented at that point applies here as well. The last group of factors contains the dependence on the geometry. It can be seen that, in addition to the Čerenkov threshold dependence, the coupling also goes to zero as the thickness of the slab goes to zero, and is a result that could easily be anticipated.

The other trends in the gain can be understood as follows: On the fundamental mode, the value of pd varies from 0 at $\omega = 0$ up to $\pi/2$ as $\omega, k \to \infty$. On the higher branches, it varies from $n\pi$ at cutoff ($\omega = ck$) to $(2n + 1)\pi/2$ as the curve asymptotically approaches the speed of light in the dielectric. The value of $\sin^2 pd$ thus varies monotonically from zero to one. Assuming that the velocity synchronism is maintained along the dispersion curve, the gain will vanish at $\omega = ck$, because in this limit, $\gamma \to \infty$, and it becomes increasingly difficult to modulate the beam. Furthermore, as $\beta \to 1/\sqrt{\varepsilon}$, the gain also vanishes due to the factor $(1-1/\beta^2\varepsilon)$ in the coefficient.

The gain thus vanishes at both ends of the dispersion curve and peaks in between. A sketch of the general behavior is shown in Fig. 11.

The maximum value that the gain can achieve is similar to that of the filled guide case. Some typical results for a thin, quartz slab waveguide are shown in Figs. 12a and 12b. In these plots, the factor $(\beta\omega_p^2/c^{2\ 1/3})$ has been omitted for convenience. The remaining factors contain all the relevant frequency and energy dependencies. Maximum values somewhat greater than unity are obtain for this particular set of parameters. The omitted term $(\beta\omega_p^2/c^{2\ 1/3})$ is actually the beam current density in A/cm^2 divided by I_o (= 17 kA) all to the one-third power. It is relatively easy to obtain values of 0.1 for this number, hence the plots shown in Figs. 12a and 12b demonstrate that with a quartz slab guide, it is possible in principle to have relatively large gain (α = .233) gives (1db/cm) well into the submillimeter part of the spectrum.

The gain plot in Fig. 12 also indicates that the gain is a bit higher on the higher order modes. This trend is a reflection of the $\omega^{1/3}$ factor in the gain. It is real, but it depends upon two assumptions whose validity are also frequency dependent. These are: first, that the beam is infinitesimally close to the dielectric and second, that the beam is monoenergetic. The first of these will be discussed now and the second point will be covered in a later section.

II C. 4. Finite Gap Between Beam and Resonator

If we assume that there is a small gap between the beam and the dielectric surface, we would have a situation such as that shown in Fig. 13. The analysis procedes as before, but the resulting dispersion relation

$$\frac{\omega_p^2 e^{-qd_2}}{2(\omega - kv_o)^2} = \frac{q\varepsilon \cot pd - p}{p} \qquad (44)$$

is, at first sight, much more complicated. However, if we again assume that the roots at synchronism lie along the dispersion curve for the free modes, the situation simplifies considerably and the end result is that the gain is modified by an exponential factor which depends upon the size of the gap:

$$\alpha = \alpha(d) \quad e^{-kd_2/\gamma^3} \qquad (45)$$

As long as kd_2/γ is small, the gain on the higher order modes will be comparable to or greater than the gain on the fundamental mode. Values of d_2 of about 1 millimeter would be conservative and fractions of this are easily obtained. Hence, provided that ones uses $\beta\gamma \geq 1$, the quart guide system discussed above will still be viable well into the submillimeter region of the spectrum.

We have been assuming that the beam extends indefinitely in the positive y-direction. As long as the beam is

at least a few e-foldings thick, this assumption does not affect the gain. Since we are primarily interested in high frequencies, this assumption will normally be valid.

The fall-off of the field in the transverse direction may also be useful in obtaining some mode selection. If a relatively thin beam is used, the fields for the lower order modes may penetrate through to the other side. If a lossy material is placed above the beam, it may be possible to further reduce the gain on the lower order mode.

In the fall-off of the electric field, operation at arbitrarily short wavelengths could be obtained if γ is allowed to become large, i.e. kd_2/γ will remain small. This will involve a penalty in the maximum value of gain obtainable, but since it is relatively large to begin with, the resulting system will still be potentially useful. In this way, with more relativistic e-beams, it might be possible to operate well into the infrared portion of the spectrum. This will be discussed further in a later section.

II D. THE EFFECT OF BEAM VELOCITY SPREAD

Prior to this point in our discussion, we have assumed that the electron beam was perfectly monoenergetic. It is intuitively plausible that this is a wavelength-dependent assumption, and we will now examine its consequences. The discussion will be divided into three parts. First, we will determine wavelength limit for a simple beam space charge wave. Then, this result will be compared with a similar criterion for a Čerenkov instability. Finally, having set the limiting wavelength for treating the beam as monoenergetic we will derive gain expressions valid in the region where the assumption is violated.

II D. 1. Beam Space Charge Waves

The linearized equation of motion for a strongly-magnetized electron beam is given by eq. (1). If this is taken along with the equation of continuity eq. (3a), Poisson's equation, and assumptions similar to those of that section, the dispersion relation for space charge waves

$$\omega = kv_o \pm \omega_p/\gamma^{3/2} \qquad (46)$$

may be easily derived.

The upper (lower) sign in eq. (46) corresponds to a fast (slow) space charge wave. See Fig. 14a.

We will concern ourselves with a slow space charge wave. Shown in Fig. 14b is a sketch which illustrates the meaning of the statement: "the wave is resolved from the beam". The wave is clearly resolved when the beam may be regarded as a delta function in frequency space, (the arrows located at ω and kv_o). If, on the other hand, the velocity spread of the beam, Δv, is such that the self-consistent frequency separation, $\Delta\omega = \omega - kv_o$ (derived under the assumption that the beam was monoenergetic) is less that $k\Delta v$, the assumption is violated. A quantitative criterion for this critical k is:

$$k_c \Delta v = \frac{\omega_p}{\gamma^{3/2}} \tag{47}$$

Equation (47) may be re-expressed in terms of physically more intuitive variables if we write: $k_c = \omega/c\beta = 2\pi/\lambda_c\beta$, Δv in terms of $\Delta\gamma$ and β, and ω_p in terms of the beam current density J_b. Then we have:

$$\lambda_c = \pi \frac{\Delta\gamma}{\gamma}\left(\frac{I_o}{\beta\gamma J_b}\right)^{\frac{1}{2}} \tag{48}$$

where I_o is still ec/r_o = 17 kA. If $\beta\gamma$ is of order unity, $\Delta\gamma/\gamma$ is of order 10^{-2} and J_b is a reasonable fraction of an ampere/millimeter^2 than λ_c is a fraction of a millimeter. These are relatively modest requirements, and thus we predict that it should be possible to make effectively cold beams well into the submillimeter part of the spectrum.

The critical wavelengths given by eqs. (47) and (48) are dependent upon the assumption of a simple space charge wave. When we are considering a Čerenkov instability, however, $\Delta\omega = \omega - kv_o$ is actually larger than $\omega_p/\gamma^{3/2}$, and hence the beam can be effectively colder at a given wavelength. The criterion for resolution is:

$$k_c \Delta v = \frac{\omega_I}{2} \tag{49}$$

where the right-hand side of eq. (49) is the real part of the detuning (eq. 13b). Substitution of the expressions for ω_I can be made for the appropriate case.

When the beam propagates through the dielectric, eq. (13b) applies directly and we have:

$$\lambda_c = \sqrt{2\pi}\left(\frac{\Delta\gamma}{\beta\gamma}\right)^{3/2}\left(\frac{I_o}{\beta\gamma J_b}\right)^{1/2} \cdot \frac{1}{\sqrt{1-1/\gamma}} \cdot \frac{1}{\sqrt{\gamma^2/\gamma_T{}^2-1}} \tag{50}$$

The current density dependence is similar to that of eq. (48), but provided the beam is at least mildly relativistic ($\beta\gamma \geq 1$), the energy dependence is more favorable. Overall, presuming that γ_T and γ/γ_T are not excessively large, the value λ_c, given by eq. (50), will be at least as small as that given by eq. (48). The addition of the form factor associated with a more practical resonator will not alter this essential conclusion.

II D. 2. Gain in the Warm Beam Limit

When the criteria given in the preceding paragraphs are violated, the beam is to be regarded as "warm" at the wavelength in question. The gain does not vanish in this limit, but it does begin to drop as ω^{-1}, as opposed to the general $\omega^{1/3}$ trend in the cold beam limit. This trend means that oscillators can probably be built in the warm beam limit, but amplifiers will be impractical.

In calculating the gain, we will use the Vlasov equation as the basic equation of motion and we will retain the assumption that the beam is strongly magnetized. In this case, the Vlasov equation is:

$$\frac{\partial f}{\partial t} + v_z \frac{\partial f}{\partial z} + p_z \frac{\partial f}{\partial p_z} = 0 \qquad (51)$$

If this is linearized, $f = f_o + \delta f$, and is Fourier-transformed, we have for the perturbed component distribution:

$$\delta f = - ie E_z \frac{\partial f_o / \partial p_z}{\omega - k v_z} \qquad (52)$$

The current is now given by:

$$J_z = \int v_z \, \delta f \, \partial p \qquad (53a)$$

$$= ie E_z \int v_z \frac{(\partial f_o / \partial p_z)}{\omega - k v_o} \, dv_z \qquad (53b)$$

Substitution of this into eq. (8) will then lead to a dispersion relation. If the beam distribution is a delta function, then the integral can be performed immediately and the current given by eq. (4b) is recovered. However, we are now interested in the limit where the beam velocity spread is finite.

An exact solution of a dispersion relation containing a integral kernel, such as that of eq. (54), can be found using numerical techniques. The results of such a procedure will be discussed below. However, some insight into the general behavior can be obtained in the limit where k times the width of the beam distribution is broad in comparison with the gain which would be obtained from a calculation in which it were assumed that the beam were cold (monoenergetic).

The dispersion relation obtained from the above procedure is:

$$\frac{\omega^2\varepsilon}{c^2} - k^2 - p^2 + \frac{\omega_p^2}{\omega\varepsilon}(\omega^2\varepsilon/c^2-k)\int_{-\infty}^{\infty}\frac{mv\partial f/\partial p dp}{\omega-kv} = 0 \quad (54)$$

In its present form, the integral which appears in eq. (54) is to be performed along the real momentum line, and hence the procedure for handling the singularity at synchronism is not yet defined. Borrowing from the theory of plasma physics, we handle it by formally extending the integral into the complex plane. First, we re-express eq. (54) as a

velocity integral. Then:

$$\frac{\omega^2\varepsilon}{c^2} - k^2 - p^2 + \omega_p^2 \frac{\left(\omega^2\varepsilon/c^2-k^2\right)}{\omega\varepsilon} \int \frac{v\partial F/\partial v dv}{\gamma^3(\omega-kv)} = 0 \qquad (55)$$

we now let

$$\frac{1}{\omega-kv} = P\frac{1}{\omega-kv} - i\pi\delta(\omega-kv) \qquad (56)$$

where P stands for the principal part of the integral. Multiplying through by c^2/ε and using the condition $v = \omega/k\omega\varepsilon$, we find for the imaginary part of the dispersion relation:

$$D'' = -\frac{\pi\omega_p^2\beta^2(1-1/\beta^2\varepsilon)}{\varepsilon\gamma^3}\frac{\partial F(\omega/k)}{\partial(\omega/k)} \qquad (57)$$

It is sufficient for the purpose of the present discussion to ignore the small correction to the real part of the dispersion represented by the principle part of the integral. In the limit, the real part of the dispersion is:

$$D' = \omega^2 - \omega_k^2 \qquad (58a)$$

and providing the growth is small, the imaginary part of the frequency is adequately represented by:

$$\omega_I = \frac{D''}{\partial D'/\partial\omega}\Big|_{\omega=\omega_k} \qquad (58b)$$

or

$$\omega_I = \pi\omega_p^2 \frac{\beta^2(1-1/\beta^2\varepsilon)}{2\varepsilon\omega_k\gamma^3} \frac{\partial F(\omega_k/k)}{\partial\omega_k/k} \qquad (58c)$$

Obviously, there will be wave growth (inverse Landau damping) in the region of velocity space where ω_k/kcv_o). Sketches of the unperturbed dispersion relation, $\omega = \omega_k$ and ω_I are shown in Fig. 15. The region of positive ω_I lies on the larger k side of the synchronous wave number, $k_s = \omega/v_o$, and peaks at a velocity which is below v_o by an amount approximately equal to the half width of the velocity distribution.

Thus, the wave growth in the warm beam limit has a shape which is complimentary to that obtained in the cold beam limit. This result may seem to imply that the growth due to inverse Landau damping is fundamentally different from the growth obtained in the warm beam limit. However, this is not the case. If the roots of eq. (55) are followed as the beam width is varied from a value of zero up to $k\Delta v\omega_I$ (cold), we find that one regime passes smoothly into the other. The peak absorption shown in Fig. 15 is always somewhat less than the gain. It is a composite of the long wavelength, cold beam gain and Landau damping caused by that part of the beam which has $\partial F/\partial v < 0$. The peak gain obtainable in the warm beam limit will always be less that ω_I (cold). This occurs because, as the beam distribution becomes arbitrarily sharp, the self-consistent beam density

dependent frequency shift will move the phase velocity of the wave downward relative to the position of maximum $\partial F/\partial v$.

In spite of this, the warm beam limit may very well be of interest. An assessment of this requires that we estimate eq. (58c) which, in general, depends upon the detailed shape of the beam distribution. We can, however, proceed without undue complication if we recognize that if $\backsim 1/\Delta v$, and thus $\partial F/\gamma v$ at its maximum is $\backsim 1/\Delta v^2$. Then, in terms of $\Delta\gamma$, an approximate expression for ω_I becomes:

$$\omega_I \backsim \frac{\pi\omega^2 p}{2\varepsilon} \cdot \frac{\gamma}{\omega} \cdot \left(\frac{\beta\gamma^2}{\Delta\gamma}\right)(1-1/\beta^2\varepsilon) \qquad (59a)$$

or

$$\alpha \backsim \frac{\lambda}{\varepsilon} \cdot \frac{J_b}{I_o} \cdot \left(\frac{\gamma^2}{\Delta\gamma}\right) \cdot \frac{(\gamma^2/\gamma_T^2-1)}{\beta^2\gamma} \qquad (59b)$$

It is interesting to evaluate the possible gain in the 10μ range. In this case, $\lambda = 10^{-3}$ centimeters. If we can achieve $J_b/I_o \backsim 10^{-3}$ and $\Delta\partial/\gamma > 10^{-2}$, it appears that $\alpha \backsim .1$ cm.$^{-1}$ are within the realm of possibility. Thus, it might be possible to construct Čerenkov lasers down to wavelengths comparable to those achieved in stimulated Compton devices.

It is also interesting to evaluate eq. (59b), when λ is equal to λ_c. Upon substitution, we obtain:

$$\alpha = \sqrt{2\pi}\left(\frac{\gamma}{\Delta\gamma}\right)^{\frac{1}{2}}\left(\frac{J_b}{\gamma I_o}\right)^{\frac{1}{2}}(\gamma^2/\gamma_T^2-1)^{\frac{1}{2}} \qquad (60)$$

Examination of eq. (60) supports the conjecture that $\alpha \geq = .1\text{cm.}^{-1}$ are attainable in cold to warm crossover region ($\lambda \backsimeq \lambda_c$).

II E. COMMENTS ON NONLINEAR BEHAVIOR

It would be possible at this point to develop a reasonably complete nonlinear theory for single-mode Cerenkov devices. This would, in part, follow lines of argument originally established to explain microwave tubes, beam plasma interactions, and more recently, free-electron lasers. In the wavelength regime which is of primary interest, however, the ratio L/λ is large and there will be, at the very least, a few axial modes within the half-width of the gain curve. There may also be a mixture of transverse modes, although if the device can be made to operate on a single transverse mode, it will be advantageous to do so. Relatively less is known about electron beam devices in the multimode region, and the development of a complete nonlinear theory, analogous to that developed by Lamb[24] for the gas laser, should take account of multimode operations. This would be a substantial undertaking. It could be productive, however, since we generally expect that Čerenkov devices will exhibit many phenomena intrinsic to all multimode oscillators, and that some of these may be useful in applications (e.g., mode locking). Hence, because the development would at this point omit some of the most interesting parts of the problem (on account of its length and because the motivation for experimental development rests primarily on the prediction of the linear gain which would be expected in specific wavelength regions) we will restrict discussion of nonlinear problems to a few simple scaling arguments.

II E. 1. Nonlinear Scaling Arguments

In the operating regime where the beam velocity distribution can be regarded as cold and the motion one-dimensional, the relative density modulation is given by:

$$\frac{\delta n}{n_o} = \frac{kv}{\omega - kv_o} \tag{61}$$

Now the change from electron orbits, which move progressively forward compared to the phase of the wave (untrapped) to orbits which are winding up (trapped), occurs in the vicinity of $|\delta n/n_o| \simeq 1$. Thus it occurs where

$$k\delta v \simeq |\omega - kv_o| \tag{62a}$$

or

$$k\delta v \simeq \omega_I \tag{62b}$$

This can be converted to a prediction of the magnitude of the axial component of the electric field at which saturation of the linear growth is in progress. We find from eq. (1) and eqs. (61a) and (61b):

$$|E_z| \simeq \frac{m\gamma^3}{e} \frac{\omega_I^2}{k} \tag{63}$$

The Poynting's flux, and hence also the total power carried to the wave, will be proportional to E_z^2 and thus up to ω_I^4. The latter will in turn be proportional to $(I/I_o)^{4/3}$.

Hence, up to form factors (which can vary between small numbers and unity) the overall power at the separatrix crossing value of E_z (eq. (62)) will be:

$$P_{wave} \sim \left(\frac{I}{I_o}\right)^{1/3} P_{beam} \qquad (64)$$

This is a conversion factor which can be expected in any traveling wave device. Enhanced conversion could be obtained by tapering the phase velocity and thus "deepening" the trapping well. Still more energy could be recovered if the beam were collected at high potential (depressed collector operation). An estimate of the overall efficiency obtainable from a Čerenkov device is thus a subtle and complex matter. In the final analysis, however, tube-like efficiencies of perhaps fifty percent could be attainable.

III. A. THE ELECTRON BEAM

The single most important component of an electron beam-driven radiation source is the beam itself. Its parameters will, in large part, determine the performance of the system. In order to examine the potential of Cerenkov sources in the millimeter and submillimeter parts of the spectrum, it will be useful to examine the parameters of some typical electron beam generators which may be used in this application.

A few general types of electron beam generators and their parameters are listed in Table 1. All of the beams are at least mildly relativistic; a choice is dictated by coupling considerations developed in earlier sections. However, the values of the beam current and the modes of operation vary widely. We will begin our discussion of the entries in the table by considering the role of the beam energy.

The beam energy helps to determine the operating wavelength in several interrelated ways: first, by synchronism; second, by the magnitude of the gap between the beam and the resonator, which must be present in any real system; and third, by its entry into the equations which determine the beam modulation. The first of these alone does not place any stringent limit on the attainable wavelength. This is

because the design of dielectric resonators which will support a wave of any reasonable phase velocity does not present a problem. The second and third aspects of the energy dependence will therefore be more important in setting the short wavelength limit to a device. The rate at which the electric field decreases as the distance from the resonator increases is given by $q = 2\pi/\lambda\beta\gamma$. The gain, however, increases with frequency and hence we would expect it to peak somewhere in the vicinity of $qa \backsimeq 1$, where a is a characteristic distance between the beam and resonator. A modest value for a would be approximately one millimeter, and a more difficult but attainable value would be about one-tenth of this. Taking this range and assuming $qa \backsimeq 1$, we can determine the limiting wavelength for good beam-to-resonator coupling. The range of this wavelength is shown in the table. Examination of the table and the figure will show that relatively compact machines could ultimately be expected to work well into the submillimeter region of the spectrum, while if one extends the range of beam generator complexity, operation in the infrared could be possible.

While the beam-to-resonator coupling decreases away from the resonator due to the fall-off of the electric field with distance, an arbitrary increase in beam energy will lower the minimum wavelength by a corresponding amount. However, the

beam energy also enters into consideration through the equations of motion for the electrons, and increasing γ furthers the difficulty of attaining good beam modulation. Hence, these two effects must be traded against each other. When the beam is strongly magnetized, the energy-dependence of the growth is approximately $\alpha \backsim \gamma^{-1}$, and when it is not magnetized, $\alpha \backsim \gamma^{-1/3}$. Since the criterion for strong magnetization becomes more difficult to meet as λ decreases, short wavelength operation will probably require unmagnetized, or at least weakly magnetized, electron beams.

The current available from the variety of generators listed in Table 1 also covers a wide range. When the beam is cold, the gain will scale as $(J_b/I_o)^{1/3}$, and thus a beam with 17_o A/cm^2 will make this parameter 0.1. We have seen earlier that if this is used with reasonable values of the other parameters, the gain will be in the .1 - .5 cm.$^{-1}$ range. The first and third entries in the table can probably achieve values in this vicinity, while the second and fourth entries could do so without question. The greater current available from the second and fourth type of generator might also make up for difficiencies in another parameter.

Field emission diode generators produce very large currents. Hence, they are in principle capable of producing a lot of gain. It was partly for this reason that a generator of this type was used in early experiments designed to demonstrate the utility of stimulated Čerenkov radiation. They also have the ability to produce beams

whose energy is sufficient to couple well into the sub-millimeter region. Their drawback for short wavlength operation may, ironically, be the fact that the current is large. This is because the self-fields, which have been neglected in our analysis of gain, may lead to larger $\Delta\gamma/\gamma$, and hence to a limit of the usable range of wavelength.

The accelerators listed in the table will also be capable of operating at current densities which give usable gain. The peak current will be low, but the focussing could be better. The current in a linear accelerator will also have a complicated time structure (the typical value of I is the peak in the micropulse), and this will complicate the gain calculations. If used, however, such a generator will be designed to work at short wavelengths and the microstructure may be a minor feature. Both this complication and the role of self-fields are worth further analysis.

The pulse length and peak power entries in the table are largely self-explanatory, although one consequence of the pulse versus continuous operation is worthy of comment. We will see below that when the Q of a cavity is reasonable, the current density required to initiate oscillation will be quite modest. Thus, systems with relatively low gain, α - 0.01 to 0.1, may be very usable as oscillators well into the infrared, whereas the same beam generator would not be a suitable source for an amplifier. Overall, it is to be expected that the pulsed beam generators, due primarily to

the larger current densities available, could be used as both oscillators and amplifiers while the steady-state generators would be largely restricted to application as oscillators.

In addition to its relation to the gain of the device, the current density plays a role in determining the wavelength of which the beam may no longer be regarded as "cold". Clearly, if all parameters other than current remain fixed, increasing the current decreases the wavelength for which the beam must be regarded as warm. The current density, the energy and the energy spread are not truly independent, but we will, for the purpose of discussion, treat them as though they were.

Restating the expression $k\Delta v = \omega_I/2$ in terms of the spatial gain, $\alpha(\text{cm.}^{-1})$, and a beam energy spread $\Delta\gamma$, we have for the wavelength at which the cold/warm transition occurs:

$$\lambda_c = \left(\frac{4\pi}{(\beta\gamma)^2}\right)\left(\frac{\Delta\gamma}{\beta\gamma}\right)\frac{1}{\alpha} \qquad (65)$$

It is clear that the beam generator in the lower energy end of the range considered must achieve relatively better energy collimation if it is to operate in the "cold" regime at any given wavelength. The lower energy, pulsed electrostatic devices with their larger currents can be expected to operate in this mode for wavelengths in the upper submillimeter- to one-millimeter range. As the beam energy rises,

Coherent output radiation has been obtained at wavelengths extending from about 1 centimeter to below 1.5 millimeters. The wavelength of the radiation depends upon the guide radius, the relative amount of dielectric and its dielectric constant, and the beam voltage. Configurations which should work in the fundamental mode over the 1 centimeter - 3 millimeter range have been studied, and reasonable agreement with the theory of Section II is found. The diameter of the copper guide which supports the quartz tube is approximately 1.5 centimeter, and tubes with 1-3 millimeter wall thicknesses have been used most recently. Thus output wavelengths which are less than the transverse dimension of the waveguide have already been obtained.

At the longer wavelengths, the frequency has been determined with the Fabry-Pérot interferometer, and some typical data illustrating the behavior is shown in Fig. 17. In Fig. 17a, a calibration trace made with a 35 hz Gunn diode source is displayed, and in Fig. 17b, experimental data with approximately the same wavelength is shown. The trace shown in Fig. 17b consists of many repetitions of the e-beam pulser, and it shows that the average spectral width, which is itself quite narrow (.1-1 percent), is primarily due to shot-to-shot reproducibility. The output of a single pulse is apparently very coherent. An interferometer for shorter wavelengths is under construction. The shorter wavelengths have been measured with cutoff filters.

The output is monitored by ordinary microwave diodes, either IN23's, IN26's, or IN53's, with the latter being used down to wavelengths below 1.5 millimeters. Attenuation levels of 30-60 db are required in order to insure that the output levels are below the burnout levels of the diodes. The absolute output power levels are not yet precisely determined except within an experimental uncertainty which becomes greater at shorter wavelengths and varies between .1 and 5 percent of the beam power. All of the factors which control this conversion efficiency are not yet well understood. The loaded Q of the resonator is modest, and the system is probably operating as a super-radiant oscillator. If this is so the previously-stated conversion efficiencies are plausible, but as is the case with the theory, nonlinear behavior of the experimental device is practically unexplored.

The experiment described above is in a relatively early stage of development. It does appear, though, that millimeter-submillimeter Čerenkov devices are a realistic possibility.

interest to make a detailed comparison of these two systems. We will conclude this section with a brief discussion of two possible configurations which might be used in the 1μ range. The first is shown in Fig. 18.

Shown in the figure is a thin dielectric guide with tapered ends. An electron beam passes over the guide and couples to the evanescent field. When the beam has a high enough energy, the coupling will be good. The tapered ends face mirrors which, together with the guide, form an optical resonator.

It might also be useful to taper the thickness of the guide near its ends. By doing this, the field energy in the guide can be increased at the expense of that stored above the guide. If the taper is adiabatic on the scale of k^{-1}, the dispersion relation will vary smoothly as will the field distribution. Shown in Fig. 19 are the results of one possible experimental configuration including a taper. As the guide thickens, the field distribution is pulled down into the guide and formed into a half-sinusoid. The latter form, which is closed to the normal mode distribution of a guide which is covered top and bottom, should give better control of the input-output coupling.

Another possible version of a short wavelength system is shown in Fig. 20. In this system, the output optics are placed below the beam. Incident radiation comes through the end face of the guide and normal to the face, but the angle formed with the top surface is greater than that required for total internal reflection. This guide is also

tapered. As it thins out, the field is pushed out to increase the coupling. It is then pulled in again and passed to a second mirror.

The two configurations just discussed are highly schematic. The beam-to-field coupling will be a straightforward matter, but the overall optical system may be quite complex. Self-reproducing patterns of the general type discussed should exist, however, and well-collimated relativistic beams, together with the resonator, could form the basis of far-infrared Čerenkov devices.

ACKNOWLEDGMENTS

This is a report of work in progress. It owes debts to those who have already contributed and to those who are currently engaged in the research. I would most especially thank Robert Layman for continuing to carry a major portion of the burden of the experimental work, of which only a small portion has been reported herein. In addition, Kenneth Busby and Kevin Felch have helped build the first apparatus and took the first measurements. John Bagger and Geoffrey Crew performed calculations during the early stages of the work. Portions of their senior theses appear in Section II. To be thanked also are John Branscum, John Golub, David Kapilow, James Murphy, David Speer, and Douglas Wise, who currently bear a major part of the responsibility for the experimental and theoretical program. Finally, thanks to Desiree Rastrom for research and administrative assistance.

Support for this work has been provided by Dartmouth College, by the Air Force Office of Scientific Research, by the Army Research Office, and by the Office of Naval Research.

REFERENCES

1. Cerenkov, P.A. (1934). Dokl. Akad. Nauk. SSSR 2,451.

2. Frank, I.M., and Tamm, I (1937). Dokl. Akad. Nauk. SSSR 14,109.

3. Heaviside, O. (1888). Phil. Mag. Feb. p.130, Mar. p.202, May. p.379, Oct. p.360, Nov. p.434, Dec. p.488.

4. Sommerfeld, A. (1904). Götting, Nachricht 99,363.

5. Curie, E. (1941). "Madame Curie." Heinemann, London.

6. Mallett, L. (1926). C.R. Acad. Sci. a) 183,274. b) 187,222. c) 188,445. Paris.

7. Jelly, J.V. (1958). "Čerenkov Radiation and its Applications." Pergamon, London.

8. Zrelov, Z.P. (1970). "Čerenkov Radiation in High Energy Physics." Israeli Program for Scientific Translations.

9. Bolotovski, B.M. (1961). Usp. Fiz. Nauk. 75,295. (1962) Soviet Physics Uspekhi 4,781.

10. Ginzburg, V.L. (1947). Dokl. Akad. Nauk. SSSR 3,253.

11. Coleman, P., and Enderby, C. (1960). J. Appl. Phys. 31, 1695.

12. Danos, M. (1953). J. Appl. Phys. 26,2.

13. Lashinsky, H. (1956). J. Appl. Phys. 27,631.

Figure 9: The basic slab guide geometry and axial field dependence.

Figure 10: The dispersion relation for the slab guide.

Figure 11: Gain curve shape vs. beam velocity for the beam-slab guide system.

Figure 12: Numerical values of dispersion (a) and spatial gain (b) vs. beam velocity for a .025 cm. thick quartz guide.

Figure 13: Geometry of slab guide/beam system when there is a finite gap between the beam and the guide.

Figure 14: The relative positions of the phase velocity and the beam velocity distribution function (F_β) when the beam is "cold" and when it is "warm".

Figure 15: Qualitative shape of the dispersion and gain in the "warm" beam limit.

Figure 16: The configuration of an experimental device designed to prodce mm-wavelength stimulated Čerenkov radiation. a) the device; b) typical voltage and radiation pulse.

Figure 17: Fabry-Perot interferometer output. a) calibration (35 Ghz source); b) stimulated Čerenkov radiation.

Figure 18: Slab guide resonator configuration for a possible far-infrared device.

Figure 19: The effect of tapering the slab guide thickness. a) the guide; b) the field distribution.

Figure 20: Another possible configuration for short wavelength operation.

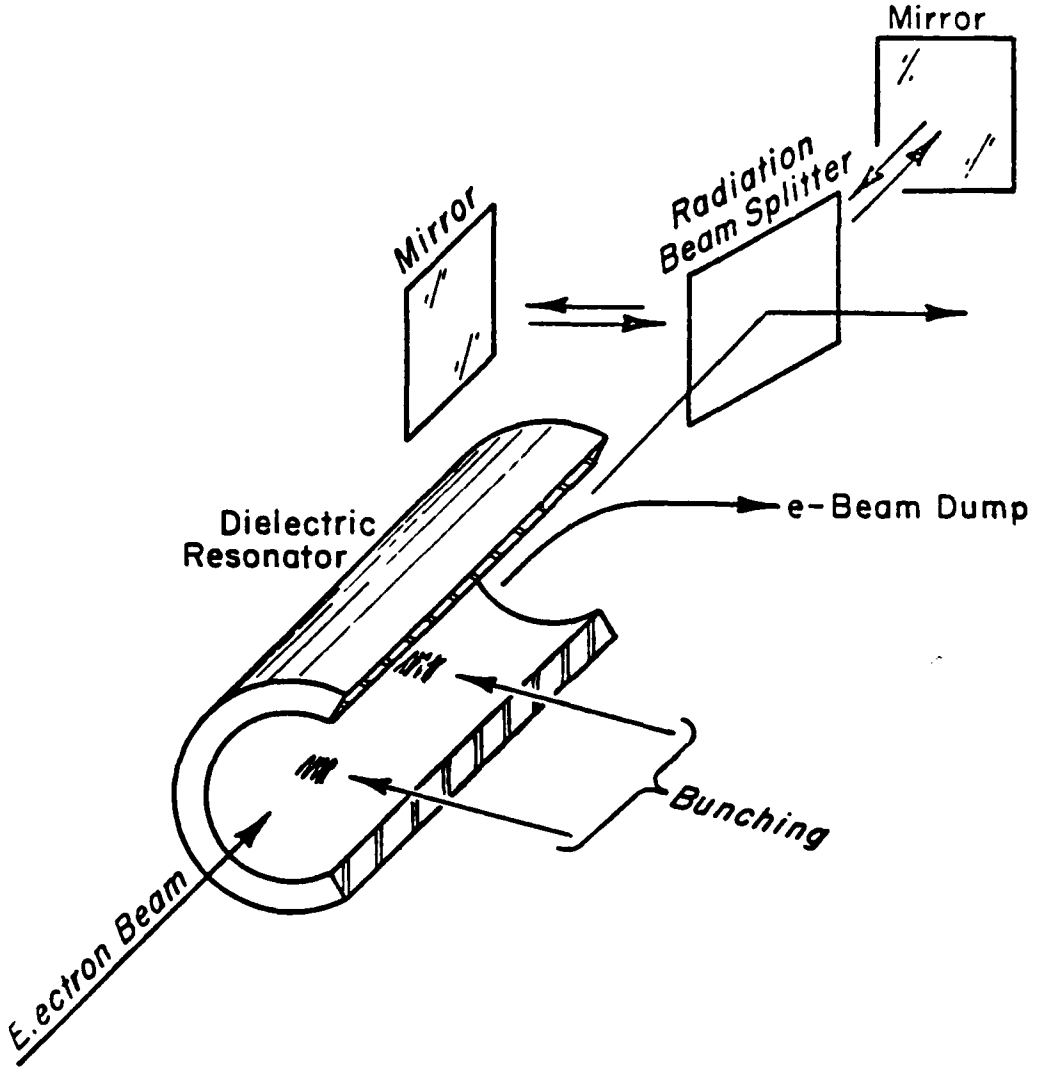

CERENKOV MASER

Figure 1.

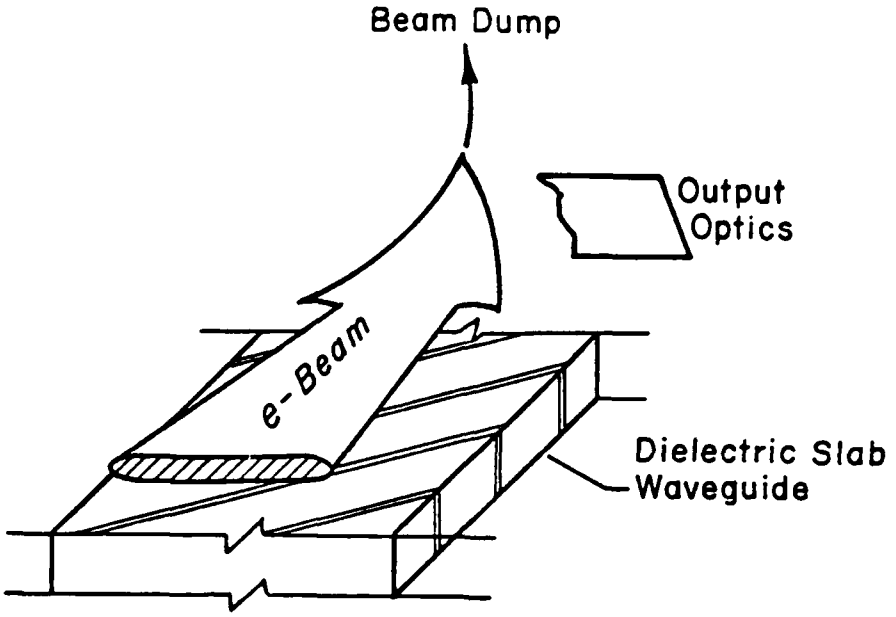
Beam Dump
Output
Optics
e-Beam
Dielectric Slab
Waveguide

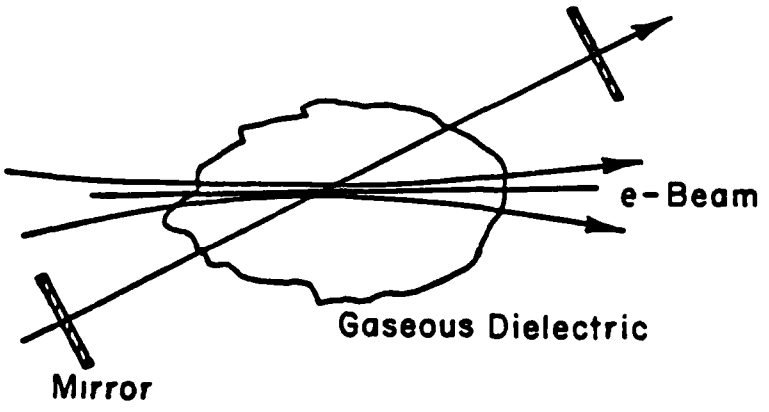
e-Beam
Gaseous Dielectric
Mirror

Figure 2. a), b)

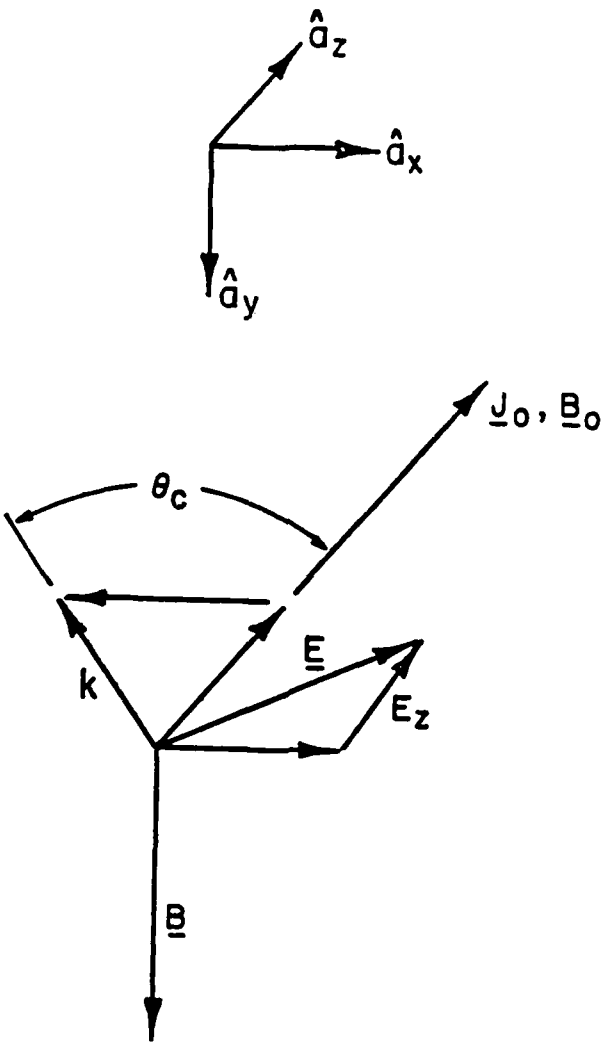
$\hat{a}_z$
$\hat{a}_x$
$\hat{a}_y$
$\underline{J}_o, \underline{B}_o$
θ_c
$\underline{E}$
E_z
k
$\underline{B}$

Figure 3.

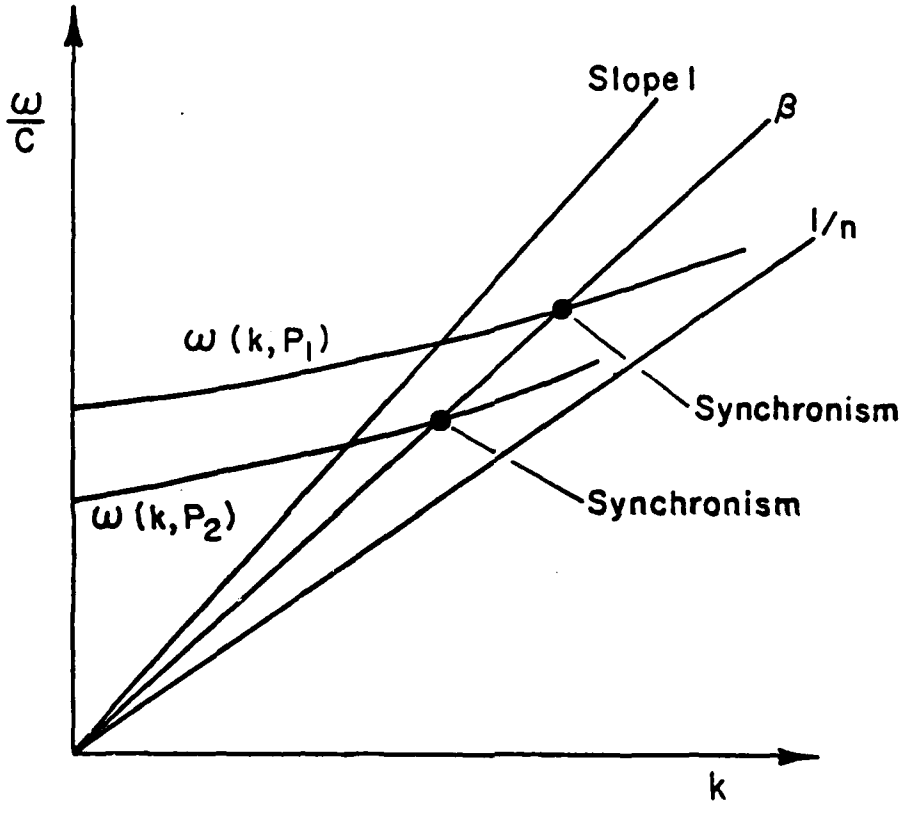

Figure 4.

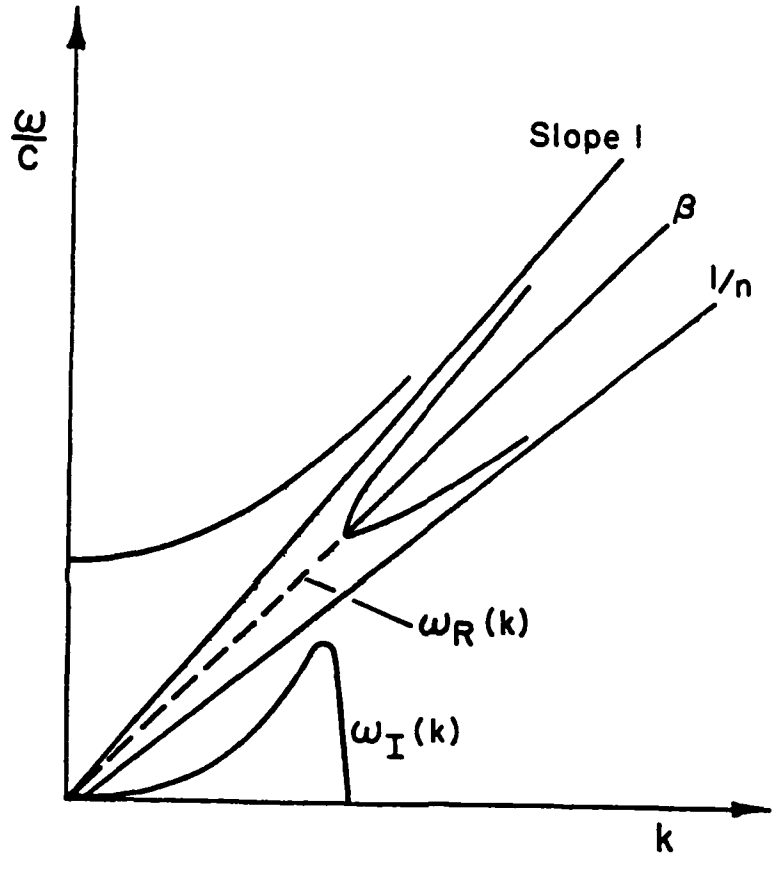

Figure 5.

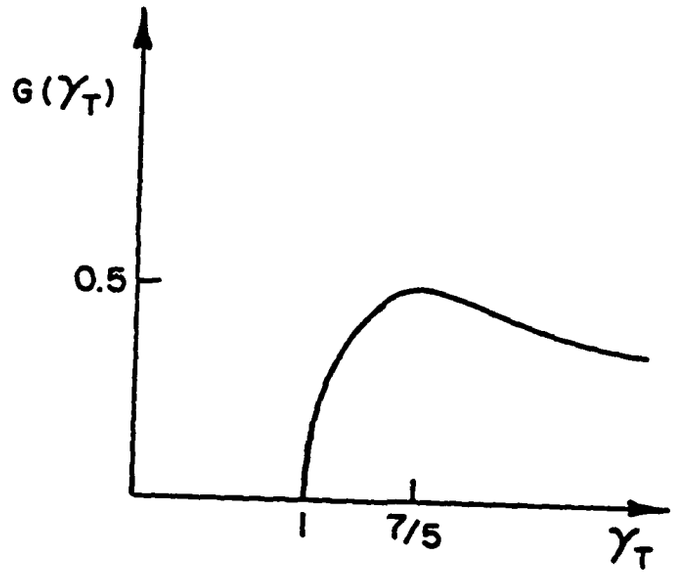

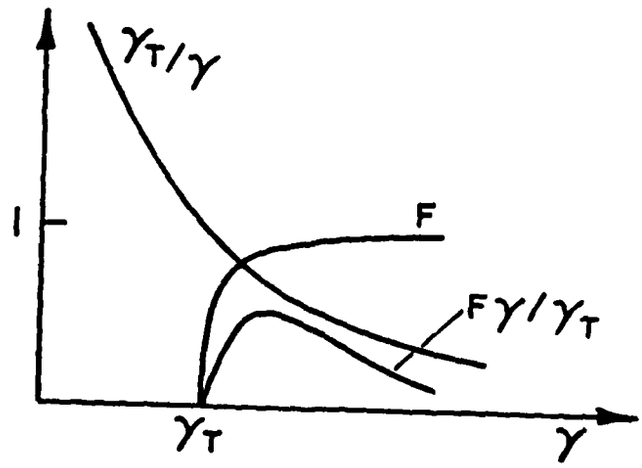

Figure 6. a), b).

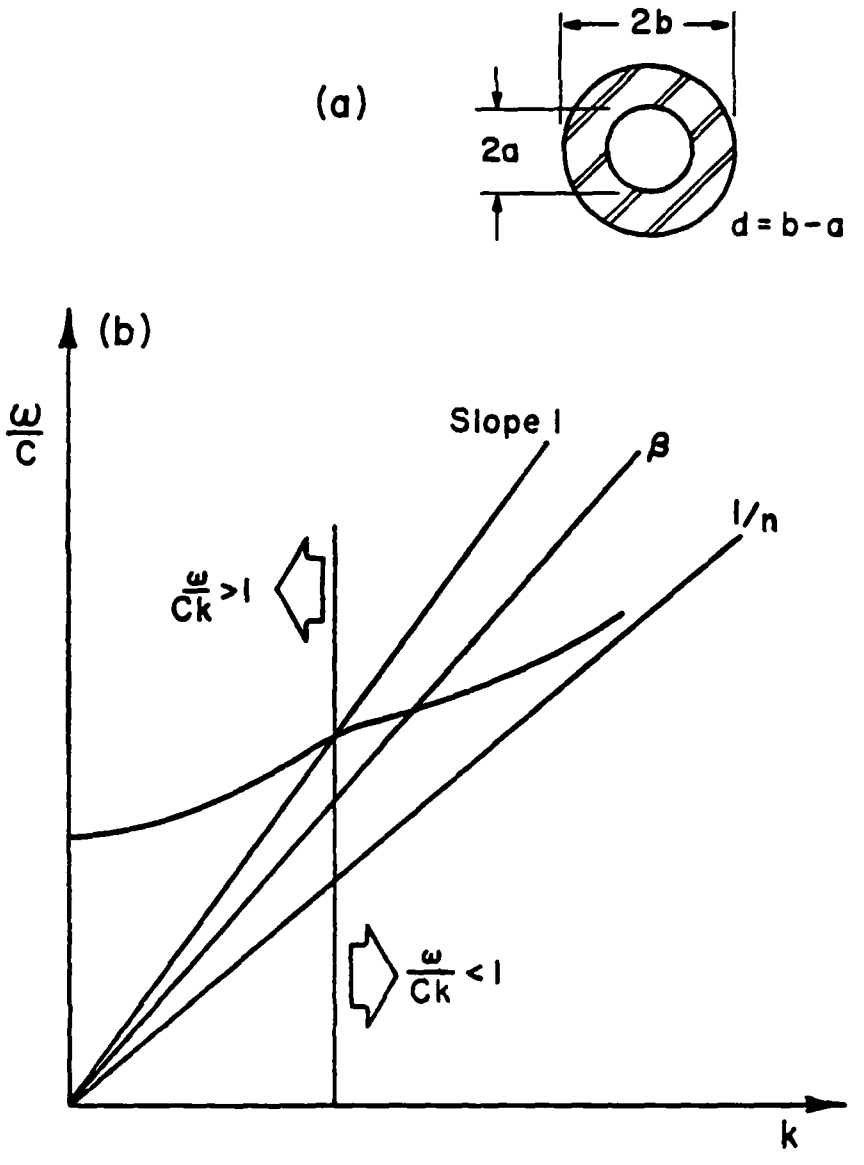

Figure 7.

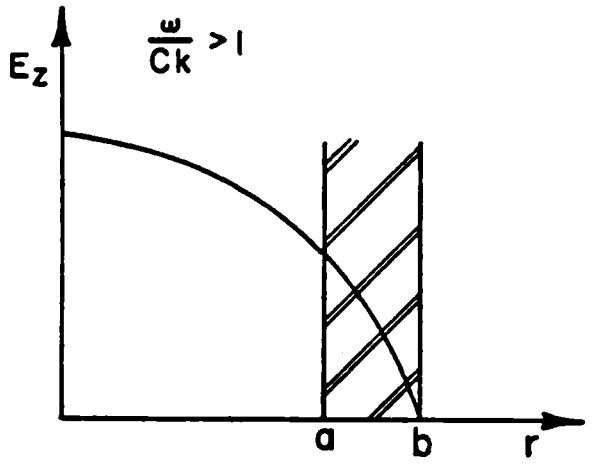

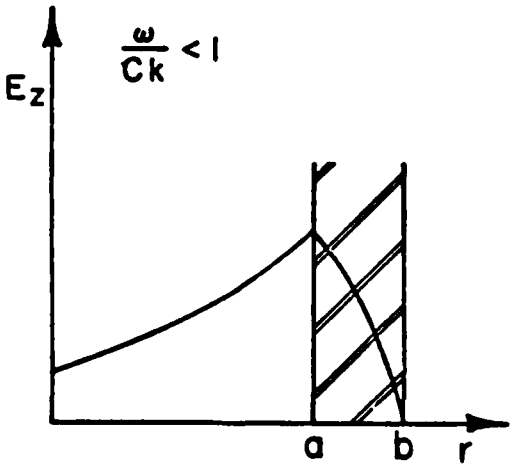

Figure 8. a), b).

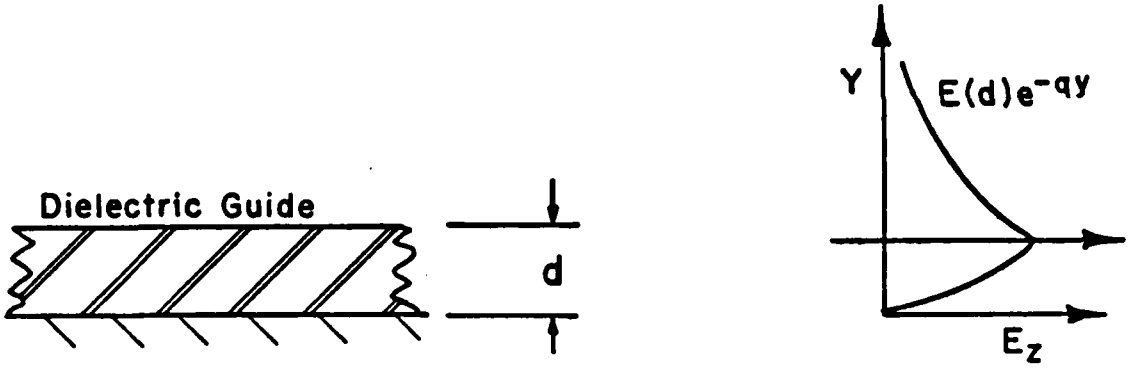

Figure 9.

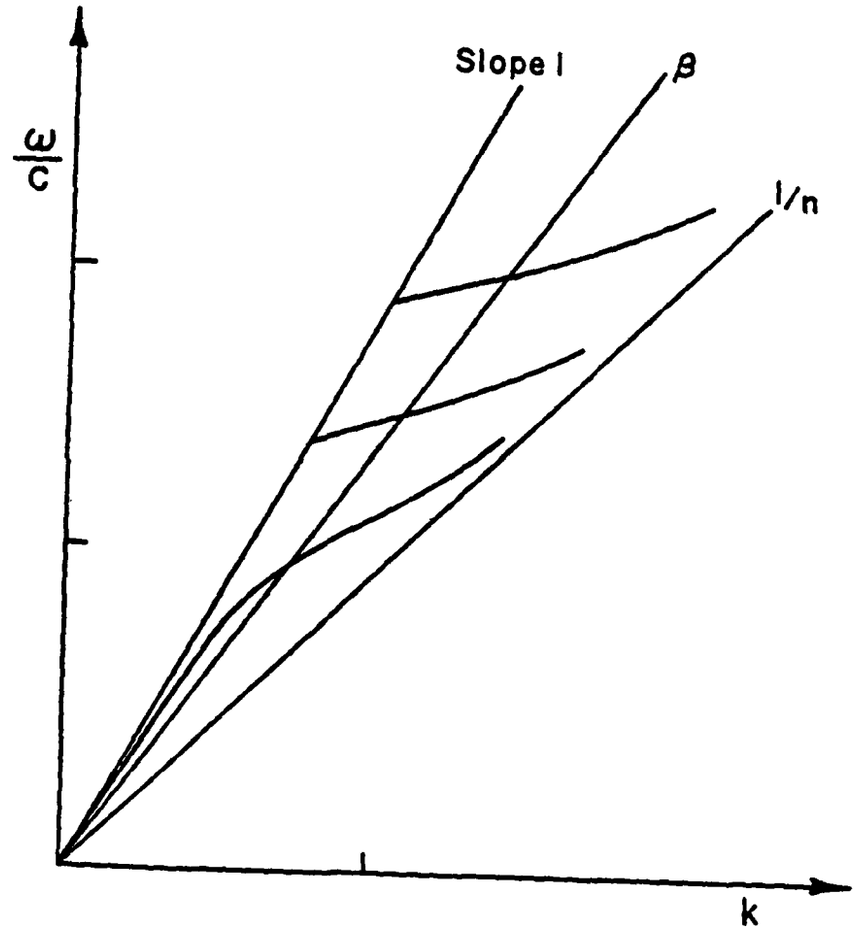

Figure 10.

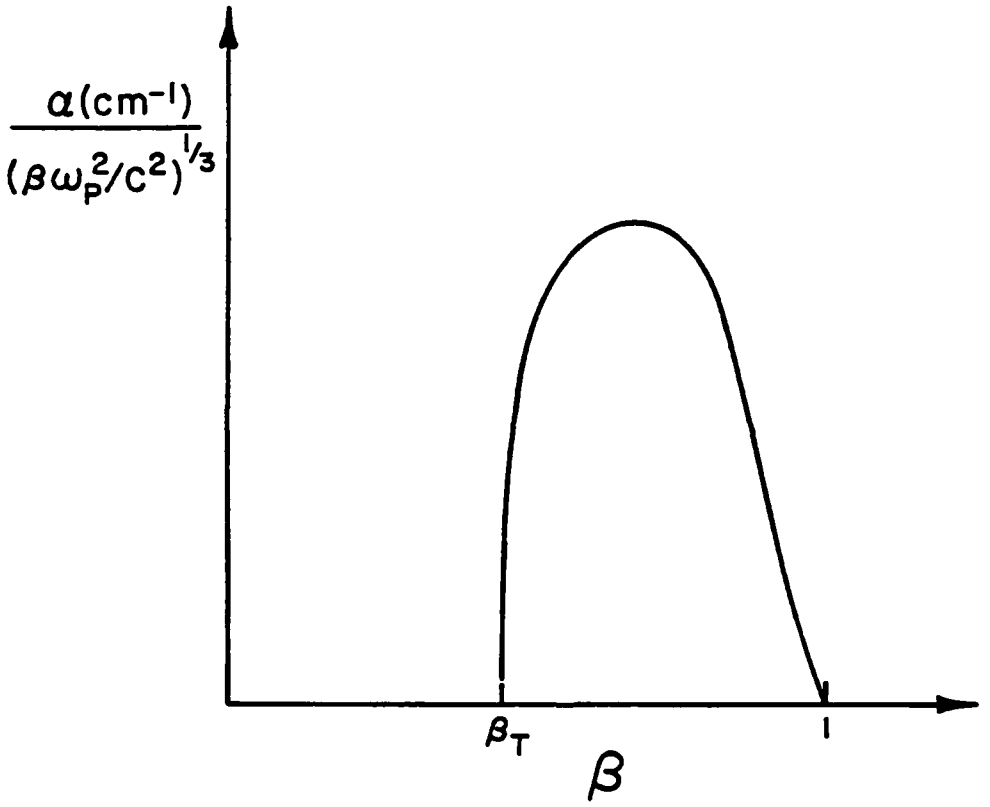

Figure 11.

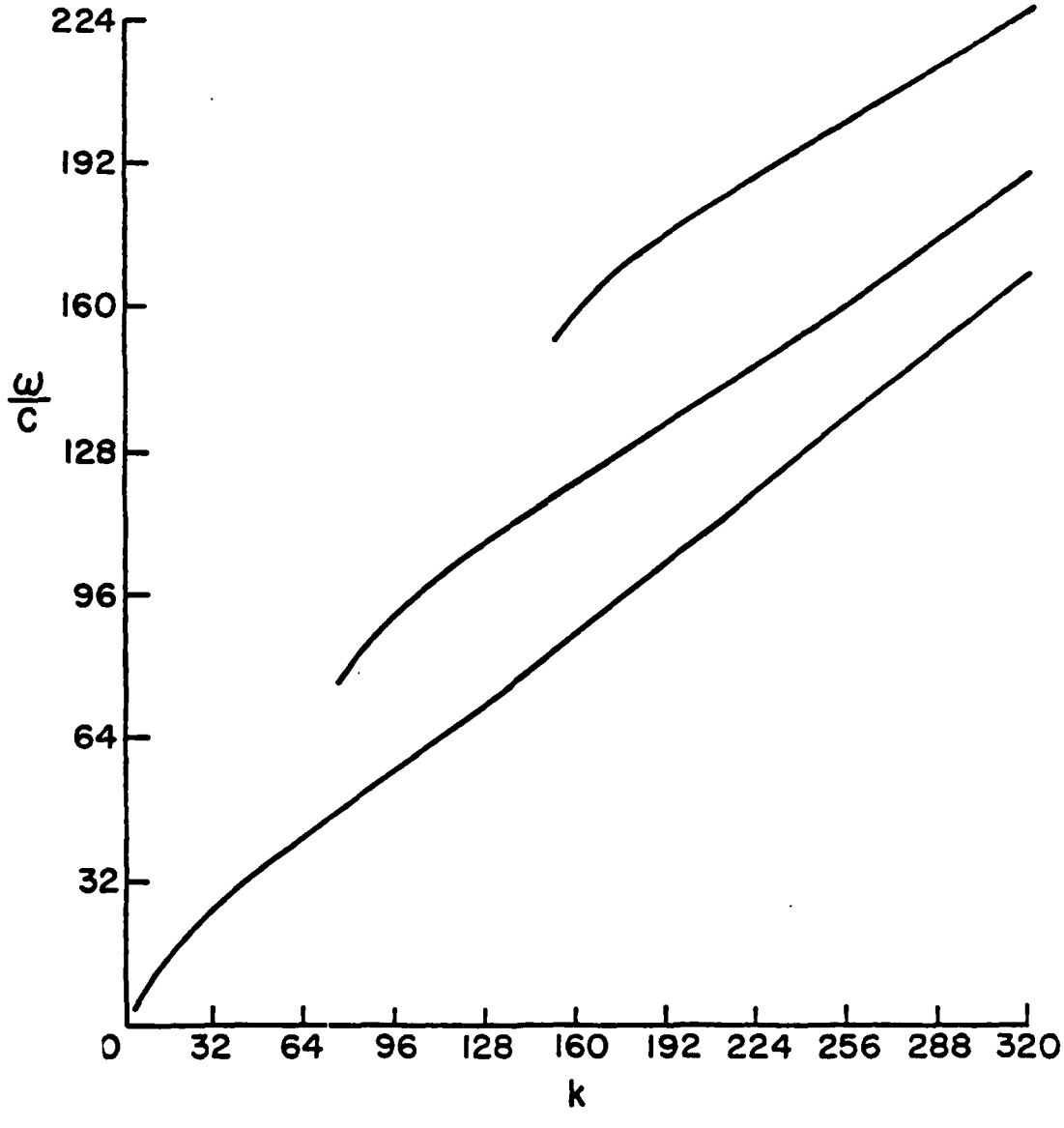

Figure 12. a)

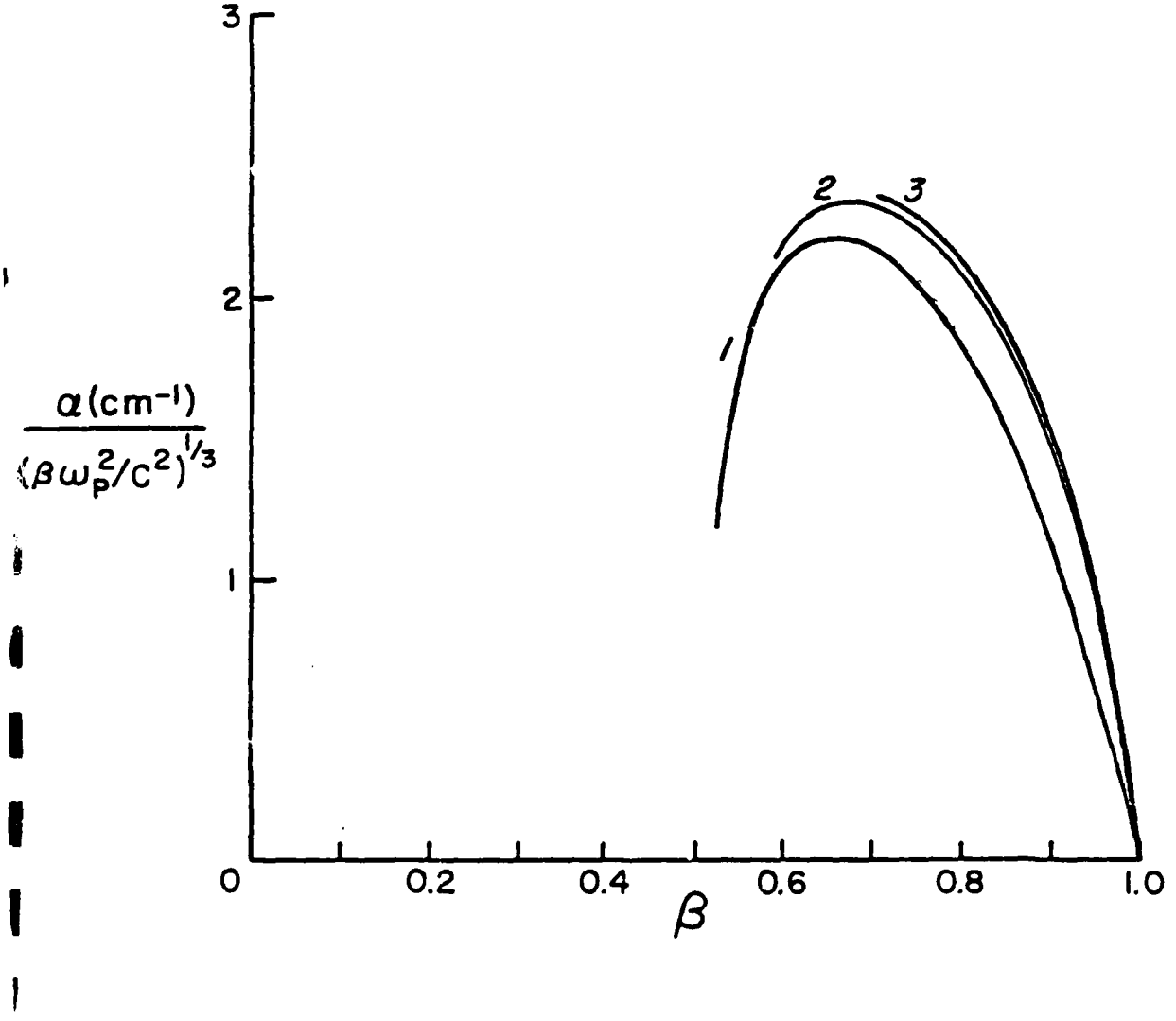

Figure 12. b)

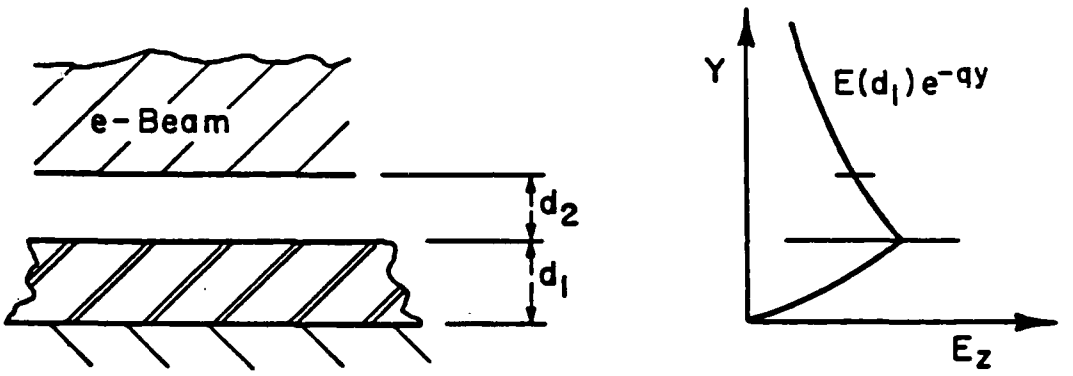

Figure 13.

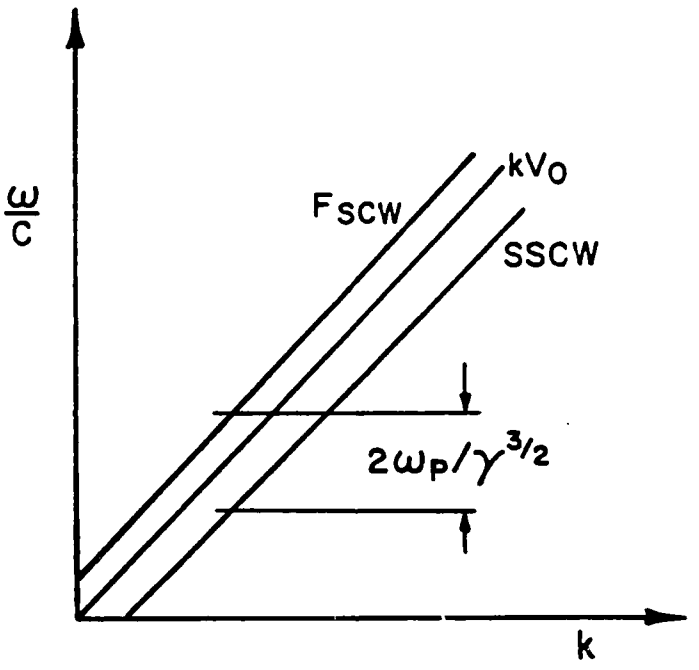

Figure 14. a)

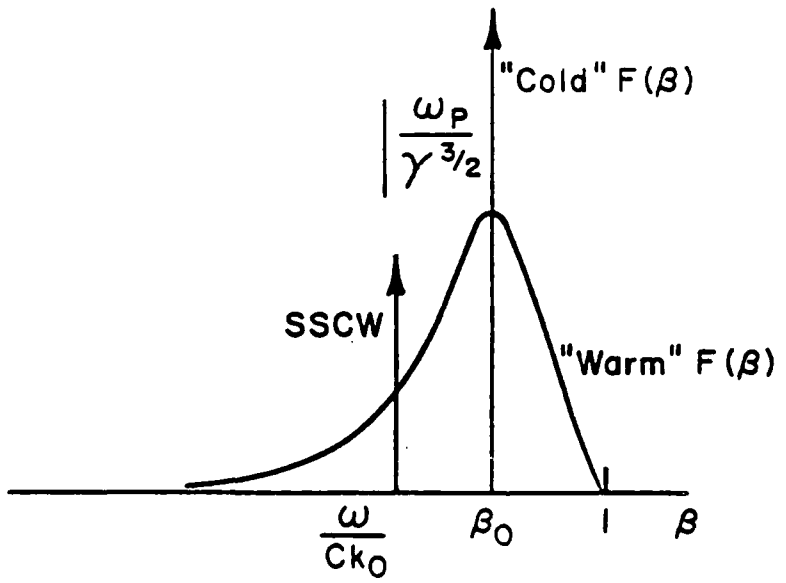

Figure 14. b)

AD-A136 473 STIMULATED CERENKOV-RAMAN SCATTERING(U) DARTMOUTH COLL HANOVER N H DEPT OF PHYSICS AND ASTRONOMY J E WALSH 14 DEC 83 N00014-79-C-0760 2/2

UNCLASSIFIED F/G 20/8 NL

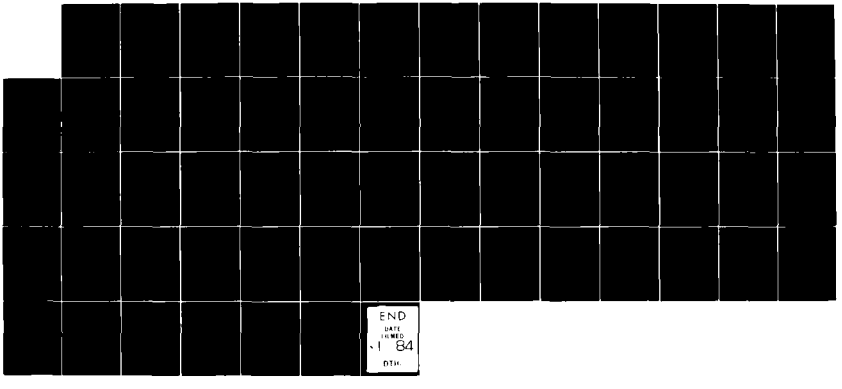

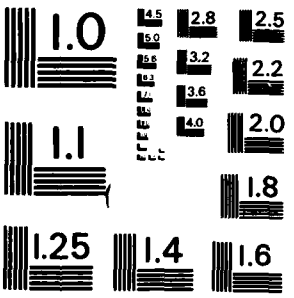

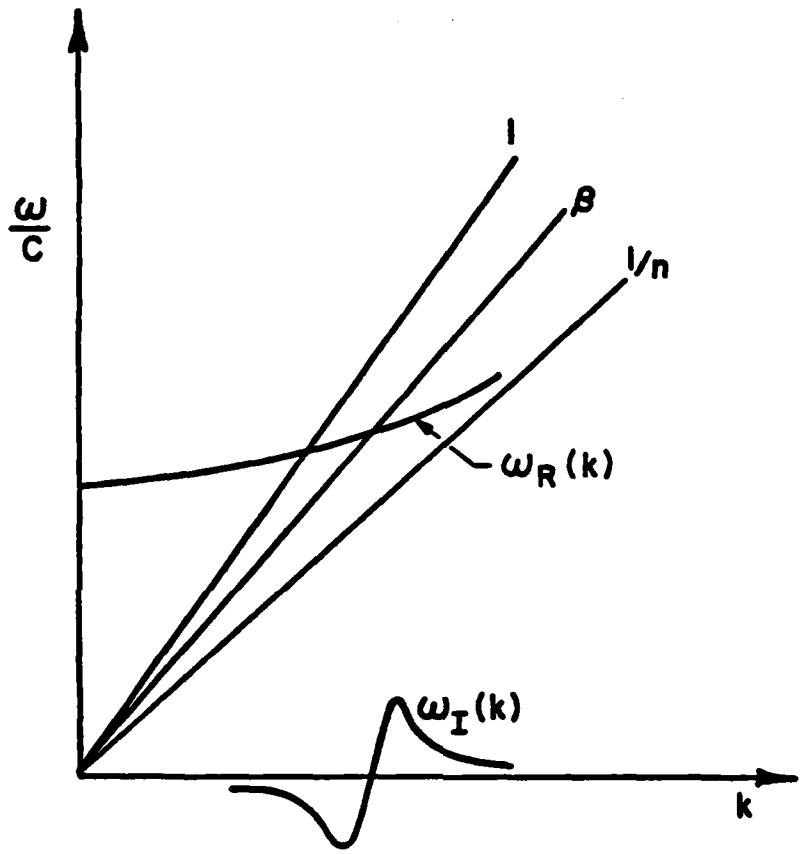

Figure 15.

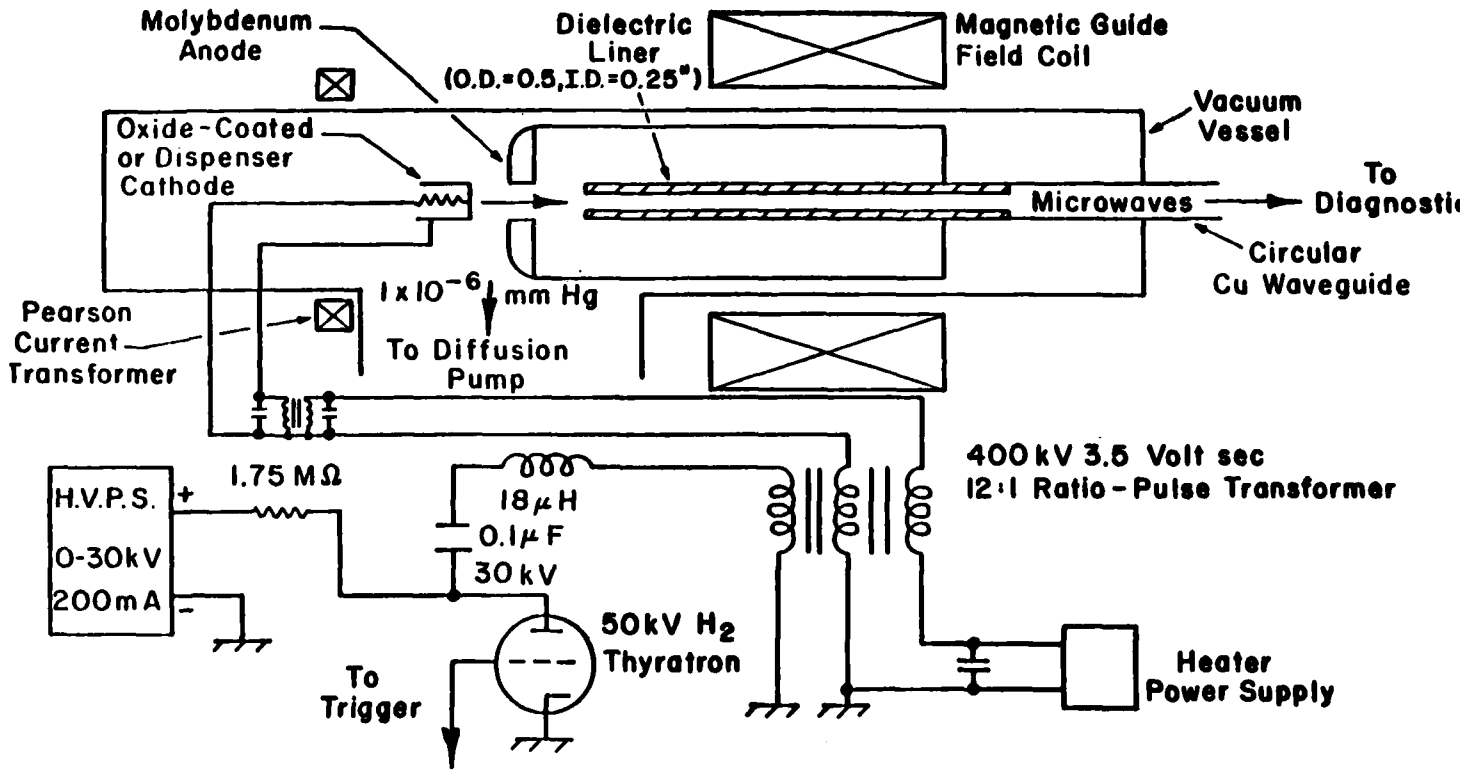
Molybdenum Anode
Dielectric Liner (O.D.=0.5, I.D.=0.25")
Magnetic Guide Field Coil
Vacuum Vessel
Oxide-Coated or Dispenser Cathode
Microwaves
To Diagnostic
Circular Cu Waveguide
1 x 10⁻⁶ mm Hg
To Diffusion Pump
Pearson Current Transformer
400 kV 3.5 Volt sec 12:1 Ratio - Pulse Transformer
H.V.P.S. 0-30kV 200mA
1.75 MΩ
18 μH
0.1 μF
30 kV
50kV H₂ Thyratron
To Trigger
Heater Power Supply

Figure 16. a)

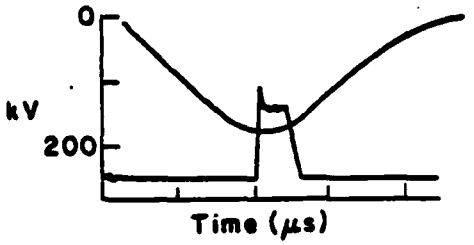

Figure 16. b)

T555 – .2V/cm
k155μV Meter – 100mV Range
15 x 18 Mesh
1N53 Detector

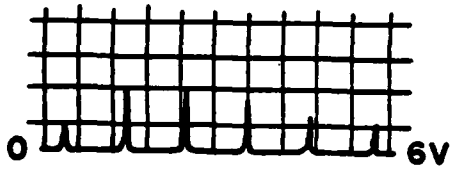

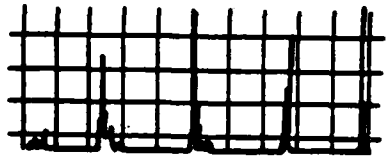

0720 30 Aug. 80
35 GHz
.65" S/S DX
1.46" E-S DX
1.38" D-S DX

#5
22 Aug.

#7

Figure 17.

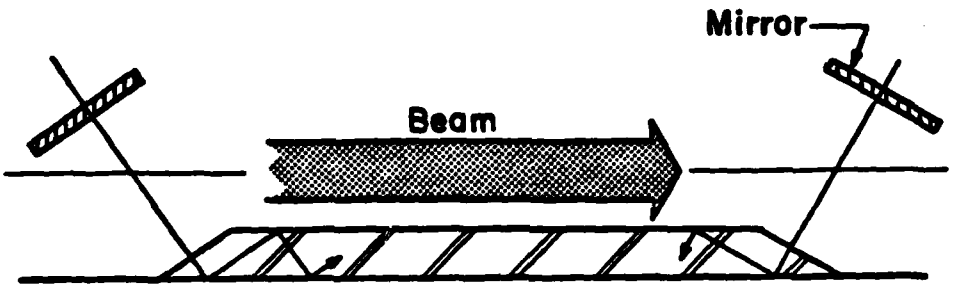

Figure 18.

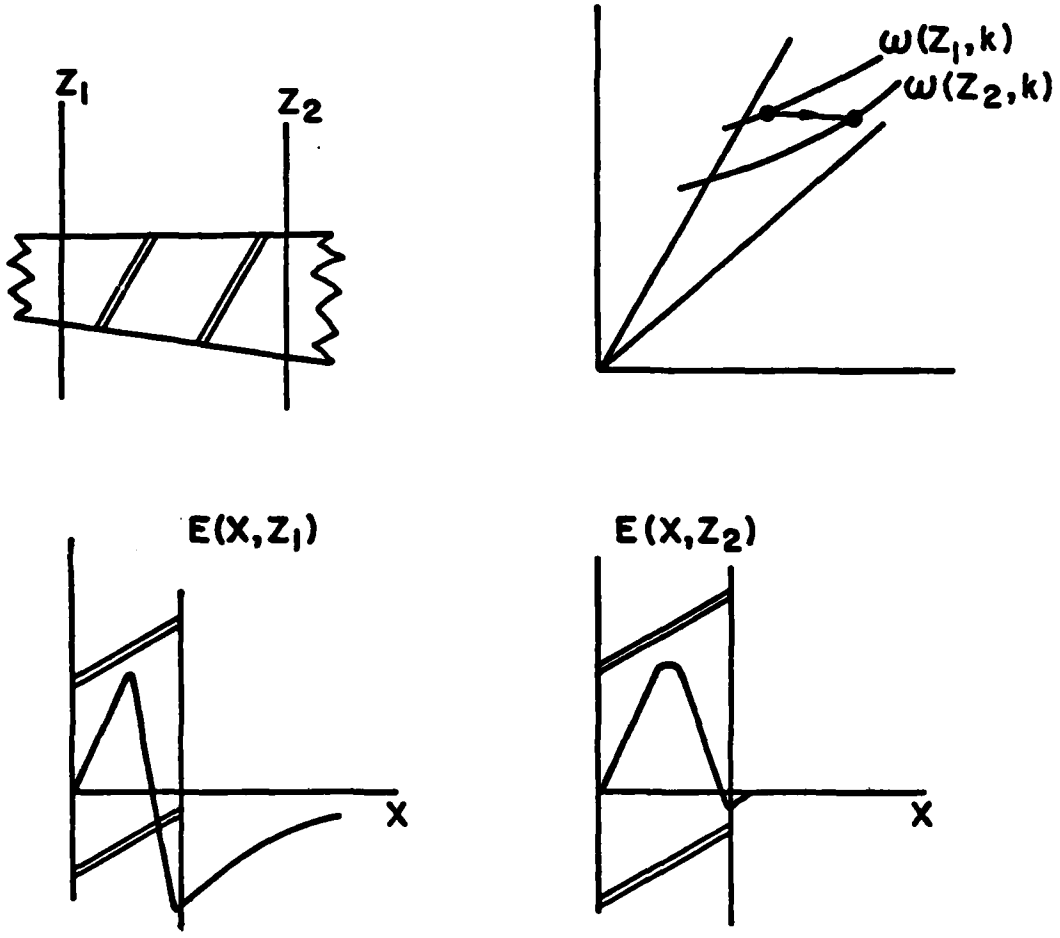

Figure 19.

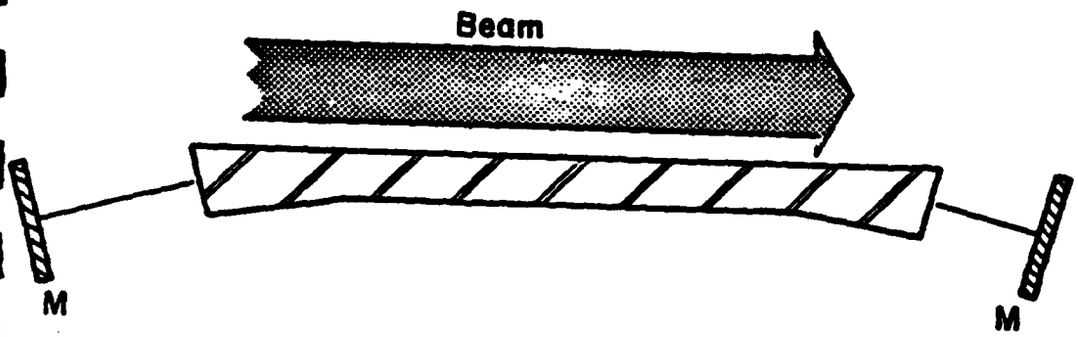

Figure 20.

CERENKOV AND CERENKOV-RAMAN RADIATION SOURCES

JOHN E. WALSH

INTRODUCTION

Cerenkov radiation[1] takes its name from P.A. Cerenkov whose pioneering experimental research clearly established the nature of the electromagnetic radiation produced by a charged particle when it moves with superluminal velocity in a dielectric medium. The electron sources used by Cerenkov were weak and thus he studied the radiation produced by single particles (spontaneous emission). The analysis of Frank and Tamm[2] also applied to the single electron case. We will be concerned in this paper with a tutorial discussion of practical radiation sources which make use of the Cerenkov process and hence we will be interested in stimulated as well as spontaneous Cerenkov emission. The former one of these is like the latter a potential source of short wavelength radiation. Cerenkov's original experiments were in the visible range of

the spectrum and more recently it has been demonstrated that a highly relativistic electron beam-noble gas combination is a bright incoherent source of radiation in the vacuum ultraviolet region[3]. In other experiments mm wavelength Cerenkov radiation has been obtained[4,5,6]. It is of interest therefore, to consider the possibility of constructing Cerenkov lasers over the entire range of the electromagnetic spectrum for which suitable dispersive materials can be found.

Cerenkov radiation can be thought of as a decay process in which an electron moving through a dielectric emits a photon and drops to a lower energy state. We will also be interested in a related process where an electron either scatters an incoming photon or emits two photons. Unlike Cerenkov radiation which has no vacuum counterpart the first of these is analogous to Compton scattering. The dynamics of the scattering are, however, both complicated and enriched by the presence of the dielectric. In a Cerenkov oscillator or amplifier the single electron is replaced by a beam whose intensity is sufficient to cause stimulated emission. A related device in which an electron beam in a dielectric interacts with an incident photon beam, can be imagined. If the electron beam is intense enough to support collective plasma oscillations the incident photons scatter off of these and the device would be called a Cerenkov-Raman laser or maser. As the wavelength of the scattered photon is decreased the electron beam loses its collective nature and the scattering becomes a single particle process. Stimulated scattering still occurs in this limit, however, and devices operating in this range are designated Cerenkov-Compton radiation sources. The

definition of the division between Cerenkov-Raman and Cerenkov-Compton devices adopted here is consistent with that used for devices[7] operated without a dielectric.

As is the case with straight Cerenkov sources, Cerenkov-Raman or Compton devices are in principle capable of working at wavelengths as short as the visible or vuv regions of the spectrum . At the present time, however, practical devices have been operated in the mm range[8]. A primary purpose of these tutorial notes is to explore in some detail the criteria which must be met if short wavelength operation is to be achieved.

The notion that superluminal velocity charged particles could be used as a radiation source is quite old. Heaviside[9] in 1889 and Sommerfield[10] again in 1904 solved for the electromagnetic fields produced by a charged particle moving with greater than light velocity. Both of these analyses preceded special relativity and assumed that it was possible for a particle to have a velocity greater than that of light in a vacuum. If, however, the velocity of light c is replaced by c over the index of refraction n, their solutions are consistent with the work of Frank and Tamm[2]. There are also some scattered observations of Cerenkov radiation. M. Curie[11] in 1911 deduced that one component of radiation produced in the walls of a glass container containing radioactive materical was due to the presence of high speed electrons, and Mallett[12] in 1926 performed several related experiments. Taken as a whole, however, none of the early work was sufficiently complete or correct to jeopordize the position of Cerenkov and of Frank and Tamm as the founders of the subject of Cerenkov radiation.

Following this original[1,2] work a very large number of papers devoted to the subject have been written. A review article by Bolotovskii[13] contains over four hundred references. Much of the emphasis in this work was on the application of Cerenkov radiation to the production of useful radiation sources in the millimeter, the submillimeter and the far infrared regions of the electromagnetic spectrum. Almost every concievable electron beam dielectric structure combination has been analyzed.

It is, of course, not practical to propagate an electron beam through a solid dielectric and hence particular importance is attached to the radiation produced by electrons moving along the axis of a channel in a dielectric. Ginzburg[14], analyzed a number of these problems in detail. He found that in addition to the fact that spontaneous Cerenkov emission is relatively weak in all regions of the spectrum below the visible[15], there is not surprisingly also a relation between the size of the channel and the wavelength of the radiation produced. One method of circumventing the relative weakness of the process at longer wavelengths is to bunch the electrons. If the scale[16] length of the bunch is small compared to the wavelength the radiation intensity is increased by the square of the number of electrons in the bunch. A number of experiments using this technique were performed. Notable amoung these were the experiments of Coleman[4] and of Lashinksy[5]. In all of the analyses and experiments mentioned the electron beam intensity and dielectric resonator designs were such that stimulated emission was not a factor.

Most, although not all of the early work was devoted to straight Cerenkov radiation. The problem of the

radiation produced by an oscillator moving through a dielectric was, however, analyzed by Frank[17] and a later analysis of this and similar problems with emphasis on its use as a radiation source was performed by Ginzburg[18]. In the latter work expressions for the power radiated by both sub and superluminal oscillators were given. More recently in a series of publications Schneider and Spitzer[19] have analyzed the problem of photon-electron scattering in a dielectric medium. All of these analyses were devoted to single particle spontaneous emission processes.

The efficient production of stimulated Cerenkov or stimulated Cerenkov-Raman radiation requires electron beam densities and velocities which are in excess of those required by conventional microwave tubes. This is the primary reason why these mechanisms have not yet been used in practical radiation sources. However, the need for high power coherent sources in the shorter part of the millimeter range and for high or moderate power tuneable coherent sources in the submillimeter and far infrared regions of the spectrum has led to some acceptance of electron beams with parameters which are more than adequate for the production of stimulated Cerenkov radiation. An intense electron beam has been used to produce megawatt levels of radiation[20] and an electron beam generator similar to that used in high power klystrons has been used to produce both stimulated Cerenkov[6] and stimulated Cerenkov-Raman[8] radiation. The details of these experiments will be discussed elsewhere[22]. The remaining sections of these notes will be devoted to exploring the fundamental principles of device operation.

KINEMATIC CONSTRAINTS ON CERENKOV AND
CERENKOV-COMPTON SCATTERING

A number of useful conclusons can be drawn from an analysis of the constraints which energy and momentum

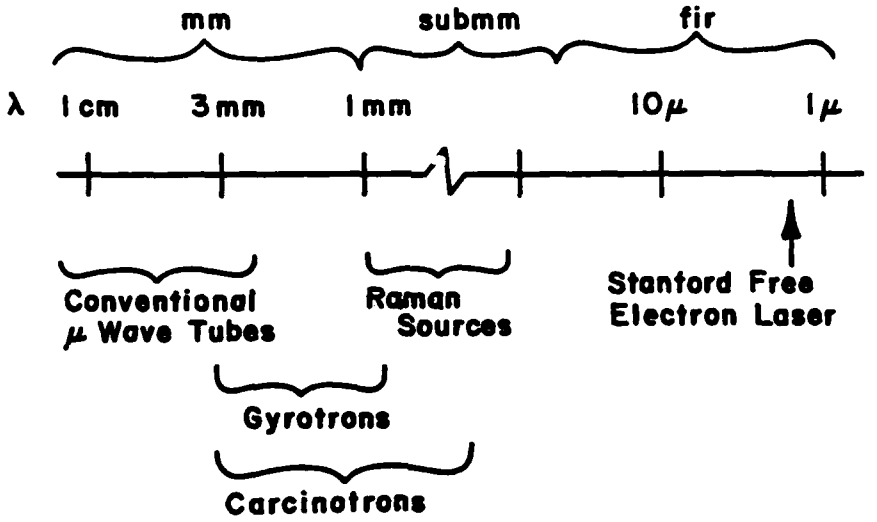

Fig. 1. Free electron radiation sources.

conservation impose on Cerenkov and Cerenkov-Compton scattering. In order to see why this is so we consider the diagramatic representation of a section of the electromagnetic spectrum shown in Fig. 1. On the left we have conventional microwave tubes. These were developed during an earlier effort to overcome the difficulties encountered when attempts were made to develop radiation sources in the cm wavelength range. They are all characterized by the fact that at least one critical dimension, ℓ, is of the order of the operating wavelength λ_o.

If an attempt is made to simply extend the successful microwave devices down in wavelength a number of fundamental difficulties[23,24] become apparent. The quality factor, Q, of any (closed) resonator drops as $\lambda^{1/2}$ and furthermore as the resonator volume decreases power density increases and heat dissipation becomes a severe practical problem. Furthermore, if we choose $\ell >> \lambda_o$ the resonator Q must rise at least as fast as $(\ell/\lambda_o)^3$ if the modes are to be resolved. In two and one dimensional resonators this restriction becomes $(\ell/\lambda_o)^2$ and (ℓ/λ_o) respectively. Thus open resonators will be an advantage if we require $\lambda_o << \ell$. Clearly however, something other than resonator geometry alone must determine the operating wavelength λ_o for an electron beam device if it is to operate at λ_o much less than say one mm.

In a conventional laser λ_o is, of course, set by atomic or molecular structure. For the short wavelength free electron sources mentioned on Fig. 1 several different techniques are used to fix the wavelength. The Stanford[25] free electron laser and the stimulated Raman scattering experiments performed at the Naval Research Laboratory[26] and at Columbia University[27] use the relativistic doppler shift. Hence λ_o in those experiments is set by the wavelength of an incoming (pump) source (a static rippled or helical magnetic field with wavelength λ_p) and the beam energy. This is a good technique since it does not rely on resonator geometry but suffers from the disadvantage that λ_o goes down approximately as the inverse of the electron beam energy squared and short λ_o operation requires large beam energies. In the gyrotron, wavelength is determined by the cyclotron resonance. These are prime candidates for mm wavelength

tubes but operation at wavelengths below one mm requires very large magnetic fields. The carcinotron is essentially a backward wave oscillator. The wavelength in these is set by geometry and because of this carcinotrons are probably the ultimate straightforward[28] extension of microwave tubes.

ENERGY-MOMENTUM CONSERVATION FOR CERENKOV SCATTERING. By considering the kinematics of Cerenkov radiation we will be able to determine the extent to which this mechanism can determine a value for λ_o which is much less than ℓ. A quantum view of the radiation process is shown schematically in Fig. 2a. Applying the laws of conservation of energy and momentum and subsequently eliminating the momentum we obtain:

$$\hbar\omega\,[\hbar\omega(n^2-1) + E_o(\beta_o n\cos\theta_c - 1)] = 0 \qquad (1)$$

where,

$$\beta_o = v_o c$$

is the initial electron velocity measured in units of the light velocity and E_o the electron energy is in the conventional notation:

$$E_o = \gamma_o mc^2 \qquad (2a)$$

$$\gamma_o = 1/(1-\beta_o^2)^{1/2} \qquad (2b)$$

The index of refraction, $n(\omega)$, may depend upon frequency. If $\beta_o n < 1$ the only solution of Eq. (1) is $\omega = 0$. When the beam velocity exceeds the Cerenkov threshold, $\beta_o n = 1$, however, the Cerenkov decay process is allowed and we find:

$$\cos\theta_c = 1/\beta_o n + \hbar\omega(n^2-1)/E_o \qquad (3)$$

The second term on the right hand side of Eq. 3 is very small at any possible ω and hence in regions where n is frequency independent the emission threshold is also frequency independent. In the absence of dispersion we will

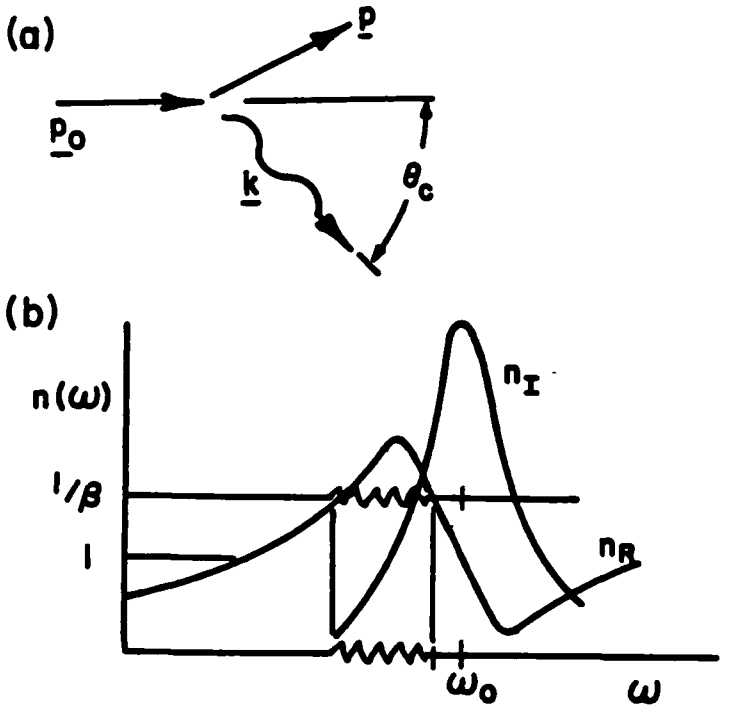

Fig. 2. a). Cerenkov scattering. b). Emission for $\beta n_R > 1$.

also find that the emission spectrum varies slowly with frequency. One method whereby the emission spectrum can be narrowed depends upon the rise in index of refraction near an absorption line. This is illustrated in Fig. 2b. The fact that the emission is near an absorption line means of

course that a good deal of the emitted radiation can be reabsorbed. It is a technique which has been used in particle counting applications[29] and in producing bright incoherent vuv radiation[3]. Furthermore, elementary calculations indicate that strong stimulated emission can be obtained in the vuv from an electron beam noble gas combination[30]. There is as yet no experimental verification of this latter prediction, a fact which is due in part to the great practical difficulties.

CERENKOV SCATTERING IN BOUNDED MEDIA. There are highly transparent solid materials available over much of the spectrum shown in Fig. 1. These can be configured in a wide variety of electron beam dielectric resonator combinations. Some of these have been tested experimentally[20,21] and found to work. Since they also show promise of working in the middle of the spectral range shown in Fig. 1 where moderate and high power sources are not now available, we will concentrate much of our discussion on this approach. Shown in Fig. 3 is a sketch of a dielectric tube waveguide and the dispersion curve for a TM guide mode. This mode is chosen in order to conform to the symmetry of the classical picture of Cerenkov radiation in an infinite dielectric which is that of a wake of radiation propagating at cone angle θ_c.

A detailed analysis of this problem is straightforward but quite complicated in detail. Fortunately, however, it is possible to deduce the most important conclusions with the aid of simple qualitative arguments. First we see that if $\beta n > 1$ there will be a coupling between an electron moving along the axis of the tube and the guide mode. Furthermore, due to the fact that

there is a unique relation between ω and k the Cerenkov emission will occur at a discrete frequency given by:

$$\omega = c\, k\, \beta \tag{4}$$

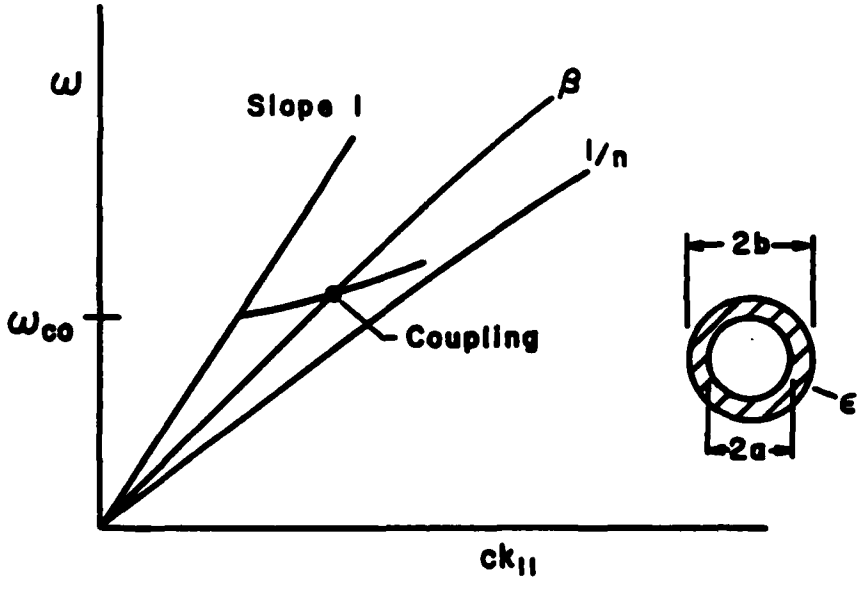

Fig. 3. Dispersion and coupling in a dielectric resonator.

Provided the guide modes are resolved with respect to transverse wave number, a series of lines, one for each mode, will be produced. As the emission occurs one can imagine the electron moving along the dispersion curve toward higher ω and k until the coupling is so reduced that emission no longer occurs. Treatment of the coupling is not

a purely kinematic process and hence it will be deferred until a later section.

Another important conclusion can be reached with the aid of Fig. 3. The cutoff frequency (ω_{co}) will depend inversely upon the wall thickness d and the square of the index of refraction of the material ($n^2 = \varepsilon$). Hence:

$$\omega_{co} = 1/d(\varepsilon-1)^{\frac{1}{2}} \tag{5}$$

and in general,

$$\omega \simeq 1/d(\beta^2\varepsilon-1)^{\frac{1}{2}} \tag{6}$$

The frequency at which the interaction occurs can be controlled both by d and by $\beta^2\varepsilon$. Thus insofar as kinematic constraints are concerned we have achieved conditions such that λ, the wavelength of the frequency produced can be much less than the characteristic dimension 2a. Furthermore, by judiciously combining the use of d and $\beta^2\varepsilon$ some control over the separation of different transverse modes can be obtained. Before the choice of all parameters is made, however, the coupling must be investigated.

CERENKOV-COMPTON SCATTERING. Shown in Fig. 4 are sketches of two possible Cerenkov-Compton (electron photon scattering in a dielectric) scattering processes. In the first of these, Fig. 4a, $\beta_o < 1/n$ and the event is analogous to ordinary Compton scattering in that an incident photon k_p (for pump) scatters off an electron which drops to a lower energy as it emits a photon k_s. There is, however, a very important difference. Application of the laws of energy

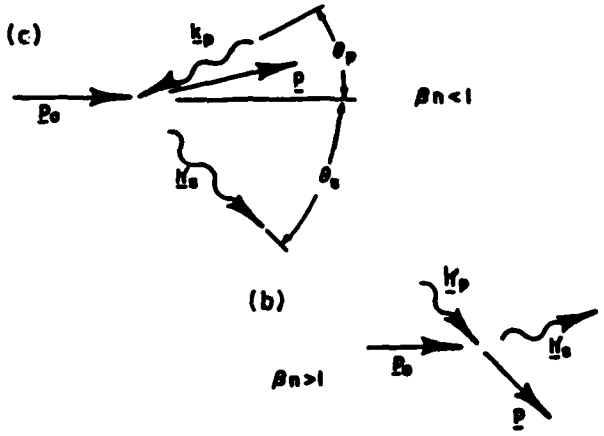

Fig. 4. Cerenkov-Compton scattering, $\beta n \gtrless 1$.

and momentum conservation lead to the conclusion that:

$$\frac{\omega_s}{\omega_p} = \frac{1+\beta_o\, n(\omega_p)\cos\theta_p}{1-\beta_o\, n(\omega_s)\cos\theta_s} \tag{7}$$

Hence ω_s becomes arbitrarily large as $\beta_o n(\omega_s) \to 1$. When electron recoil and or dispersion are included the frequency shift becomes finite but still very large in this same limit. Thus unlike similar stimulated scattering devices[10,26,27] which operate without a dielectric, extremely high energies are not a prerequisite for large ω_s and hence this is a conclusion of some practical significance.

The presence of the medium makes possible $\beta n > 1$ and thus there are scattering processes which have no vacuum analog. These are shown in Fig. 4b. Application of the

conservation laws in this case leads to the relation:

$$\frac{\omega_s}{\omega_p} = \frac{\beta_o\, n(\omega_p)\cos\theta_p + 1}{\beta_o\, n(\omega_s)\cos\theta_s - 1} \tag{8}$$

for which comments similar to those made for Fig. 4a may be made in the limit $\beta_o n(\omega_s) \to 1$. There is, however, one difference, as $\beta_o n(\omega_s) \to 1$ from above unity the solution to the conservation equation moves into the complex plane and the process as expected, becomes forbidden.

If the effects of dispersion are included, multiple roots of Eqs. 7 and 8 can be obtained[17,18,19]. These will be of some importance both in gasses when ω_s is near an absorption line and in the case where a dielectric waveguide is used to support the wave. Before analyzing the waveguide case, however, a very important practical modification to the scattering processes should be considered.

THE ZERO FREQUENCY PUMP. It might be anticipated that an intense source of incident, "pump", photons would be required if a useful level of stimulated radiation at ω_s is to be produced. This would be an important practical limitation if it were not for the fact that a rippled or helical static magnetic field with wavelength λ_p will serve[31] as well. This so called zero frequency pump ($\omega_p = 0$, $k_p = 2\pi/\lambda_p$), which is also used in the vacuum version of stimulated scattering sources, is capable of providing enorous equivalent pump power in the rest frame of the electron.

Analysis of the kinematic relations which lead to Eqs. 7 and 8 with the assumption that ω_p is now zero leads

immediately to:

$$\omega_s = \frac{c\beta_o k_p \cos\theta_p}{1-\beta_o n(\omega_s)\cos\theta_s} \tag{9a}$$

and,

$$\omega_s = \frac{c\beta_o k_p \cos\theta_p}{\beta_o n(\omega_s)\cos\theta_s - 1} \tag{9b}$$

for the subluminal and superluminal cases respectively. The advantages of a zero frequency pump thus apply to the Cerenkov-Compton processes. A further advantage not available in a vacuum is that now k_p can be chosen in order to get good depth of modulation. The frequency shift is controlled independently by $\beta_o n(\omega_s)$.

CERENKOV-COMPTON SCATTERING IN A WAVE GUIDE. The motion imparted to an electron by the pump is primarily transverse and hence this motion can couple to the TE modes of a guide. Shown in Fig. 5 is a sketch of the dispersion relation for a partially filled guide[32] which is bounded by metal walls. Also shown are the beam line $ck\beta$ for the case $\beta n < 1$ and the zero frequency pump which is designated as a horizontal line segment of length k_p. It is clear from the diagram how the pump makes up the momentum difference between a beam mode and the scattered mode. Furthermore, it is also clear that there will in general be two solutions to the kinematic relations and a beam energy threshold below which the scattering process is forbidden. A sketch of the beam energy versus frequency curve is also shown on Fig. 5.

Comments made in a previous section regarding the role of d and ε in controlling the frequency of the fundamental mode generally apply to the Cerenkov mode as

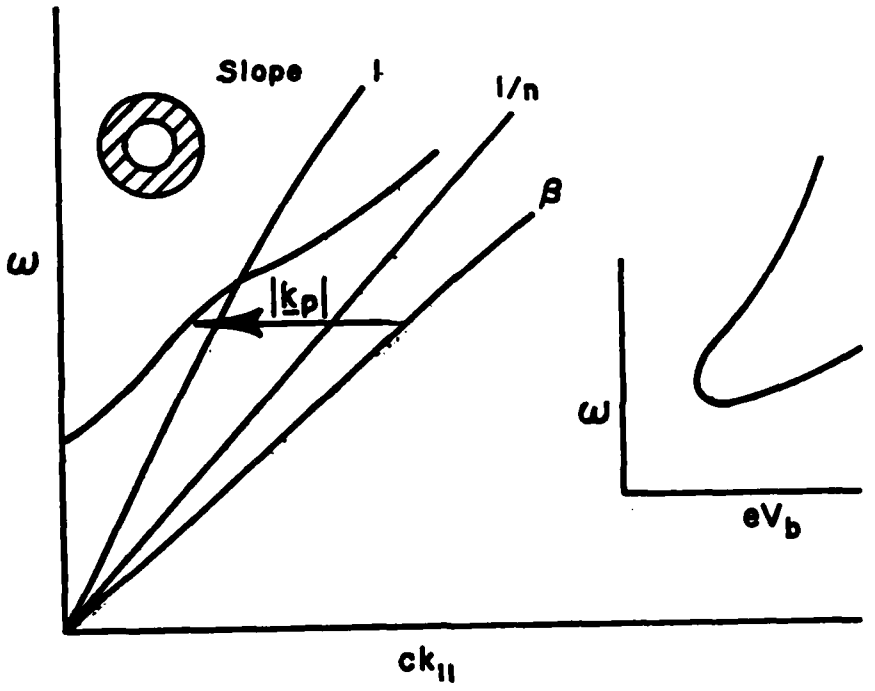

Fig. 5. Cerenkov-Compton scattering in a dielectric resonator.

well. There is one further significant difference. When $\omega/ck < 1$ the fields in the vacuum region must evanesce away from the dielectric (Fig. 6) and although some control over the decay length can be maintained by using large energy electron beams it will ultimately lead to weak coupling at large ω. When Cerenkov-Compton scattering is used, however, we can also couple to waves with $\omega/ck > 1$ and hence to fields which peak rather than evanesce in the region of the

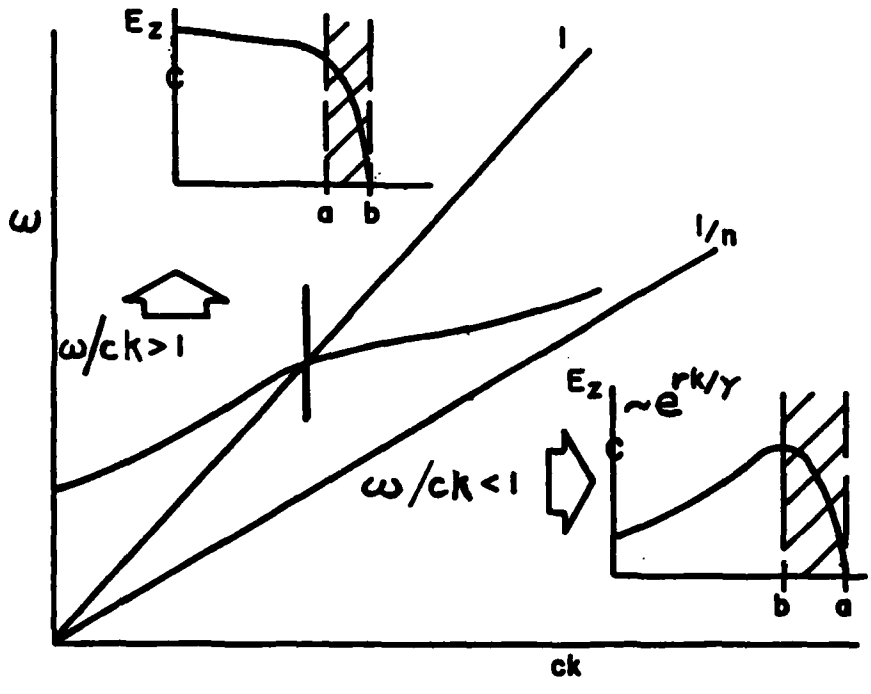

Fig. 6. Axial field strength $\omega/ck \gtrless 1$

electron. The advantage of the dielectric is not lost in this operating regime because the point where $\omega/ck = 1$ will still depend upon $(d^2(\varepsilon - 1))^{-1/2}$ and the point near $\beta n = 1$ will still produce large frequency shifts at beam energies which are comparatively modest. The preceding discussion is primarily aimed at the regime $\beta_o n < 1$ since there are practical advantages to operating with lower beam energies. Devices need not be restricted to this region, however,

since the cross section for the process becomes large for both $\beta_o n \lesssim 1$. Analysis of the related dynamical processes will show that gain can be achieved in both regimes.

CONCLUSIONS. We can conclude from the kinematic arguments presented in the preceding sections that one requirement for producing a high frequency free electron device, $\ell >> \lambda_o$, can be met by Cerenkov and Cerenkov-Compton devices. Whether those possibilities are realized will depend also on the electron dynamics and the parameters of the electron beam used to drive the device. This will be taken up in the next sections.

CERENKOV EMISSION RATES

The spontaneous and stimulated emission rates for Cerenkov radiation can be computed either classically or quantum mechanically. In the quantum calculation one would begin with the kinematic constraints discussed previously and use perturbation theory in the standard way to arrive at experssions for the emission rates. When the recoil terms $(\hbar\omega/E_o)$ are small however, the resulting expressions are independent of $\hbar$. This is true in both the nonrelativistic and the extreme relativistic limit. It is a result of the fact that the electron is making transitions between continuum states and does not depend upon an assumption that there are a large number of photons present. Cerenkov radiation is thus an essentially classical process, and we will use classical formalism, Maxwell's equations and the relativistic Vlasov equation, in order to arrive at

expressions for the emission rates.

SPONTANEOUS CERENKOV EMISSION. The classical picture of Cerenkov emission is that of a wake produced when the particle velocity exceeds the speed of light in the medium. A sketch is shown in Fig. 7. The symmetry of the problem

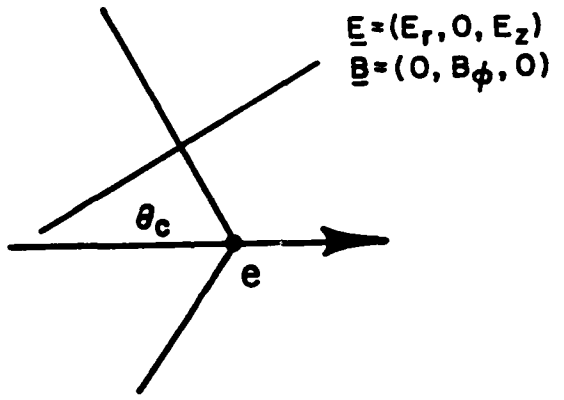

Fig. 7. Cerenkov wake and field components.

immediately dictates which electromagnetic field components, also stated on Fig. 7, are nonvanishing. Derivations of explicit expressions for these are readily available and need not be repeated. We will simply summarize the main conclusions.

If recoil and dispersion are neglected, closed form expressions for the fields as functions of r and z can be obtained. These diverge on the shock front defined by the Cerenkov cone however, and hence they are not the most useful form for further work. It is better to Fourier

transform the charge,

$$\rho = -e \frac{\delta(r)}{2\pi r} \delta(z-vt) \tag{10a}$$

and current,

$$\underline{J} = \underline{v} \rho \tag{10b}$$

which results in

$$\rho_{k,\omega} = -e \frac{\delta(r)}{r} \delta(\omega-kv) \tag{11a}$$

and

$$\underline{J}_{k,\omega} = \underline{v} \rho_{k,\omega} \tag{11b}$$

and use these as source terms in equations for the scalar and vector potentials. The equations governing the radial dependence are then Bessel equations. This in turn suggests that a Fourier-Bessel expansion is the best way to decompose the fields. In an infinite medium the Hankel transform is used, and an expression for the work done by the particle on each component of its own polarization field can be readily computed. The resulting expression is the well known formula for the intensity of radiation produced per unit path length per unit frequency interval:

$$\frac{dI(\omega)}{dz} = e^2\omega(1-1/\beta^2\varepsilon(\omega))/c^2 \tag{12}$$

Integration of Eq. 12 over all ω would result in the total power lost per unit path length. If dispersion is neglected however, this expression again diverges. This is a purely formal difficulty however, since $\epsilon(\omega) \to 1$ as $\omega \to \infty$ for any material and it is obvious that the integral is to be done only for regions where $\beta^2\epsilon > 1$. As a measure of intensity per unit ω Eq. 12 is accurate even in regions when $\epsilon(\omega)$ is sensibly constant.

Evaluation of Eq. 12 also readily shows that very little radiation is produced until ω reaches the uv region of the spectrum. This conclusion is true even if a substantial beam of electrons is used in place of a single electron. If a beam of finite cross section is propagated in a dielectric the power produced per unit length of beam becomes

$$\frac{dP(\omega)}{dz} = \frac{eI}{c} \frac{\omega}{c} (1-1/\beta^2\epsilon(\omega)) \tag{13}$$

where I is the beam current. If the current is expressed in amperes and the power density in watts we obtain:

$$\frac{dP(\omega)}{dz} = 10^{-8} I(A) \frac{\omega}{c} (1-1/\beta^2\epsilon) \tag{14}$$

watts/cm for the power. Pure spontaneous Cerenkov radiation is therefore, a weak process throughout the wavelength range longer than a few tenths of a micron. We will find, however, that both radiation in a superadiant configuration and stimulated radiation are potentially strong processes.

Before leaving the topic of spontaneous Cerenkov

radiation it is useful to point out the differences which occur in the radiation formulas when a bounded medium is introduced. In the discussion of Fig. 3 we concluded that the emission in a dielectric tube was confined to a series of discrete frequencies, one for each mode. The discreteness would remain so long as the overall Q was such that the modes could be resolved. Straightforward extension of the techniques used in the infinite medium can be used to obtain

$$\frac{dI}{dz} = \frac{2e^2}{a^2} \frac{1}{J_1^2(x_{o\ell})} \tag{15}$$

for the power emited into a mode whose field dependence is $J_o(x_{o\ell}r/a)$ where $x_{o\ell}$ is a root of the Bessel function J_o, and a is the guide radius. When a beam of current I is used, the expression analogous to Eq. 5 becomes:

$$\frac{dP}{dz} = \frac{2e}{a^2} \frac{I}{J_1^2(x_{o\ell})} \tag{16a}$$

$$= 2.88 \times 10^{-12} \, I(A)/a^2 J_1^2(x_{o\ell}) \tag{16b}$$

watts/ampere/cm. Again this is a very small amount of power but the comments pertaining to changes in the system which lead to either superadient or stimulated emission lead to predictions of high available power output.

STIMULATED CERENKOV EMISSION RATES. The early theoretical and experimental attempts to turn Cerenkov radiation into a useful source made use of what could be termed pre-bunching.

Clearly if a short (compared to the desired wavelength) bunch of electrons were used the intensity of the radiation would increase by the square of the number of electrons in the bunch. In principle the enhancement could be very large but in practice it is difficult to produce dense bunches with a scale length which is short enough to be interesting. It is better to use the process of stimulated emission. The scale length in this case is that of the stimulating radiation.

There are two basic regimes in which the stimulated process is important. In the first, which pertains to weak beams, spontaneously emitted photons are trapped in a resonator and these stimulate further emission. The energy build-up in this regime will be sensitive to resonator length and other cavity details and for this reason it will be defined as the interferential gain regime.[34] In order for subsequent electrons to add energy to the spontaneously emitted field left by earlier electrons, control of the overall phasing of beam and radiation must be maintained. The growth of radiation within the beam is not exponential and the reaction of the radiation back on the beam in this regime need not be treated self-consistently.

In the second regime the beam is strong enough to cause exponential amplification of the spontaneously created field within the beam itself, and the role of the cavity, if one is used, is somewhat different. Discussion of the details of the role played by resonators will be deferred until a later section. The gain in the exponential regime is subdivided according to whether the beam can be regarded as cold (negligible thermal spread) or warm (the thermal spread affects the gain). We can easily show that the

decision about whether the beam can be regarded as warm or cold depends upon the beam density and the wavelength as well as the velocity spread. Consider a monoenergetic electron beam which is supporting a slow space charge wave propagating in the same direction as the beam. Assuming the fields are weak enough to allow the neglect of nonlinear effects, the dispersion relation of such a mode is easily derived with the aid of the equations of motion,

$$\frac{d(\gamma v_z)}{dt} = \frac{-e}{m} E_z \tag{17}$$

of continuity,

$$\frac{\partial n}{\partial t} + \nabla \cdot (n\underline{v}) = 0 \tag{18}$$

and Poisson's equation,

$$\underline{\nabla} \cdot \underline{E} = -4\pi e (n-n_o) \tag{19}$$

Fourier transforming we obtain for the slow space charge mode

$$\omega = kv_o - \Omega_b/\gamma_o^{3/2} \tag{20a}$$

where

$$\Omega_b^2 = 4\pi n_o e^2/m \tag{20b}$$

is the beam plasma frequency and $\gamma_o = (1 - \beta_o^2)^{-1/2}$ is related to the zero order energy of a beam electron.

The relation between the phase velocity of this mode and the beam velocity is shown in Fig. 8. Also shown in Fig. 8 are two typical velocity distributions. In one the beam and the modes are resolved in velocity and the beam is approximately "cold". In the other it is not and the beam

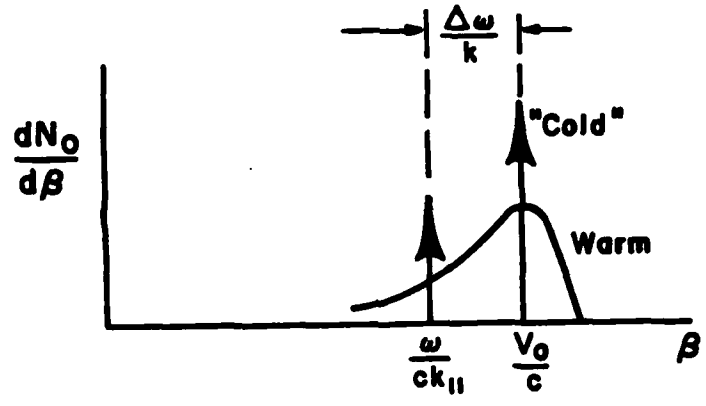

Fig. 8. Beam-space charge waves.

is "warm". Measured in the laboratory frame the velocity difference between the mode and the beam is

$$\Delta v = \Omega_b / \gamma_o^{3/2} k \qquad (21)$$

If we now consider a beam whose velocity spread is equal to Δv we have a criterion for determining the wave length at which a beam can no longer be regarded as cold. It is convenient to express this in terms of energy spread:

$$\Delta v_b = c\Delta\gamma/\beta_o\gamma_o^3 \tag{22}$$

Equating (21) and (22) and using $k = 2\pi/\lambda$ we find a wavelength,

$$\lambda_c = 2\pi c\,\Delta\gamma/\Omega_b\gamma_o^{3/2} \tag{23a}$$

which for $\lambda \gtrless \lambda_c$ defines a cold (warm) beam. If we rewrite the plasma frequency in terms of beam current we have an alternative expression

$$\lambda_c = 2\pi a \frac{\Delta\gamma}{\gamma}\left(\frac{I_o}{\beta_o\gamma_o I}\right)^{\frac{1}{2}} \tag{23b}$$

where a is the beam radius, I is the beam current, and

$$I_o = ec/r_o$$

is the "current" carried by an electron crossing a classical electron radius at velocity c and is equal to 17.5 KA. Discussion of the role of λ_c will be continued below.

Emission in the cold limit. The stimulated Cerenkov emission rate has been derived elsewhere. We will simply summarize the results of this calculation. The symmetry of the beam and the fields are the same as that of the spontaneous case and thus we will have for the equations of motion:

$$[\nabla_\perp^2 + (\frac{\omega^2\epsilon}{c^2} - k^2)]\ \underline{A} = \frac{-4\pi}{c}\ \underline{J} \tag{24a}$$

and

$$[\nabla_\perp^2 + \frac{\omega^2\varepsilon}{c^2} - k^2]\phi = \frac{-4\pi}{c}\frac{c\rho}{\varepsilon} \tag{24b}$$

In writing these we have already Fourier transformed in time and in z (the beam axis coordinate). We have also assumed that the beam is passing directly through the medium. This is not realistic for any case except perhaps a gas in the limit of extreme relativistic beam energy. In a practical configuration there will be one (or more) beam channels in a dielectric resonator. The boundary value problem is greatly complicated by this state of affairs and thus it is difficult to gain a grasp of the physical situation if all possible complications are put in at the beginning. We will assume, therefore, that the beam passes axially through a cylindrical resonator. The form factors which result when practical cases are considered will be discussed further in the concluding sections.

The charge and current in the cold beam limit may be computed either with fluid equations or the Vlasov equation. These depend upon $\underline{A}$ and ϕ. Expanding the entire set of equations in a Fourier-Bessel expansion then yields a dispersion relation:

$$\omega^2 - \omega_k^2 = \frac{\Omega_b^2(\omega^2 - c^2k^2/\varepsilon)}{\varepsilon\gamma^3(\omega - ck\beta)^2} \tag{25a}$$

where

$$\omega_k^2 = c^2(p^2+k^2)/\varepsilon \qquad (25b)$$

is the dispersion of the undriven guide, and p is the radial wavenumber. In deriving (25) we are also assuming that a strongly magnetized beam is used. The other quantities have been defined previously. The dispersion curves in the limit of zero coupling and finite coupling are shown in Figs. 9a

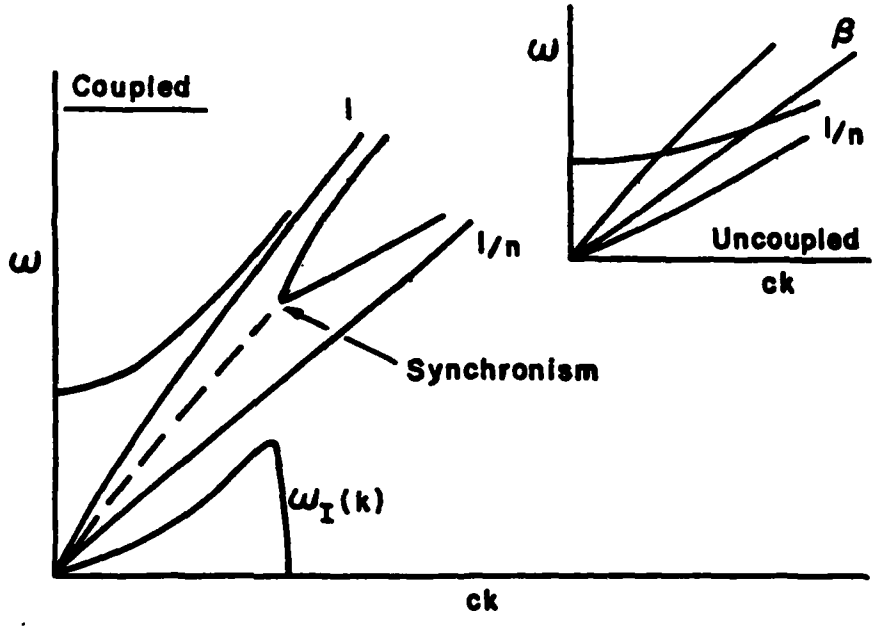

Fig. 9. Dispersion curves in the cold beam limit.

and 9b. There are four roots, two associated with the beam space charge modes and two with the unperturbed guide modes. When $\beta < 1/n$ all four roots are real while for $\beta > 1/n$ we have a complex conjugate pair of roots. The imaginary part

of the frequency (the gain curve) for this limit is also shown in Fig. 9b. The gain not unexpectedly peaks near the region of strongest coupling:

$$\omega_k = ck\beta_o \tag{26}$$

Near this point the dispersion relation reduces approximately to a cubic and we have

$$(\omega - ck\beta_o)^3 - \Omega_b{}^2\, ck\beta\, (1-1/\beta^2\varepsilon)/2\gamma^3 = 0 \tag{27}$$

Since we are on a root of the unperturbed guide mode we also have:

$$k = p/(\beta^2\varepsilon-1)^{\frac{1}{2}} \tag{28}$$

Rewriting $\Omega_b{}^2$ in terms of the current and p in terms of the radius a, ($p = x_{o\ell}/a$), Eq. 27 can be expressed in terms of physically more intuitive variables:

$$(\omega-ck\beta)^3 - \frac{2I}{\beta I_o}\ \frac{(1-1/\beta^2\varepsilon)^{\frac{1}{2}}}{(\varepsilon)^{\frac{1}{2}}}\ \left|\frac{c}{a\gamma}\right|^3 = 0 \tag{29}$$

Thus the gain and the frequency shift on resonance become

$$\omega_I = \frac{(3)^{\frac{1}{2}}}{2}\left(\frac{2Ix_{o\ell}}{(\varepsilon)^{\frac{1}{2}}\beta_o I_o}\right)^{1/3}(1-1/\beta^2\varepsilon)^{1/6}\ \frac{c}{a\gamma} \tag{30a}$$

and

$$\Delta\omega_R = -\frac{\omega_I}{(3)^{\frac{1}{2}}} \tag{30b}$$

respectively. The gain and the frequency shift in spatial units are obtained by dividing Eqs. 30a and 30b by c . Relatively modest electron beam parameters result in substantial gains. A typical example is given in Table 1.

Table 1

Example of gains calculated for typical beam parameters.

ε	2.5	4
V_b(kv)	250	120
I_b(A)	17.5	17.5
$\alpha_I a$	.138	.232

Cerenkov emission rate in the warm beam limit. A discussion of the growth, or stimulated emission rate in the limit where the beam can no longer be regarded as monenergetic may also be found in the references.[33] Hence the discussion here will be brief. Assuming that a strong guide magnetic

field coaxial with the beam direction renders the small signal motion one dimensional, the equations for the z components of the vector potential and the gradient of the scalar potential may with the aid of the equation of continuity be combined to give one equation for the axial component of the electric field:

$$[\nabla_\perp^2 + (\frac{\omega^2\varepsilon}{c^2} - k^2)]E_z = \frac{-4\pi i}{c^2} \frac{(\omega^2 - c^2k^2/\varepsilon)\rho}{k} \quad (31)$$

In the preceding section the charge density ρ was computed using the fluid equations, now to account for thermal spread we will use the Vlasov equation:

$$\frac{\partial f}{\partial t} + v_z \frac{\partial f}{\partial z} + \dot{v}_z \frac{\partial f}{\partial v_z} = 0 \quad (32)$$

where in writing Eq. 32 we have used a velocity distribution and incorporated the assumption that the motion of the particles takes place primarily along the z direction.

Linearizing the Vlasov equation and Fourier transforming in t and z we obtain in the usual way an expression for ρ:

$$\rho = in_o e \int \frac{v_z(\partial f_o/\partial v_z)}{\omega - kv_z} dv_z \quad (33)$$

If we substitute for $\dot{v}_z$ from the equation of motion:

$$\frac{d}{dt}(\gamma v_z) = \frac{-e}{m} E_z \tag{34}$$

and substitute the resulting expression for ρ in the equation for E_z we then have

$$[\nabla^2 + \frac{\omega^2 \varepsilon}{c^2} - k^2] E_z = \frac{-\Omega_b^2}{c^2} \frac{(\omega^2 - c^2 k^2/\varepsilon)}{k} \tag{35}$$
$$x \int \frac{\partial f_o / \partial v_z}{\omega - k v_z} dv_z E_z$$

If a delta function distribution in velocity is assumed the dispersion relation for the cold beam limit obtained in the preceding section is recovered. Restricting ourselves to the opposite limit we may use

$$\frac{1}{\omega - kv} = P \frac{1}{\omega - kv} - i\pi\delta(\omega - kv) \tag{36}$$

to obtain for the imaginary part of the frequency:

$$\omega_I = \frac{\pi \Omega_b^2}{2\omega_k} \frac{\beta^2(1 - 1/\beta^2 \varepsilon)}{\gamma^3} \frac{\partial f(\omega/k)}{\partial(\omega/k)} \tag{37}$$

In obtaining Eq. 37 we have also made use of the condition for phase synchronism

$$\omega = ck\beta \tag{38}$$

and we have ignored the small real part of the beam density dependent frequency shift.

The exact value of ω_I will depend to some extent on the detailed shape of $f(v_z)$. However if we assume that its width in velocity is Δv and that it varies smoothly around its peak the derivative may be replaced with Δv^{-2}. Making use of the relation between Δv and energy spread $\Delta\gamma$, the previous definition of ω_p^2 and dividing by c to obtain a spatial growth rate α we then have:

$$\alpha = \frac{1}{2}\left(\frac{\beta\gamma I}{I_o}\right)\frac{\lambda}{a}\quad\frac{(1-1/\beta^2\varepsilon)}{a}\quad\left(\frac{\gamma}{\Delta\gamma}\right)^2 \tag{39}$$

This result can be further reduced by evaluating it at the wavelength λ which represents the crossover between a warm and a cold beam and by making use of the relation between ω, the transverse wavenumber $x_{o\ell}/a$ and the square of the sine of the Cerenkov angle $(1-1/\beta^2\varepsilon)$. The spatial growth measured in units of beam radius a then becomes:

$$\alpha a = \frac{\pi}{2}\left(\frac{x_{o\ell}}{2\pi}\right)^2\left(\frac{\lambda}{a}\right)^2\left(\frac{\gamma}{\Delta\gamma}\right)\left(\frac{\beta\gamma I}{I_o}\right)^{\frac{1}{2}} \tag{40}$$

Examination of Eqs. 39 and 40 shows that operation of a collective mode device in the submm-fir region of the spectrum is a realistic possibility. This point will be addressed further after the emission rate of the Cerenkov-Raman mode is computed.

CERENKOV-RAMAN EMISSION RATE

The procedure for calculation of the emission rate for the Cerenkov-Raman configuration is similar to that used in the preceding section. It is however slightly more involved since in addition to the beam oscillations, and radiation field we now also have a pump field. The discussion will be broken into two parts. In the first the interaction mechanism will be examined qualitatively and in the second the equations of motion will be developed in more detail.

CERENKOV-RAMAN COUPLING. The kinematics of Cerenkov-Compton scattering were explored in the second section. If the single electron is replaced by a beam and the photons by waves the Cerenkov-Raman instability can occur. This comes about in the following way. The electron beam supports space charge oscillations. If an electromagnetic wave propagates either along or counter to the electron beam the Lorentz force associated with the product of the transverse velocity imparted to the electrons by the electric field associated with the wave and the magnetic field of the wave will act along the direction of the beam propagation.

A synchronous or resonant coupling between three waves is possible. Imagine a beam on which there is a space charge oscillation with axial wave number k_b. If a wave with axial wave number k_p is propagating in the direction counter to the beam there is a beat force with wavenumber

$$k_s = k_b - k_p \tag{41}$$

This implies that the interaction between a space charge oscillation and a counterstreaming "pump" wave generates a scattered wave. We will see that a large amplitude pump wave can induce growth of both the space charge and the scattered waves. Because the pump wave is scattered from a collective beam oscillation the designation of the process as Raman scattering is appropriate. The prefix Cerenkov is used because in the present case we are also examining the process when a dielectric resonator is used to support the scattered wave. It is meaningful to consider the scattering in regimes where the beam speed is either above or below the usual Cerenkov velocity and perhaps it would be proper to restrict the usage of the designation Cerenkov-Raman process to the former limit. However this would unduly clutter the notation. We will use the same designation for both limits and differentiate between subluminal, $\beta n < 1$, and superluminal $\beta n > 1$ where appropriate.

In order to extract a useful amount of gain from this interaction the pump field intensity must be very large. Hence in practice it is best to use a static rippled or helical magnetic field for the pump. In the rest frame of the electron this will result in a large transverse electric field while in the lab frame the pump will have zero frequency but non zero wavelength $\lambda_p = 2\pi/k_p$. Temporal synchronism will require:

$$\omega_s = \omega_b \tag{42}$$

The approximate dispersion relations for the space charge

and scattered modes are

$$\omega_b = ck_b\beta \tag{43a}$$

and

$$\omega_s = ck_s/n \tag{43b}$$

These together with the equation for spatial synchronism result in

$$\omega_s = \frac{c\beta k_p}{1-\beta_o n} \tag{44}$$

the relation obtained from kinematic considerations in the second section. Reversal of the pump direction $k_p \rightarrow -k_p$ and the assumption $\beta n > 1$ immediately results in:

$$\omega_s = \frac{c\beta k_p}{\beta n-1} \tag{45}$$

The kinematic arguments are thus equivalent to phase matching.

THE DISPERSION RELATION FOR CERENKOV RAMAN SCATTERING. In order to calculate the gain the dynamics of the interaction must be considered in more detail. There is now a transverse as well as a longitudinal current and hence the appropriate field equations are

$$\left(\nabla^2 + \frac{\omega^2\varepsilon}{c^2} - k^2\right) \begin{bmatrix} \underline{A}_\perp \\ E_z \end{bmatrix} = \frac{-4\pi}{c} \begin{bmatrix} \underline{J}_\perp \\ i(\omega^2 - c^2k^2/\varepsilon)\rho/ck \end{bmatrix} \tag{46}$$

Again we combine the z component of the vector and scalar potentials since this will simplify computation of ρ and $\underline{J}$. In order to exhibit the basic phenomena with a minimum of complication we will also assume that there are no transverse spatial variations.

Computation of the current is begun with the introduction of a Lagrangian:

$$L = -mc^2(1-\beta^2)^{\frac{1}{2}} - e\underline{\beta} \cdot \underline{A} + e\phi \tag{47}$$

The transverse canonical momentum

$$\underline{p}_\perp = \gamma mc\underline{\beta}_\perp - \frac{e}{c}\underline{A}_\perp \tag{48}$$

is a conserved quantity. If as is usually the case the beam enters the interaction region with no initial angular momentum $\underline{p}_\perp = 0$ and we have immediately:

$$c\underline{\beta}_\perp = \frac{e}{\gamma mc}\underline{A}_\perp \tag{49}$$

It is convenient to use the ordinary momentum

$$p_z = \gamma m v_z \tag{50}$$

in the z direction and the equation of motion for this becomes

$$\dot{p}_z = -eE_z - \frac{m\gamma}{2}\left(\frac{e}{\gamma mc}\right)^2 \frac{\partial}{\partial z} A_\perp^2 \qquad (51)$$

where in obtaining this result we have used the fact that $\underline{p}_\perp$ is conserved and the assumption that there is no spatial variation in the transverse direction.

If the transverse vector potential contains both pump and scattered components the second term on the right hand side of the equation of motion results in a force with wave number k_b and frequency $\omega_b = \omega_s$. This will drive the space charge oscillation.

Computation of ρ and $\underline{J}$ requires the introduction of the Vlasov equation. It is best in this equation to use the mixed set of coordinates $\underline{p}_\perp$, v_z, z, and t. Linearizing we then have:

$$\rho = i n_o e \int \frac{\dot{v}_z (\partial f_o/\partial v_z) dv_z d\underline{p}_\perp}{\omega - kv_z} \qquad (52a)$$

and

$$\underline{J}_\perp = i n_o e \int \frac{\underline{v}_\perp \dot{v}_z (\partial f_o/\partial v_z)}{(\omega - kv_z)} dv_z d\underline{p}_\perp \qquad (52b)$$

The expression $\gamma_\perp^2$ equals $1/(1-\beta_\perp^2)^{1/2}$ and as we will see, the

wave number k is actually k_b.

The expression for ρ contains a term linear in E_z obtained earlier for the Cerenkov mode and a nonlinear drive term which depends upon the ponderomotive potential $A_\perp^2$. The expression for $\underline{J}_\perp$ contains only nonlinear terms, the most important one of which is the one resulting from the product of E_z and $\underline{v}_\perp$. This term drives the equation for $\underline{A}_\perp$ at the frequency ω_s.

Further progress requires evaluation of the integrals in Eqs. 52. In the wavelength limit where the beam may be regarded as cold we can assume:

$$f_o(v_z, \underline{p}_\perp, z, t) = \delta(\underline{p}_\perp)\, \delta(v_z - v_o) \tag{53}$$

and the integrals can be done immediately, yielding for the nonlinear contributions:

$$\rho^{NL} = \frac{in_o e^2}{m} \frac{\gamma_\perp^2}{\gamma^3} \frac{k_b}{(\omega - k_b v_o)^2} \frac{e}{\gamma mc} \frac{\partial}{\partial z} A_\perp^2 \tag{54a}$$

and

$$\underline{J}^{NL} = \frac{in_o e^2}{m} \frac{\gamma_\perp^2}{\gamma^3} \frac{k_b}{(\omega - k_b v_o)^2} \frac{e}{\gamma mc} \underline{A}_\perp E_z \tag{54b}$$

The linear terms in ρ and $\underline{J}$ simply are absorbed into the dispersion relation for the uncoupled waves.

The pump field is actually a spatial standing wave

and hence it has components which vary as $\exp(\pm ik_p z)$. The component with the positive sign will combine with a term in the vector potential of the scattered wave with a similar sign to provide a resonant drive for the space charge mode. In the nonlinear current the pump term with the negative sign combines with a forward propagating component of the space charge wave to provide a resonant drive for the scattered wave.

Defining the magnitude of the relative velocity modulation provided by the pump as:

$$\beta_p = \frac{e}{\gamma mc^2} A_p \tag{55}$$

we arrive finally at a pair of coupled equations for the scattered and space charge waves:

$$D^T A_s = \frac{-i\Omega_b^2 k_b \beta_p \gamma^2}{\gamma^3(\omega - k_b v_o)^2} E_z \tag{56a}$$

$$D^L E_z = \frac{-i\Omega_b^2 k_b \beta_p \gamma^2}{\gamma^3(\omega - k_b v_o)^2} A_s \tag{56b}$$

The symbols D^T and D^L stand for the linear parts of the dispersion relations of the scattered (transverse) and space charge (longitudinal) waves respectively. The former one of these is:

$$D^T = \frac{\omega^2 \varepsilon}{c^2} - k^2 - \frac{\Omega_b^2}{\gamma c^2} \tag{57}$$

and the latter is:

$$D^L = 1 - \frac{\Omega_b^2}{\gamma^3 (\omega - k v_o)^2} \tag{58}$$

A determinantal equation for the coupled modes could now be computed and its roots evaluated. However, in spite of the many simplifying assumptions made so far this remains a formidable task. The following procedure will be adopted.

Optimum coupling will occur near the region where the uncoupled waves are resonant modes, i.e. near where each satisfies its own linear dispersion relation. Near this frequency the coupled equations can be rewritten in the form:

$$\frac{\partial A_s}{\partial t} = -i \left(\frac{\Gamma}{\partial D^T / \partial \omega} \right)_{\omega_s} E_z \tag{59a}$$

$$\frac{\partial E_z}{\partial t} = -i \left(\frac{\Gamma}{\partial D^L / \partial \omega} \right)_{\omega_s} A_s \tag{59b}$$

where Γ denotes the factors which appear as coefficients on the right hand side of Eqs. (56). We are also now assuming the mode amplitudes A_s and E_z vary slowly as a result of the coupling although this is not the same as the original

definition which included the exponential factors and tacitly assumed that the amplitudes were constant.

A determinantal equation for Eqs. (59) can now be formed easily. We find for the imaginary part of the frequency

$$\omega_I = \gamma_\perp^2 (\Omega_b \omega_s)^{\frac{1}{2}} \beta_p / 2\gamma^{3/4} \tag{60}$$

It is also useful to state this in spatial units of the beam radius

$$\alpha a = \gamma_\perp^2 \beta_p (k_s a)^{\frac{1}{2}} \left(\frac{4I}{\beta \gamma^3 I_o} \right)^{\frac{1}{2}} \tag{61}$$

The growth rate increases as the square root of the scattered frequency and hence this is an intrinsically short wave length process provided the beam may be regarded as cold. As was the case with the pure Cerenkov mode the growth in the warm limit will decrease with decreasing wave length and hence the warm-cold transition wavelength discussed in the earlier sections although not an absolute limit for device operation is a useful figure of merit for estimating the high-low gain transition.

CONCLUSIONS

We have derived expressions for the frequency and the stimulated emission rate for Cerenkov and Cerenkov-Raman

emission processes. In the limit where the driving electron beam can be regarded as monoenergetic the growth rate rises with frequency (as $\omega^{1/3}$ and $\omega^{1/2}$ respectively) for both processes and hence they are both intrinsically short wavelength interactions. Furthermore, by controlling the filling factor and the relative dielectric constant of the dielectric waveguide resonators, practical operation in a regime where the operating wavelength is much less than the characteristic transverse dimension of the resonator, has been achieved. The fundamental limitation to operation of these devices in the collective regime at short wavelengths would thus appear to be the electron beam quality. The dielectric resonator makes use of beams which although substantial, are nevertheless modest when compared to those used in other short wavelength free electron radiation sources. Operation in the lower part of the mm region of the spectrum has already been attained and operation in the submm regime appears very likely. The basic dielectric resonator-electron beam technique can most probably be made to work into the far infrared portion of the electromagnetic spectrum. The basic physical principles governing free electron radiation sources operation is very much the same for all devices. Hence we would expect that in general, devices such as we have discussed, would work at as short a wavelength as any other free electron laser.

ACKNOWLEDGEMENTS

The author would like to acknowledge innumerable enlightening discussions with Ken Busby, Kevin Felch, Geoff Crew, and Professor William Case of Hobart and William Smith

Colleges. Support from Dartmouth College, the Department of the Army Grant DAAG39-78-C0032, the Air Force Office of Scientific Research Grant 77-3410, and the Office of Naval Research is also gratefully acknowledged.

REFERENCES

1. P.A. Cerenkov, Dokl. Adad. Nauk. SSSR 2, 451 (1934).
2. I.M. Frank, and Ig. Tamm, Dokl. Akad. Nauk. SSSR, 14, 109 (1937).
3. M.A. Piestrup, R.A. Powell, G.B. Rothbart, C.K.Chen, and R.H. Pantell, Appl. Phys. Lett. 28, 92 1976.
4. P. Coleman and C. Enderby, J. Appl. Phys. 31, 1695 (1960).
5. H. Lashinsky, J. Appl. Phys. 27, 631 (1956).
6. K. Felch, K. Busby, J. Walsh, and R. Layman, Bull. Am. Phys. Soc. 23, 749 (1978).
7. A. Hasegawa, Bell System Tech. Jour. 57, 3069, 1978.
8. K. Busby, K. Felch, R.W. Layman, J.E. Walsh, 1979 IEEE Conf. on Plasma Science---Conf. Record, 107.
9. O. Heaviside, Phil. Mag. 1888: Feb. p 130, Mar. p 202, May p 379, Oct. p 360, Nov. p 434, Dec. p 488.
10. A. Sommerfeld, Gotting, Nachricht. 99, 363 (1904).
11. E. Curie, Madame Curie (Heinemann, London 1941).
12. L. Mallett, C.R. Acad. Sci (Paris) 183, 274 187, 222 188, 445.
13. B.M. Bolotovskii, Usp. Fiz. Nauk. 75, 295 (1961); Soviet Physics Uspekhi 4, 781 (1962).
14. V.L. Ginzburg Dok. Akad. Nauk. SSSR 3, 253, 1947.
15. Cerenkov losses do not compete with other collisional radiation until the vuv region is reached.

16. Prebunching will not necessarily be self-consistent.
17. I.M. Frank, J. of Phys. 2, 49 (1943).
18. V.L. Ginzburg Dok. Akad. Nauk. SSSR 56, 145, (1947).
19. S. Schneider, and R. Spitzer, Nature 250, 643, (1974), I.E.E.E. Trans MIT 25, 551 (1977).
20. J.E. Walsh, T.C. Marshall and S.P. Schlesinger, Phys. Fluids 20, 709 (1977).
21. K. Busby, K. Felch, R.W. Layman, J.E. Walsh, Bull. Am. Phys. Soc. 24, 607 (1979).
22. Recent experimental results are discussed elsewhere in this volume.
23. J.R. Pierce, Phys. Today 3, 24 (1950).
24. I. Kaufman, Proc. I.R.E. 47, 381 (1959).
25. D.A.G. Deacon, L.R. Elias, J.M.J. Madey, G.J. Ramian, H.A. Schwettmann, and T.I. Smith, Phys. Rev. Lett. 38, 892-894 (1977).
26. P. Sprangle, R.A. Smith, and V.L. Granatstein, NRL Memorandum Report 3888 (1978).
27. R.M. Gilgenbach, T.C. Marshall, and S.P. Schlesinger, Physics of Fluids, 22, 5, 971-977 (1979).
28. Carcinotrons have been operated well into the submillimeter regime.
29. J.V. Jelley, Cerenkov Radiation and its Applications, (Pergamon, London, 1958).
30. M. Stockton, J. Walsh, J. Opt. Soc. Am. 68, 1629 (1978).
31. R.M. Phillips, IRE Trans. Electron Devices, ED-7, 231 (1960).
32. N. Marcuvitz, Waveguide Handbook (McGraw-Hill, New York, 1951).

33. J.E. Walsh, "Stimulated Cerenkov Radiation," in Physics of Quantum Electronics, edited by S. Jacobs, M. Sargent, M. Scully (Addison-Wesley, Reading, Mass., 1978), Vol. 5.

34. A. Gover, A. Yariv, Applied Physics, 16, 121 (1978).

JOURNAL DE PHYSIQUE
Colloque C1, supplément au n°2, Tome 44, février 1983 *page* C1-389

CERENKOV LASERS*

J. Walsh, B. Johnson, E. Garate, R. Cook, J. Murphy and P. Heim

Department of Physics and Astronomy, Dartmouth College, Hanover, N.H. 03755, U.S.A.

Abstract.-

A Cerenkov laser consists of an electron beam, a dielectric resonator, and suitable output coupling optics[1]. The beam may pass directly through the dielectric at greater-than-light speed for that medium, in which case it will emit spontaneous Cerenkov radiation. If, in addition, there are mirrors forming an optical cavity, the reflected radiation stimulates further Cerenkov emission, and gain can result. In order to achieve gain, however, the beam velocity spread must be kept very low and hence in this most elementary case a gaseous dielectric and a highly energetic beam is needed. The Cerenkov threshold energy γ_T expressed in terms of the index of refraction n is given by:

$$\gamma_T = n/\sqrt{n^2 - 1}$$

When typical gasses at moderate pressure are considered, γ_T will range between 20 and 200.

It is also possible to propagate a beam through a channel or near to the surface of a dielectric.' In this case the threshold energy is greatly reduced. Substantial power[2] in the lower mm wavelength range can be obtained from devices driven by beams in the 100-200 KV range.

*Supported in part by the Air Force Office of Scientific Research, the Army Research Office, and the Office of Naval Research.

If the beam energy is increased, a device of this kind may also be useful at much shorter wavelengths. This follows from two basic considerations. The first is the scale length of the region over which the fields slowed by the dielectric resonator evanesce. It can be shown on very general terms that this is governed by:

$$\lambda\beta\gamma \quad \backsim \quad b$$

where b is the scale length of the order of the beam diameter and beam-wave velocity synchronism is assumed. When b is a fraction of a millimeter, $\beta\gamma$ in the 2-20 range place λ in the far infrared part of the spectrum.

In calculating the gain in the short wavelength region, a non-collective approach may be adopted. A field with a component directed along the beam is assumed to exist. This produces a modulation current and the stimulated emission is the result of the work done by the beam back on the field. It is most convenient to express this as a reciprocal quality factor

$$\frac{1}{Q_b} \equiv \frac{R_e}{2\omega\mathcal{E}} \int_{\text{beam}} \underline{j} \cdot \underline{E}^* d\,V$$

where $\mathcal{E}$ is the energy stored in the whole resonator, $\underline{E}$ and $\underline{j}$ are the electric field and the modulation current, and ω is the angular frequency of the emitted radiation. When $1/Q_b < 0$, gain is positive.

The gain expression can be placed in a relatively general form. If we assume that the beam may be regarded as monoenergetic at the wavelength of interest ($\lambda > L\delta\gamma/(\beta\gamma)^3$, L-resonator length) we can show:

$$\frac{1}{Q_b} = \frac{1}{(\beta\gamma)^3} \frac{I}{I_o} \frac{L^3|E_z|^2}{8\pi\mathcal{E}} \frac{\bar{n}}{n_o} \frac{\partial}{\partial\theta} \frac{(1-\cos\theta)}{\theta^2}$$

where $\theta = (kv-\omega)L/v$ is the relative transit angle, and current, I, have been measured in units of $I_o = ec/r_o$ ($r_o = e^2/mc^2$). The terms in the expression which involve the field component in the beam direction and the stored energy are of the order of L^2/mode area, times a factor which is specifically dependent on the resonator. In addition, an effective relative beam density $\bar{n}/n_o$ is obtained from the transverse dependence of the fields. Typical designs for short wavelength devices and the results of recent experiments will be discussed.

References.-

1. Stimulated Cerenkov Radiation, in Advances in Electronics and Electron Physics, Vol. 58 (Academic Press, 1982).
2. A High Power Cerenkov Maser, with S. Von Laven, J. Branscum, J. Golub, and R. Layman, Appl. Phys. Lett., to be published September 1982.

380158

A Cerenkov gas laser

J. E. Walsh, B. Johnson

Department of Physics and Astronomy, Dartmouth College
H.B. # 6127, Hanover, New Hampshire 03755

Abstract

A Cerenkov gas laser would consist of a suitable gas at near atmospheric pressure, a highly relativistic electron beam, and an optical cavity. The electron beam emits spontaneous Cerenkov radiation which is reflected on the beam at the Cerenkov angle by the cavity. This, in turn, stimulates further emission. In an idealized situation the predicted gain of such a system, when operated in the visible region of the spectrum, could be quite high (many percent/pass). Results of an idealized calculation and departures therefrom caused by finite beam emittance and energy spread, velocity space diffusion of the beam in the resonator, and constraints imposed by beam and cavity characteristics will be discussed.

Introduction

The idea of a Cerenkov radiation gas-filled visible wavelength source has long been an attractive one.[1] Since the index of refraction n ($n = \sqrt{\epsilon}$; ϵ = dielectric constant) varies with frequency ω, light of different wavelengths is emitted at different angles defined by $\cos\theta_C = 1/\beta n(\omega)$. For $\beta \lesssim 1$ a gas can be used to provide n only slightly different from unity. Consequently, large variations in $(n - 1)$ can be achieved through variations in pressure. Thus, for a given beam energy and gas pressure, the wavelength and corresponding angle of emission are completely determined. The advent of highly relativistic electron beams and fast-pulse detection systems makes this idea feasible. A device is proposed in which spontaneous emission is reflected back onto the beam, thereby inducing stimulated emission and enhancing output.

Several factors must be considered in the design of such a device. Beam energy, energy spread, and angular divergence must be examined. Cavity parameters such as gas type, gas pressure, cavity dimensions, and mirror reflectivity, as well as output detection must be analyzed. These considerations, together with an estimate of spontaneous and stimulated emission rates, determine the gain threshold conditions.

Effects of the medium on the electron beam

Our choice of suitable gases is dictated by the need to maximize Cerenkov output while keeping energy losses at a minimum. As a representative low Z gas, we choose Helium at STP. The threshold energy for emission of Cerenkov radiation in the visible region is ≈ 61 MeV. We define a critical energy E_s above which the electrons in the atoms effectively screen the nuclear charge from the incident electrons. In Helium, $E_s \approx 78$ MeV, therefore, if we assume an electron energy of 80 MeV, we can hope to minimize energy losses due to collisions. In addition, we choose a nominal cavity length of 1 meter and find that the energy loss due to collisional ionization is approximately $4.7 \cdot 10^{-2}$ MeV,[2] and that due to Bremsstrahlung is on the order of $1.3 \cdot 10^{-4}$ MeV.[3] Thus, for an initial electron energy of 80 MeV, we find the percent energy loss in 1 meter of Helium from both effects to be $\Delta E_{TOT}/E \approx .075\%$. We then conclude that the particle velocity is not significantly affected and, ignoring electron-electron interactions in the beam, we can calculate the angular scattering of an electron in the beam via the method of Scott and Snyder.[4] If one assumes the beam enters the cavity well-collimated, the angular distribution of the electrons is approximately Gaussian. The calculated value of $\sqrt{\langle\phi_{1/e}\rangle^2}$, where $\phi_{1/e}$ the angle at which the angular distribution is 1/e th its peak value, is ≈ 2.5 mrad. In comparison, the Cerenkov angle at 5000 Å is on the order of 10 mrad.

Spontaneous emission rate

The calculation of the spontaneous emission, both in terms of the number of photons per pulse and energy per pulse is straightforward.[5] For a pulsed electron beam of pulse length 3 picosecond and beam cross-sectional area of 1 mm^2, the number of photons per pulse per cm is $\approx 2 \cdot 10^6$. The energy per pulse in 1 meter is on the order of $4 \cdot 10^{-11}$J. These are detectable quantities; however, the major source of gain is intended to be the stimulated emission which will significantly enhance the output.

Stimulated Emission Rate

The dependence of the stimulated emission rate on the key parameters can be displayed easily if we assume, in the first approximation, that the beam moves in one dimension (along z) and can be represented by a delta function distribution in momentum. We assume that the spontaneous emission, which represents the perturbing field, is reflected onto the beam at the Cerenkov angle, and use the linearized Vlasov equation:[6]

$$\frac{d}{dt}\,\delta f = -\dot{\bar{p}} \cdot \frac{\partial f_o}{\partial \bar{p}} \quad . \tag{1}$$

Integrating over a zeroth order orbit we find an expression for δf. We then define a current

$$\bar{J} = -n'e \int d\bar{p}\; \delta f\, \bar{v} \quad , \quad n' \equiv \text{electron density}, \tag{2}$$

such that

$$\frac{dE}{dt} = -\frac{1}{2}\,\mathrm{Re} \int dV\; \bar{J} \cdot \bar{E}^* \tag{3}$$

Finally, we define

$$1/Q = -\frac{1}{\omega E}\,\frac{dE}{dt} \quad . \tag{4}$$

In the one-dimensional case,

$$\dot{p} = -e E_z = -eE_{zo}\, e^{i(kz - \omega t)} \tag{5}$$

where $E_{zo} = E_o \sin\theta_c$.

Substituting into the expression for Q^{-1} and collecting terms yields the result

$$1/Q = 4\pi \frac{A_b L^2}{A_m}\,\frac{J}{I_o}\,\frac{\sin^2\theta_c}{(\beta\gamma)^3}\,\frac{\partial}{\partial\theta}\left(\frac{1-\cos\theta}{\theta^2}\right) \quad , \tag{6}$$

where

$\beta = \frac{v}{c}$ and $\gamma = (1-\beta^2)^{-\frac{1}{2}}$,

$J = I/A_b$, $I \equiv$ the beam current

$A_b \equiv$ cross-sectional beam area, $A_m \equiv$ cross-sectional mode interaction area,

$\sin^2\theta_c = 1 - \cos^2\theta_c = 1 - \frac{1}{\beta^2 n^2}$ where n is the refractive index of the gas, and

$\theta = (k_z v - \omega)\,\frac{L}{v}$.

The Cerenkov angle dependence and the dependence on mode area enter through the relation

$$\frac{E_{zo}^2}{E^2} = \frac{8\pi}{\Gamma A_m} \tag{7}$$

The general range of obtainable Q^{-1} (or, alternatively, gain/pass $G = -L\omega/vQ$) can be easily extracted from an examination of Eq. (6). Assuming E = 78 MeV, I = 10 amp, L = 1 m, and n = 1.000129, we have for peak Q^{-1} and G, $-7\cdot10^{-8}$ and 23%, respectively. In obtaining these results we have also assumed that the beam is located at the maximum value of

$$\frac{\partial}{\partial\theta}\left(\frac{1-\cos\theta}{\theta^2}\right) .$$

The value of $\sin^2\theta_c$ was chosen assuming ω is not close to an absorption line. In the frequency region near the absorption line, n rises, the threshold energy decreases, and the value of $\sin^2\theta_c$ increases. Hence gain is enhanced in this region. In order to

evaluate the potential benefits of operating in this region the associated increase in absorption must also be assessed.

This method has also been applied to a two-dimensional beam where the z direction is parallel to the beam and the x direction is transverse to it. Furthermore, we have assumed a more realistic velocity distribution which is Gaussian in both the z and x directions. The calculations are therefore considerably more complicated and the integrations are performed numerically. In addition, we examine the value of Q^{-1} as a function of index of refraction and as a function of the transit angle θ defined as

$$\theta = (\bar{k} \cdot \bar{v} - \omega)\, L/v_z \,. \qquad (8)$$

for several parallel Gaussian widths. The results of these calculations are displayed graphically in Figures 1 and 2.

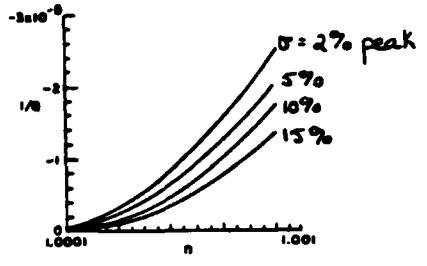

Figure 1. Gain vs. refractive index.

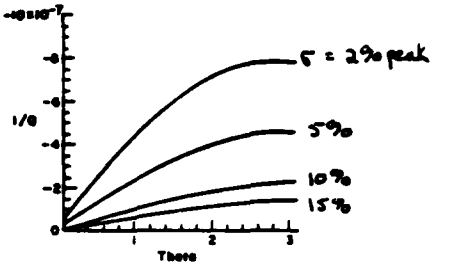

Figure 2. Gain vs. transit angle.

The higher curves represent decreasing Gaussian widths and we see the obvious result that gain increases. In addition, order-of-magnitude increases in Q^{-1} can be achieved by varying n. The easiest way to increase n is to raise the gas pressure, which has the added benefit of increasing the Cerenkov angle, thus facilitating detection. Unfortunately, such an increase also results in increased scattering energy loss and angular spread. Thus, as mentioned earlier, operation near an absorption line may be an attractive alternative.

If we compare the maximum values of Q^{-1} obtained via the above calculation to a typical optical cavity Q value,

$$\text{where } Q = \frac{2\pi L}{\lambda}\left(\frac{1}{1-\rho^2}\right), \quad \rho = \text{reflectivity}, \qquad (9)$$

We find $Q_{beam} \approx 10^6 - 10^7$ and $Q_{cavity} \approx 10^8$ for $\rho = 90\%$. Thus, the criterion for resonance, $Q_{cavity} > Q_{beam}$, can be achieved.

Conclusions

A complete description of a possible Cerenkov gas 'laser' would include the following: (see Figure 3)

a) A low z gas such as Helium, at or near atm. pressure.

b) An electron beam of electron energy $\geq$ 78 MeV;

c) Two mirrors, one of optical reflectivity on the order of 100% and one partially transmitting;

d) A detection system capable of fast-pulse (e.g. picosecond) detection.

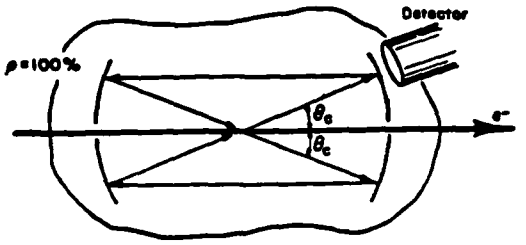

Figure 3.

Our investigation thus far indicates that a relatively high power visible wavelength source is feasible. Critical parameters must be evaluated which will minimize beam degradation while maximizing output. Future endeavors in a thorough analysis of this subject will include the effects, if any, of space charge neutralization and electron trapping, as well as dispersion characteristics and further departures from the semi-idealized two-dimensional model presented in this paper.

Acknowledgments

This work is supported in part by a grant from the Office of Naval Research, Grant # N00014-79-C-0760.

References

1. Chen, C. R.; Sheppard, J. C.; Piestrup, M. A.; Pantell, R. H.; "Analysis of Bunching of an Electron Beam at Optical Wavelengths", J. Appl. Phys., Vol. 49(1), Jan. 1978.
2. Jackson, J.D., Classical Electrodynamics, 2nd Ed., p. 629, John Wiley & Sons, 1975.
3. Ibid., p. 718.
4. Scott, W. I., "Mean-Value Calculations for Projected Multiple Scattering", Phys. Rev., Vol. 85(2), pp. 245-248, Jan. 15, 1952.
5. Jelly, J. V., Cerenkov Radiation and its Applications, Pergamon Press, 1958.
6. Walsh, J. E.; Murphy, J. B.; "Tunable Cerenkov Lasers", I.E.E.E. J. of Quant. Elec., Vol. QE-18(8), August 1982.

END

DATE
FILMED

1-84

DTIC